Title
The role of siderophores in algal-bacterial interactions in the marine environment

Author
Amin, Shady A.

Publication Date
2010

Peer reviewed

UNIVERSITY OF CALIFORNIA, SAN DIEGO

SAN DIEGO STATE UNIVERSITY

The Role of Siderophores in Algal-Bacterial Interactions in the Marine Environment

A dissertation submitted in partial satisfaction of the requirements for the degree

Doctor of Philosophy

in

Chemistry

by

Shady Ahmed Amin

Committee in charge:

Professor Carl J. Carrano, Chair
Professor Laurance G. Beauvais
Professor Brian Palenik
Professor Forest L. Rohwer
Professor F. Akif Tezcan
Professor Yitzhak Tor

2010

The Dissertation for Shady Ahmed Amin is approved, and it is acceptable in quality and form for publication in microfilm and electronically:

_____

_____

_____

_____

_____

_____
Chair

University of California, San Diego

San Diego State University

2010

To my father

TABLE OF CONTENTS

LIST OF SYMBOLS AND ABBREVIATIONS

amu	Atomic Mass Units
BPDS	Bathophenanthrolinedisulfonic acid
CAS	Chrome azurol S
CCCP	Carbonyl cyanide 3-chlorophenyhydrazone
CIS	Coordination Induced Shift
δ_C	^{13}C NMR chemical shift in ppm
DEPT	Distortionless Enhancement by Polarization Transfer
DFT	Density Functional Theory
DOM	Dissolved Organic Matter
DMSO	Dimethyl sulfoxide
DSS	3-(trimethylsilyl)-1-propanesulfonic acid-d_6, sodium salt
EDTA	Ethylenediaminetetraacetic acid
EGTA	Ethylene glycol-bis(2-aminoethylether)-N,N,N',N'-tetraacetic acid
ESI-MS	Electrospray Ionization Mass Spectrometry
Fe'	Soluble inorganic iron species in seawater
gCOSY	Gradient-Correlation Spectroscopy
HMBC	Heteronuclear Multiple Bond Correlation
HMQC	Heteronuclear Multiple Quantum Coherence
HPLC	High Performance Liquid Chromatography
k_m	Michaelis constant
K_{ML}	The overall (pH-independent) binding constant of a metal to a ligand
LMCT	Ligand-to-Metal Charge Transfer
LMW	Low molecular weight
MMFF	Merck Molecular Force Field
MS	Mass Spectrometry

NMR	Nuclear Magnetic Resonance
NOESY	Nuclear Overhauser Effect Spectroscopy
PB	Petrobactin
Rf	Rhizoferrin
TOCSY	Total Correlation Spectroscopy
VF	Vibrioferrin

LIST OF FIGURES

LIST OF TABLES

ACKNOWLEDGEMENTS

I would like to acknowledge first and foremost my research advisor Carl Carrano, who helped me and guided me through this long journey. I learned from him a great deal of knowledge and for that I will always be in debt. During my time in his lab I have had the opportunity to manage and direct research of a few undergraduates, which amounted to an unrivaled experience in my life.

My research experience in Oban, Scotland has been fantastic. I have built many friendships and learned a great deal of knowledge from people there. For this, I would like to thank David Green, who introduced me to the world of microbiology and the intricates of dinoflagellates. If I had a second PhD advisor, it would be David. I would like to also thank Frithjof Küpper for helping me during my trips to Scotland and for getting me aboard the Discovery last year. I have enjoyed knowing and working with Frithjof from the time of attending Alison Butler's Bioinorganic chemistry class at UCSB when I really did not know who he was to the amazing and adventurous hikes and trips across the Scottish Highlands. I received help from many other people in Scotland including Mark Hart and Debra Brennan who helped in the environmental samples isolation and in teaching me basic biochemical techniques, Martina Strittmatter for her help around the microbiology lab, Andrew Mogg for helping with ship setup, Toby Sherwin for leading the scientific staff and the rest of the scientific crew. Katherine Barbeau helped with obtaining large quantities of seawater throughout my PhD and she generously measured the binding constant of vibrioferrin to Fe'. I would like to also thank Alison Butler at UCSB who really inspired me to love bioinorganic chemistry and introduced me to the world of siderophores. This was a critical step in directing me towards working in this field.

Many other people contributed various things to my research including all my coauthors: Bill Sunda, Wesley Harris, Mark Hart and Stephen Schellenberg. Dr. Leroy

Lafferty generously helped with running and troubleshooting ^{11}B and 2-D NMR experiments. Funding for my salary and for research has been provided by the California SeaGrant. I would like to thank my friends Steven Willard, Amer El Batta and Reji Nair for the great time we spent together. I would like to also thank my lab partners whom I have worked with and known throughout my PhD: Guillermo Santillan, Ba Tran, Ariel Romano (who helped me with gene expression), Lyndsay Trimble (who helped with qPCR of the ship samples), Justin Hoffman, Rebekah McGirk, Madhura Rane, Andy Drake, Yukiko Uchida, and Dhuha Al Waheeb.

Last but not least, I would like to also thank my parents for all their support, encouragement and patience. Without their effort and love, reaching the end of the road would never seem possible. I also thank my wife for enticing me to work during the past two years and for her love and patience.

The text, tables, and figures of Chapters 1, 2, 3, 4, and 5 are in part reprints of the materials published in the following papers: Amin, S.A.; D.H. Green; M.C. Hart; F.C. Küpper; W.G. Sunda; C.J. Carrano. Photolysis of iron-siderophore chelates promotes bacterial-algal mutualism. *Proc. Natl. Acad. Sci. U. S. A.* **2009**, *106*, 17071-17076; Amin, S.A.; D.H. Green; F.C. Küpper; C.J. Carrano. Vibrioferrin, an unusual marine siderophore: Iron binding, photochemistry and biological implications. *Inorg. Chem.* **2009**, *48*, 11451-11458; Carrano, C.J.; S. Schellenberg; S.A. Amin; D.H. Green; F.C. Küpper. Boron and marine life: A new look at an enigmatic bioelement. *Mar. Biotechnol.* **2009**, *11*, 431-440; Harris, W.R.; S.A. Amin; F.C. Küpper; D.H. Green; C.J. Carrano. Borate binding to siderophores: structure and stability. *J. Am. Chem. Soc.* **2007**, *129*, 12263-12271; Amin, S. A.; F.C. Küpper; D.H. Green; W.R. Harris; C.J. Carrano. Boron binding by a siderophore isolated from marine bacteria associated with the toxic dinoflagellate *Gymnodinium catenatum*. *J. Am. Chem. Soc.* **2007**,*129*, 478-479. The dissertation author was the primary

researcher for the data presented and was either the primary author or a co-author on the papers included. The co-authors listed in these publications also participated in the research.

VITA AND PUBLICATIONS

Education

2010	PhD, Chemistry, University of California, San Diego, La Jolla, CA/San Diego State University, San Diego, CA (JDP).
2009	M. A., Chemistry, San Diego State University, San Diego, CA.
2003	B. Sc., Biochemistry, University of California, Santa Barbara, Santa Barbara, CA.

Awards

2008	The President's Award in Research and Scholarship at SDSU's 1st Annual Student Research Competition
2008	Award at the annual statewide CSU Student Research Competition
2007	Research Travel Scholarship from SDSU Office of International Studies
2005-2006	Pfizer Research Fellowship
2005	"*Outstanding Student Speaker*" award at the Trace Metal Biogeochemistry Symposium, 229th ACS National Meeting, San Diego, CA
2005	Research Travel Scholarship from SDSU Office of International Studies

Publications

1) **Amin, S.A.**; D.H. Green; M.C. Hart; F.C. Küpper; W.G. Sunda; C.J. Carrano. Photolysis of iron-siderophore chelates promotes bacterial-algal mutualism. *Proc. Natl. Acad. Sci. U. S. A.* **2009**, *106*, 17071-17076.

2) **Amin, S.A.**; D.H. Green; F.C. Küpper; C.J. Carrano. Vibrioferrin, an unusual marine siderophore: Iron binding, photochemistry and biological implications. *Inorg. Chem.* **2009**, *48*, 11451-11458.

3) Zhang, G.; **S.A. Amin**; F.C. Küpper; P.D. Holt; C.J. Carrano; A. Butler. Ferric stability constants of representative marine siderophores: Marinobactins, Aquachelins, and Petrobactin. *Inorg. Chem.* **2009**, *48*, 11466-11473.

4) Carrano, C.J.; S. Schellenberg; **S.A. Amin**; D.H. Green; F.C. Küpper. Boron and marine life: A new look at an enigmatic bioelement. *Mar. Biotechnol.* **2009**, *11*, 431-440.

5) Harris, W.R.; **S.A. Amin**; F.C. Küpper; D.H. Green; C.J. Carrano. Borate binding to siderophores: structure and stability. *J. Am. Chem. Soc.* **2007**, *129*, 12263-12271.

6) **Amin, S. A.**; F.C. Küpper; D.H. Green; W.R. Harris; C.J. Carrano. Boron binding by a siderophore isolated from marine bacteria associated with the toxic dinoflagellate *Gymnodinium catenatum*. *J. Am. Chem. Soc.* **2007**,*129*, 478-479.

ABSTRACT OF THE DISSERTATION

THE ROLE OF SIDEROPHORES IN ALGAL-BACTERIAL INTERACTIONS IN THE MARINE ENVIRONMENT

by

Shady Ahmed Amin

Doctor of Philosophy in Chemistry

University of California, San Diego, 2010

San Diego State University, 2010

Professor Carl J. Carrano, Chair

Iron is arguably the most important micronutrient in the marine environment due to its involvement in many vital physiological processes, such as photosynthesis, oxygen transport, electron transfer and nitrogen fixation. However, the availability of iron is hampered by its poor solubility and tendency to form biologically inaccessible colloidal and oxo-polymeric species. This lack of availability is more pronounced in the oceanic environment where the solubility of iron(III) is even lower than in most terrestrial

environments and where the majority of soluble iron is complexed by organic ligands that dominate its speciation. Consequently, iron has been shown to limit microorganisms in large areas of the ocean.

In response to iron limitation, many marine bacteria have been shown to produce siderophores, LMW complexing agents that possess high affinity for Fe(III). Recently, the traditional view of siderophores as sole iron chelators has been challenged by the discovery of their role in the transport of other metals and their interactions with cell-to-cell communication systems in bacteria. Chapters 2 and 3 of this dissertation discuss another unique trait of siderophores: the ability to efficiently bind borate. The high concentration of boron in the ocean (0.4 mM) and the affinity of two major siderophore families, the catecholates and the citrates, to this element suggest a possible unknown biological function. Further proteomic studies are underway to examine the importance of boron to marine bacteria.

Chapter 4 investigates siderophore production of a group of marine bacteria belonging to the *Marinobacter* genus, some of which were isolated from lab cultures of dinoflagellates and coccolithophores, in response to iron limitation. Two algal-associated subclades of *Marinobacter* spp. were found to produce the photoactive siderophore vibrioferrin (VF) while non-algal associated species did not. This correlation between algal association and VF production leads to what appears to be a mutualistic relationship between both organisms where the bacteria contribute iron via the photochemistry of VF and the phytoplankton release dissolved organic matter (DOM) that support the growth of the bacteria and ultimately fuel the biosynthesis of VF. The photochemistry of VF and its influence on iron speciation is further elucidated in chapter 5, where it is shown that ferric-vibrioferrin rapidly degrades in sunlight leaving behind a highly bioavailable form of iron, Fe'.

Because light is central to the photochemistry of VF and consequently to any interactions between VF-producers and phytoplankton, I sought to investigate the influence of light on gene expression of iron uptake genes in *M. algicola* DG893. Chapter 6 reveals a selective response of iron uptake genes related to only the metabolism of VF. In addition, environmental samples collected during a research cruise in the North Atlantic in 2009 demonstrate that VF-producers are concentrated near the surface during daytime. This pattern of vertical distribution demonstrates that although these organisms are not abundant in the ocean, they are relevant to iron biogeochemistry and further work is needed to elucidate the extent of their contribution to iron speciation and to algal iron uptake.

1. Introduction

1.1. Iron as a limiting micronutrient

As the fourth most abundant element in the Earth's crust, iron has become one of the most important transition metals in biology. Attesting to this importance is the involvement of iron in various essential metabolic functions in almost all organisms on earth. Some of these functions include photosynthesis, respiration, oxidative stress, oxygen storage, and nitrogen fixation. However, iron is present under aerobic conditions and at physiological pH only in the form of extremely insoluble minerals like hematite, goethite, and pyrite or as polymeric oxide-hydrates, -carbonates, and -silicates that severely restrict the bioavailability of this metal (*1-3*). The diminished bioavailability of iron is more pronounced in the marine environment as the solubility of various inorganic iron salts is reduced at the higher pH of seawater and because > 99% of soluble iron species in seawater are further complexed by yet uncharacterized organic ligands, L_1 and L_2 (*4, 5*). This has since been corroborated by a number of large-scale iron fertilization experiments in the open ocean, where macronutrients were abundant yet chlorophyll levels remained low (High Nutrient Low Chlorophyll regions; HNLC) (*6-8*). Such a limitation forces most marine microbial organisms to adopt various strategies to acquire this precious element.

1.2. Bacterial iron acquisition: siderophores

In response to iron limitation, whether in higher mammalian hosts, in soil or in the marine environment, a large number of bacteria and some fungi have been shown to produce low-molecular weight organic compounds with exceptionally high affinity for Fe(III) known as *siderophores*. As the greek-derived name suggests, siderophores are iron-bearing compounds that solubilize, chelate and transport iron to microbial cells (*9*). Although siderophores have been shown to strongly bind various other transition metals, their affinity for Fe(III) is often higher (*10*). Several hundred siderophores, whose biosyntheses are repressed by high iron

a

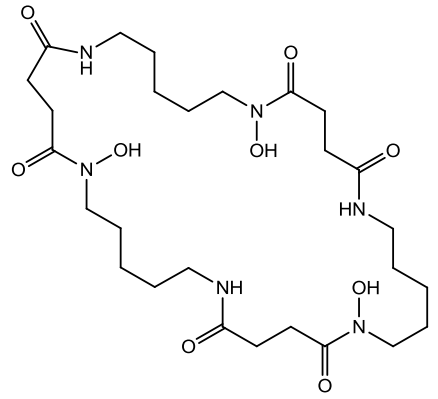

b

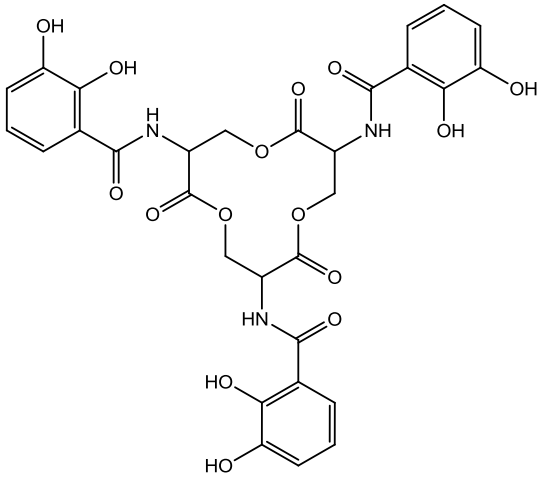

c

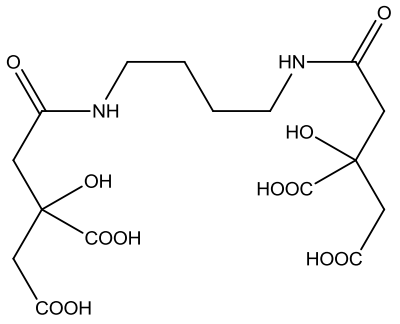

Figure 1.1. Structures of representative siderophores displaying the three common binding groups to iron. (a) the trihydroxamate Desferrioxamine E, (b) the tricatecholate enterobactin, (c) and the dicitrate rhizoferrin.

levels, are known and extensive studies of their isolation, structure, transport and molecular genetics have been undertaken in the last two decades (*11*). The structural variety of siderophores has been comprehensively reviewed (*12, 13*). Siderophores utilize various

chelating groups to complex ferric iron including hydroxamates, catecholates and citrates (Fig. 1.1).

The study of marine siderophores is in its infancy as compared to their terrestrial counterparts and the structures of only a few have been fully elucidated (*13, 14*). Although the characterization of iron complexing ligands in natural seawater has been hampered by the lack of sufficiently sensitive techniques, it has been proposed that siderophores may contribute to the pool of excess organic ligands responsible for complexing most of the soluble iron in seawater (*10, 15*). Research undertaken in the past two decades has focused on trying to construct a view of marine bacterial siderophore production and how it coincides or differs from terrestrial bacterial siderophore production. The stark differences in the physical environments and iron speciation available to marine and terrestrial bacteria are undoubtedly dictating dissimilar genetic siderophore selection to either group that suits each environmental niche. For example, the expected rapid diffusion away from cells of any freely soluble, externally secreted, siderophores necessitates an unusually efficient iron acquisition system for growth of oceanic organisms. This is evident in the large percentage of the characterized marine siderophores that can be classified as amphiphilic suggesting a different iron uptake strategy than that typically found in terrestrial microorganisms (*16-20*). The presence of long and varied lengths of fatty acid chains attached to the hydrophilic head group of the siderophore confers amphiphilic character to such structures (Fig. 1.2). This character causes the siderophore to partition with the hydrophobic cell membrane and thus lessens diffusion into the open ocean (*21*).

Another unusual feature that is almost universally observed in marine siderophores is the common presence of α-hydroxy acid groups in many marine siderophores, which renders their iron complexes photoactive (*22-24*). Sunlight driven photoreduction of the Fe(III) in such siderophores may transiently produce Fe(II) which can be utilized by other organisms. This has been argued for the amphiphilic siderophore aquachelin C, where its conditional stability

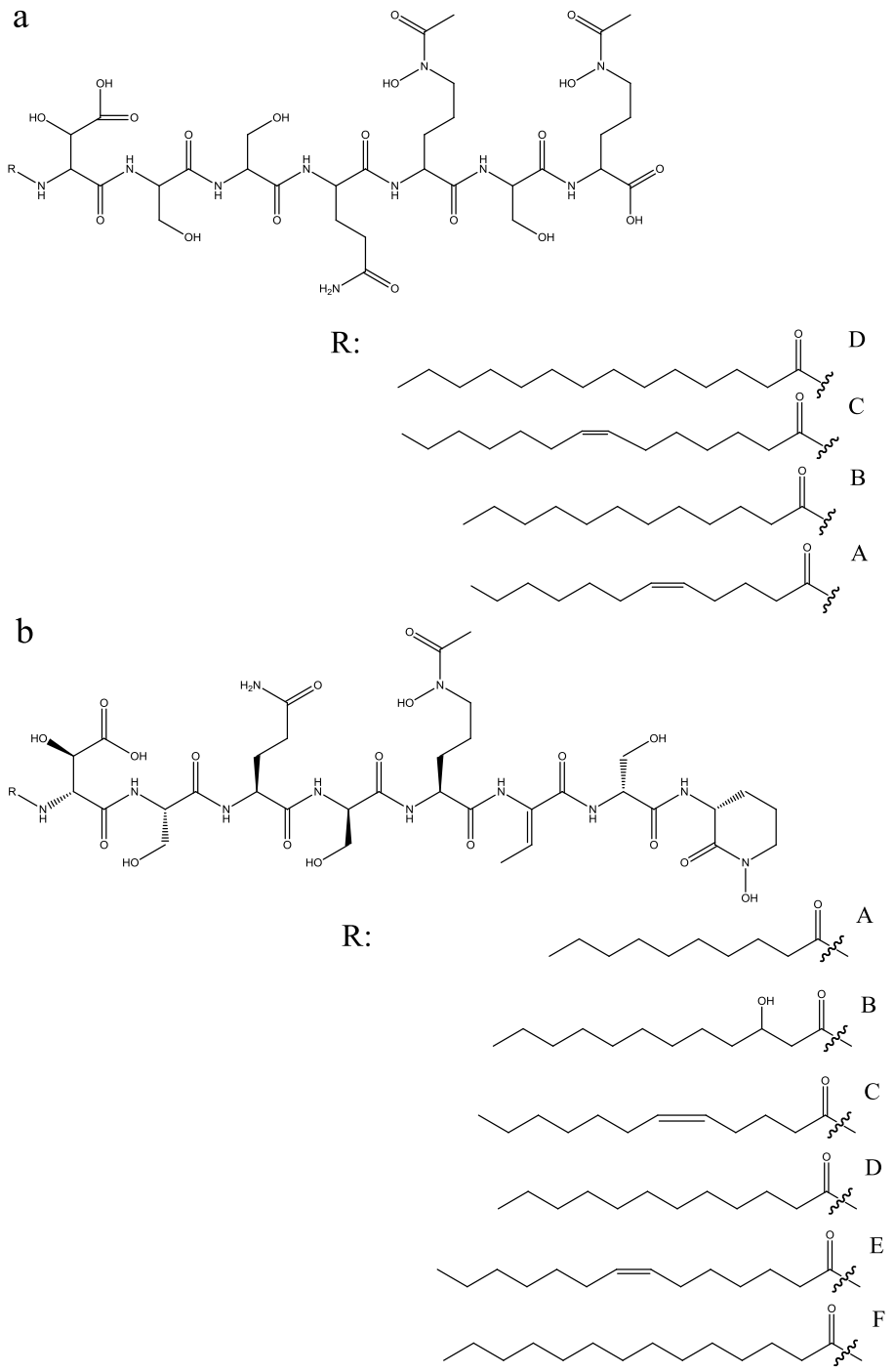

Figure 1.2. Structural examples of marine amphiphilic siderophores: the aquachelins A-D (a) and the loihichelins A-F (b).

constant with respect to soluble inorganic iron (Fe'), $K^{cond}_{FeL,Fe'}$ = $10^{11.5}$ while the stability constant for the parent siderophore is $10^{12.2}$ (Fig. 1.3) (*22*). However, in the other two examples

studied in detail involving aerobactin and petrobactin the photooxidized siderophores remained capable of binding iron surprisingly with more affinity than the parent siderophores (Fig. 1.3). Küpper *et al* reported overall stability constants of $10^{28.6}$ and $10^{27.6}$ for the photooxidized and the parent siderophores respectively (*25*). In addition, Abergel *et al* reported pM values of 24.4 and 23.0 for the photooxidized and the parent siderophores respectively, again contrasting with the aquachelin photochemistry (*26*). This was further corroborated by radioactive iron uptake studies for aerobactin, which showed that the photooxidized siderophore is involved in transporting iron into the cell of the producing organism (*25*). The photolability of marine siderophores and its possible biological and/or physical roles have been comprehensively reviewed yet it is still unclear what impact this characteristic exerts on the oceanic regime (*13, 15*).

1.3. The multiple functions of siderophores

1.3.1. Affinity towards other transition metals. The ability of siderophores to bind a wide variety of metals with high affinity has stirred interest in their use in different medical and environmental applications. Although siderophores form their most stable thermodynamic complexes with ferric iron, this has been contested for one established siderophore, desferrioxamine B (Fig. 1.4a), which has been recently shown to chelate Co(III) better than Fe(III) (*27*). This diversity in metal-chelation has recently suggested that siderophores can indeed act as metallophores under certain physiological conditions. For instance, nitrogen-fixing soil bacterium *Azotobacter vinelandii*, which has been shown to release the siderophores azotochelin and azotobactin in response to iron limitation, uses the same siderophore for molybdenum and vanadium acquisition under diazotrophic conditions (Fig. 1.4b) (*28-30*). In the marine environment the speciation of metals such as Co, Zn, Cd, Cu and Ni are dominated—much like iron—by their complexation to organic ligands in the ocean. In view of such diversity

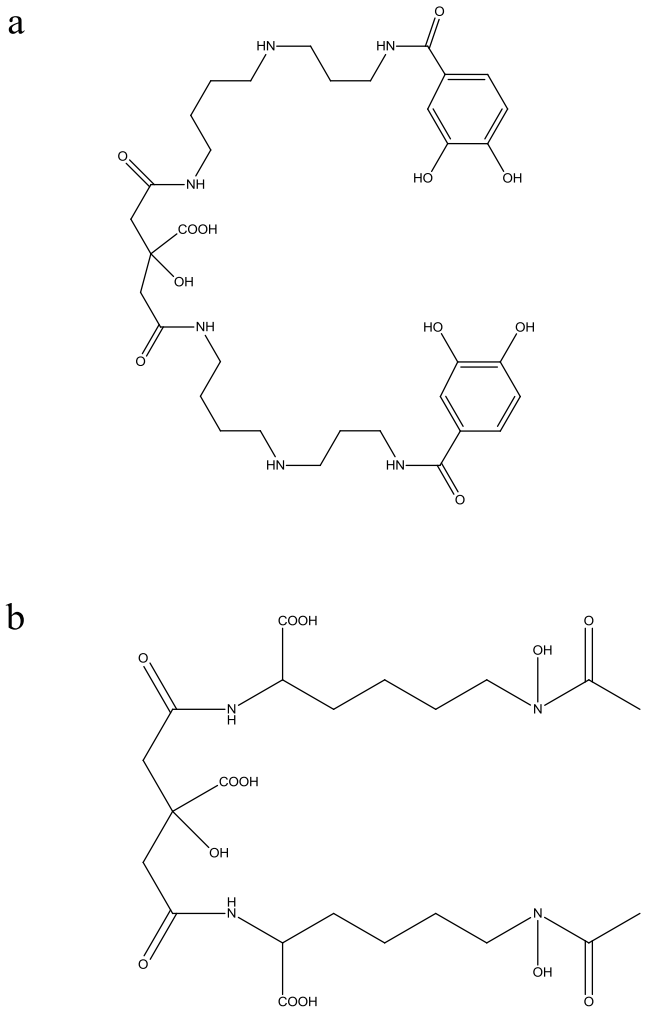

Figure 1.3. Structures of two photolabile marine siderophores: petrobactin (a) and aerobactin (b).

in metal chelation, it might be anticipated that siderophores can influence global metal speciation; however, there is no sufficient evidence to suggest this. Thus, the traditional view of siderophores solely as iron scavengers is slowly changing as more evidence indicates that siderophores perform multiple other functions in bacteria.

1.3.2. Siderophores as signaling molecules. Quorum sensing describes the cell density-dependent regulation of bacterial physiology, including gene expression. Quorum-sensing bacteria excrete low molecular weight chemical messenger molecules, called autoinducers, into

a

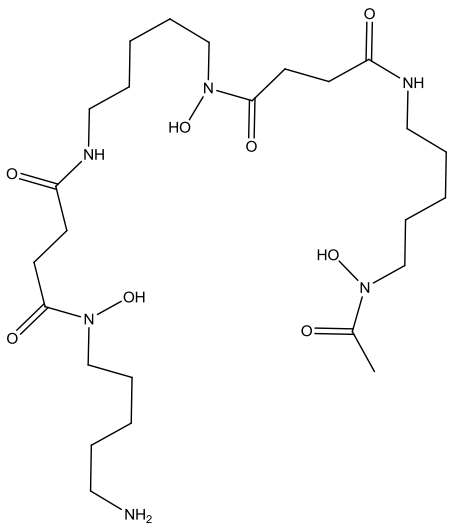

b

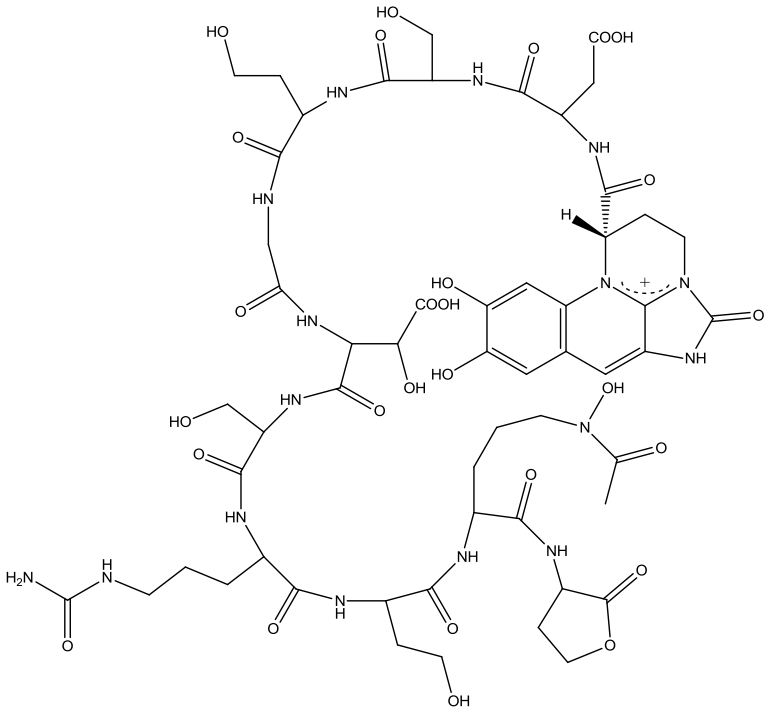

Figure 1.4. Structures of the trishydroxamato siderophore desferrioxamine B (a) and the mixed ligand siderophore azotobactin δ (b).

the environment which, when a critical concentration is reached, trigger a signal transduction cascade. This signal cascade results in the coupling of gene expression to bacterial population (*31*). Siderophore production and other iron transport genes are among those long reported to be

under quorum sensing control (*32, 33*). An additional link between quorum sensing and iron regulation is evident in the ability of some autoinducers to sufficiently bind Fe^{3+} and thus influence siderophore chemistry. Particularly, Diggle *et al* demonstrated the ability of 2-alkyl-3-hydroxy-4-quinolones class of autoinducers to form stable complexes with Fe^{3+}. Since *Pseudomonas aeruginosa*, the producing bacterium, synthesizes its own siderophores, the affinity of these autoinducers to iron might function to entrap the iron closer to the cell surface where siderophores can free the iron from the autoinducers and transport it into the cell (*34*). In addition, a tetramic acid derivative produced by the same bacterium has been reported to possess strong affinity for iron (pM = 25.8) though the authors failed to explain how such a bidentate ligand can bind iron more effectively than a hexadentate ligand such as EDTA (pM = 25.3) (*35*). Of more direct relevance are the numerous recent reports that siderophores themselves can have a cell signaling function in addition to their iron uptake and transport roles. For example, pyoverdine is reported to regulate not only its own production but also that of several other secreted virulence factors in *P. aeruginosa* (*36*). Siderophores produced by one species of marine bacteria have also been reported to induce production of siderophores from a previously nonproducing and unrelated bacterium (*37*).

A role linked to quorum sensing for siderophores might provide a convenient rationale for what has long been an enigma in the area of marine siderophores. Why should free living marine bacteria produce and excrete a metabolically expensive molecule such as a siderophore if there was such a low probability of its recapture and uptake into the cell as would be expected in an open aqueous environment? What however if there was a reasonable chance for recapture and uptake such as when there were a large number of bacteria in a small space such as a biofilm, or close association with another species such as an algae or other microhabitat. It would be reasonable for siderophores to be produced in large amounts only when conditions for successful uptake exist i.e. under a type of quorum sensing control. An alternative view of the

whole quorum sensing concept is that it is actually a diffusion sensing, rather than a direct population sensing, phenomenon (*38*, *39*).

1.3.3. Affinity towards boron. Although not conventionally considered an important biological element, especially with respect to siderophore chemistry and marine heterotrophic bacteria, recent research in this dissertation suggests a more important role for boron than previously known. Thus, a more detailed introduction to boron than provided in subsequent chapters is necessary in order to understand the impact of results presented in this thesis.

Boron was first isolated by Joseph Louis Gay-Lussac, Louis Jacques Thênard, and Humphry Davy in 1808 (*40, 41*). While there has been extensive interest in the use of boron as a surrogate of pH in paleoclimate studies in the context of climate change-related questions, the high concentration in sea water (0.4 mM) and the depth-independent (non-nutrient-like, Fig. 1.5) concentration profile of this element have led to boron being neglected as a potentially biologically relevant element in the ocean. However, recent advances in genomics, trace element detection, biochemistry, and natural products discovery have renewed interest in this previously largely neglected element.

Since the 1920s, boron has been known to be an essential micronutrient for all higher terrestrial plants and many other organisms, but also to be toxic at higher environmental concentrations (*42*, *43*). Thus, the beneficial range of boron appears rather narrow. A large volume of literature has focused on the element from the perspective of terrestrial agriculture (*44*) and established examples of both boron deprivation (*43*) and boron toxicity (*45*). In consequence, both boron-tolerant and boron-efficient cultivars have been developed. In contrast to the generally boron-poor terrestrial environment, the relatively high concentration of boron in the marine environment suggests that boron deficiency is not likely an issue for marine primary productivity despite the fact that it is an essential element for marine algae. However, the potential toxicity of boron coupled with its high concentration in the ocean, suggest the need for

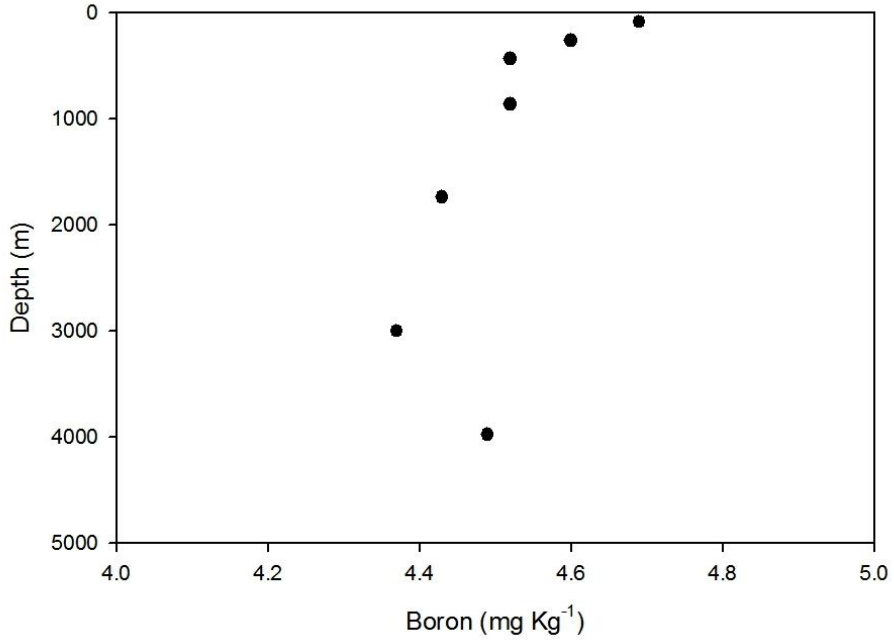

Figure 1.5. Representative depth profile of total dissolved boron concentrations at 18º 22' N, 165º 54' W (based on data from Uppstrom, 1974).

some sort of homeostatic control mechanisms in marine organisms. The control of boron concentrations is a critical issue in the context of seawater desalination (*46*). The remarkable observation that a number of marine natural products contain boron suggests that organisms have not only adapted to the presence of high boron concentrations in their environment but have made use of its abundance for a variety of biological uses.

1.3.3.1. The chemistry of boron. Boron typically exists as trigonal planar BX_3 species given its $2s^2 2p^1$ electronic configuration. However, this electron deficient element often reacts with electron pair donors via its empty p_z orbital to produce formally dative bonded tetrahedral "adducts". Thus, trigonal planar boric acid is the primary soluble form of boron in natural waters. As a very weak acid, with a pK_a of 9.15, boric acid and sodium borates exist predominantly as undissociated boric acid, $B(OH)_3$, in dilute aqueous solution below pH 7. Above pH 10, the tetrahedral metaborate anion, $B(OH)_4^-$,becomes the main species in solution. Consequently, $B(OH)_3$ and $B(OH)_4^-$ have been recognized as the primary boron species in

seawater (*47*). However, boric acid is not formally a proton donor, but rather reacts with a hydroxyl ion from water to form the $B(OH)_4^-$ adduct and releases a proton in the process via the reaction:

$$B(OH)_3 + H_2O \leftrightarrow B(OH)_4^- + H^+$$

At high boron concentrations (> 0.025 M) between pH 6 and pH 11, highly water soluble polyborate ions such as $B_3O_3(OH)_4^{-1}$, $B_4O_5(OH)_4^{-2}$, and $B_5O_6(OH)_4^{-1}$ form, but such concentrations are almost never observed in the environment and hence these species are of little importance biologically.

Although the reaction chemistry of boron can be complex with a myriad of theoretically and technologically important known boron hydrides and carboranes, the only biologically relevant reactions of likely importance in the mildly basic aqueous milieu of seawater are those with nitrogen and oxygen donors. The reactions of boric acid/borate with hydroxyl donors such as alcohols, phenols, diols, polyols, or polysaccharides to produce alkoxides or "boroesters" constitute the most important of these reactions. Indeed, the importance of boron for plants likely derives from the reaction of borate with carbohydrates that promotes the cross-linking and stabilization of the plant cell wall (see below). Both mono and diesters are possible and these are most stable when derived from "chelating" dihydroxy species. The monoesters maintain a trigonal planar configuration with no net charge, while the more important diesters form spirocyclic compounds that are anionic and tetrahedral in geometry.

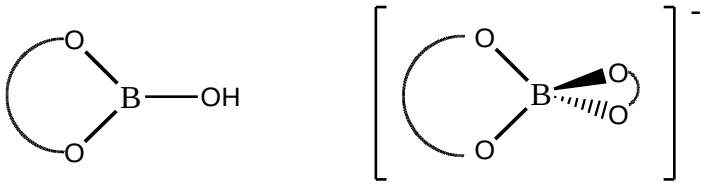

Since water is a product of these "esterifications," decreasing the activity of the solution (i.e. reaction in a less polar environment) will strongly drive the reaction toward the product.

However, even in aqueous solutions, the equilibrium constants of such "esterifications" are often sufficiently large to allow significant product formation (*48*). While 1,3-diols with six-membered chelate ring structures should be preferred on steric grounds to the more ring-strained 1,2-diols with five-membered chelate ring structures, the latter is favored energetically and is the mode most frequently observed (*49*). Also important is the relative pK_a of the reacting alcohol or phenolic species. Typically, the more acidic the alcohol, the lower the pH that significant complexation occurs. At higher pH, competition with hydroxide ion to form borate becomes important.

Considerable controversy has arisen as to whether the reactive boron species in these reactions is boric acid or borate. Initially, since such reactions with alcohols occur primarily at alkaline pH, the reactive boron species was assumed to be the borate species, which predominates at high pH. However, recent work has shown unequivocally that this view is incorrect and that the reactive species even in alkaline pH is in fact boric acid (*49, 50*).

1.3.3.2. Boron as a nutrient for marine algae. While a number of studies report that boron is essential for the growth and development of marine algae, the specific role(s) of the element remain unclear. Boron was recognized as an essential nutrient for terrestrial plants since the 1920s (*43*), whereas symptoms of boron toxicity have been reported for soil concentrations > 1 ppm (*45*).

Pioneering studies in the 1940s and 1950s reported that boron is essential for different groups of algae and cyanobacteria. For example, in the marine red algae *Bangia* and *Porphyra*, boron at seawater concentrations is essential for sustained growth (*51*). The freshwater green alga *Chlorella* has a similar boron requirement for growth (*52*), whereas boron deficiency in the cyanobacterium *Nostoc* leads to chlorosis (*53*). Consequently, boron has been recognized as an important constituent of algal culture media (*54*). Lewin demonstrated the requirement of boron for the growth of marine pennate and centric diatoms (*55-58*), with cell division being much-

reduced at boron concentrations less than 0.5 mg L^{-1} (~0.05 mM; i.e. ~10% natural seawater concentration), and ceasing completely at lower concentrations (*55*). Under boron-deficient conditions, the content of phenolic compounds in the diatom *Cylondrotheca fusiformis* is more than doubled, while the majority of other major cell constituents remain unchanged (*56*). Shortly after these diatom-based studies, the essential role of boron for the development of *Fucus edentatus* Pyl. (Phaeophyceae) was also recognized (*59*): omission of boron from the culture medium resulted in moribund embryos, but normal development could be restored by adding 1-4 μM boron. Gametogenesis in brown algal gametophytes (of the kelps *Laminaria japonica* and *L. angustata* and of the sulfuric acid-producing *Desmarestia ligulata*) is strongly affected by the availability of boron and iron which show partially antagonistic effects, with high boron concentrations acting inhibitory which can be alleviated by Fe^{3+} supplements (*60*). The partially antagonistic interplay between iron and boron is particularly striking in light of the more recent findings that Fe^{3+} and borate compete for binding to microbial siderophores (*61*, *62*), even though no functional link between the two effects has been established yet. Little is known about the boron content of marine algae, and more research is definitely needed regarding this aspect. Öy (as quoted by *63*) published some figures for minor elements in the brown algae *Ascophyllum nodosum, Laminaria* sp., *Fucus serratus* and *Fucus vesiculosus*, with boron concentrations typically in the range of 100 p.p.m. Since this concentration is higher than that of the seawater this implies that there must be some sort of active uptake and homeostatic control mechanism in place in these organisms.

The role of boron in higher plants including boron uptake and molecular aspects of boron transporters has been reviewed recently (*44*), with a major function being the cross-linking of pectins for the maintenance of cell wall integrity (*64*). In general, borate reacts most strongly with sugars that have cis-diols on a furanoid ring as a result of both steric and electronic forces. Therefore, compounds bearing cis-diols on a furanose ring form far stronger

complexes with borate than those on a pyranoid ring such as the more common alpha-D-glucose. This affinity is reflected in the differing equilibrium constants (~ 10^3 for glucose vs. ~10^7 for ribose) (*48*). In fact, only two natural sugars have the strongly boron-binding cis-diol functionality on a furanose ring, ribose and apiose. It was found that the essentiality of boron to higher plants stems from its ability to crosslink cell wall carbohydrates, Therefore, it is not surprising that the first isolated B-polysaccharide was identified as a complex of the peptic polysaccharide rhamnogalacturonan II (RG-II) (*65*). RC-II is notable in that it has the richest known diversity of sugars and linkages. Monomeric RG-II also has four side chains, two of which contain apiose. The apiosyl residues are engaged in B-binding and borate crosslinks between apiofuranosyl residues of two 2-O-methyl-D-xylose side chains resulting in a dimeric complex between two molecules of monomeric RG-II and one borate. The presence of boron crosslinks in marine plants was initially described for the sulfated polysaccharide of the green seaweed *Ulva lactuca* (*66*) and has been confirmed for red, green, and brown macroalgae by ^{11}B NMR analysis (*67*). Even though it is tempting to speculate that boron may play a key role for the cell wall integrity of marine algae, substantial further research clearly is needed for a better understanding of the biological significance of the boron requirement by marine algae.

1.3.3.3. Boron transport and regulation. A broad systematic understanding of boron uptake mechanisms is lacking for animals, though uptake is known to occur across mucous membranes of the gastrointestinal and respiratory systems. In contrast, higher plants are fairly well studied with regards to boron uptake (*44*). Boric acid is an uncharged and undissociated molecule over much of the physiological pH range and is therefore considered to be the species taken up (*68*). Boron uptake was largely assumed to occur through passive diffusion, but recent studies over the last decade have shown that uptake occurs as an active process mediated by active BOR transporters or facilitated by nodulin-like intrinsic proteins (NIPs). BOR1, a member of the SLC4 anion-exchanger superfamily (*69*) which also includes

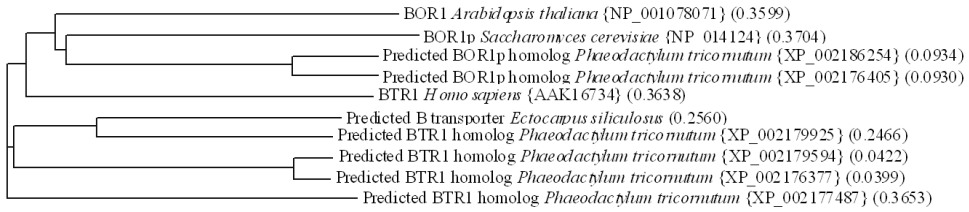

Figure 1.6. Phylogenetic analysis of putative bicarbonate/borate transporters sequences. Tree generation was done using VectorNTI (Invitrogen) based on three known borate transporters (BOR1, BOR1p, and BTR1). Nucleotide database accession numbers are provided in brackets and distances are in parentheses.

bicarbonate transporters, was identified as the first transport protein involved in active xylem loading in the higher plant model *Arabidopsis* (*70*). Shortly afterwards, the same group found a member of the major intrinsic proteins (MIPs), namely NIP5;1, to be essential for boron uptake and plant development under boron limitation (*71*).

Homologs, clustering in the same clade with BOR1, the yeast protein YNL275w (BOR1p) and the BTR1 protein of humans, are found in the genomes of the diatoms *Thalassiosira pseudonana*, *Phaeodactylum tricornutum*, and the brown seaweed *Ectocarpus siliculosus*. This observation suggests that boron transport and regulation is widespread among marine plants. However because of the similarities between the purported borate transporters and their bicarbonate analogs, detailed biochemical studies will be needed to confirm the physiological function/substrates of these gene products.

1.3.3.4. Boron-containing natural products from marine prokaryotes. Considering the abundance of boron in the Earth's crust and ocean, it is surprising how few boron-containing natural products are known – however, it is similarly striking that only one of them is of terrestrial origin with all others coming from marine microorganisms. All boron natural products known to date are prokaryotic metabolites. An obvious, intriguing question for further research is whether eukaryotes use boron in a similar manner in their metabolism and whether they produce any boron-containing natural products.

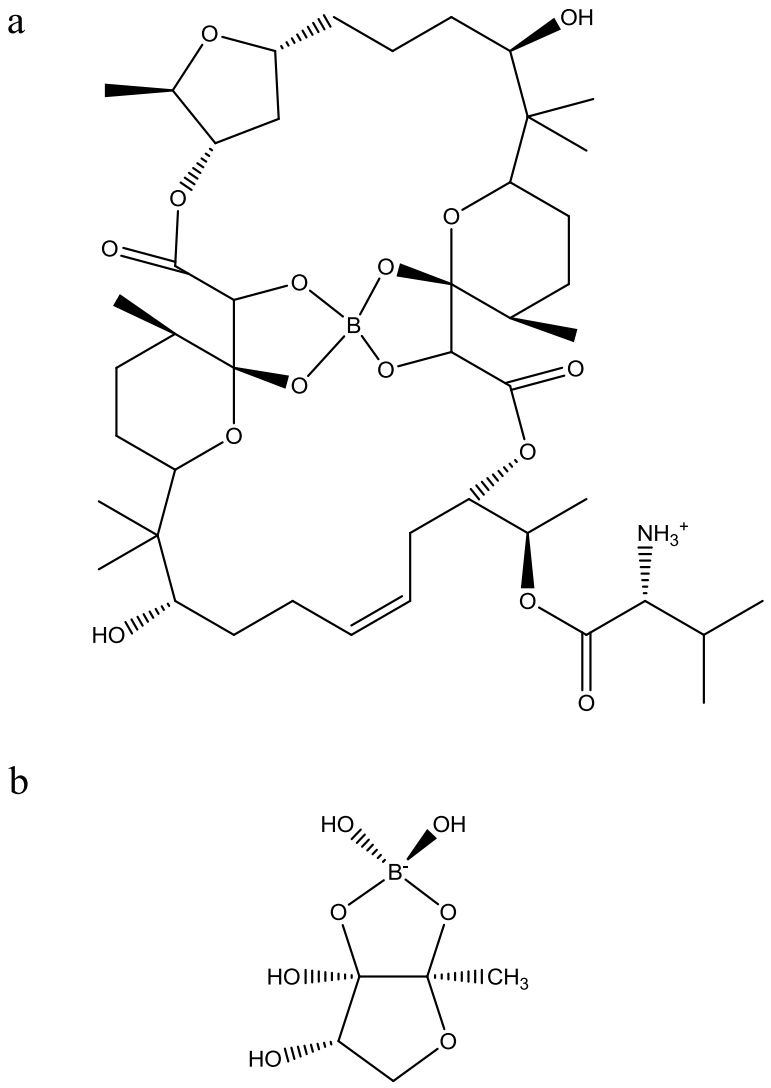

Figure 1.7. Boron-containing natural products: The streptomycete-derived antibiotic boromycin (a) and the quorum sensing autoinducer AI-2 (b).

The first identified boron-containing natural product was boromycin (Fig. 1.7a) (*72-74*), which was isolated from a culture of *Streptomyces antibioticus* ETH 28 829 that originated from a terrestrial soil sample from the Ivory Coast. The second boron natural product, the macrodiolide antibiotic aplasmomycin, was found in the related, but marine *Streptomyces griseus* (*75*).

The next high-profile natural product was the quorum-sensing molecule autoinducer-2 (AI-2), which was first isolated from the bioluminescent marine bacterium *Vibrio harveyi* (Fig.

1.7b) (*76*). In fact, its production by a range of other bacteria is remarkable and AI-2 has been postulated to function in inter-species communication (*77*). However, recently it was discovered that the active form of AI-2 found in terrestrial bacteria such as *S. typhimurium* does not contain boron but rather it is simply the furanose sugar itself. This finding was confirmed by the crystal structures of the two molecules bound to their respective receptors, which shows unequivocally that boron is bound to the AI-2 of marine bacteria but not to the AI-2 of terrestrial bacteria (*78*). This is a powerful example of how marine organisms have had to adapt to the high concentrations of boron in their environment or vice versa.

Findings in several disciplines suggest that boron, an abundant element in the ocean, is involved in a range of aspects of marine life and it is considered an essential trace element. While all boron-containing and boron-binding low-molecular weight metabolites are of prokaryotic origin, boron also plays an important role in stabilizing plant and algal cell walls by crosslinking carbohydrates. The molecular biology of boron transporters in different branches of the tree of life is beginning to emerge, but the knowledge remains far from phylogenetically representative at the current time. Studies in biological oceanography investigating the correlation of boron with phytoplankton abundance (in particular, whether boron in seawater is drawn down in algal blooms) would appear very timely. Also, the potential occurrence of low molecular-weight, boron-containing compounds in eukaryotes and much of the other remaining physiological roles of this element remain largely enigmatic at this stage and require significant, further research effort.

1.4. Algal iron acquisition

Despite the obligate requirement of iron for algal growth since it is a major component of the photosynthetic machinery, the nature of the iron species bioavailable for phytoplanktonic algal communities and its actual uptake mechanism(s) are still largely unknown. In terrestrial

plants, two basic strategies for iron uptake have been distinguished, with strategy I plants (mainly *dicotyledons*) using a mechanism involving soil acidification, lateral root formation, specific transfer cells in the rhizodermis as well as induction of an Fe(III)-chelate reductase and of transporter proteins Fe(II), transferring Fe(II) into the cells (*79, 80*). In contrast, strategy II plants (in particular, *monocotyledons*) assimilate Fe as a phytosiderophore complex.

Phytoplankton for the most part do not produce their own siderophores and their ability to directly take up bacterially derived Fe(III)-siderophore complexes has not been established. A number of studies claim that some species of phytoplankton, mostly dinoflagellates, produce detectable amounts of siderophores in solution; however, the lack of axenic culture techniques may have led to the detection of bacterial and not algal siderophore production as such results were never reproduced (*81, 82*). Some flagellates have been reported to acquire iron from particulate matter by ingesting whole bacterial cells (*83*). Iron storage proteins have been shown to provide sufficient concentrations of accessible iron to support the growth of several cyanobacterial, diatom, and coccolithophore cultures (*84*). Other studies have examined the ability of phytoplankton (most frequently diatoms), to utilize iron from exogenous Fe(III)-siderophore complexes (*85*). Iron bound to ferrioxamines B and E particularly have been shown to be preferred by *Phaeodactylum tricornutum* over soluble inorganic iron (*86*). Interestingly, it has been shown that exogenous additions of desferrioxamine B can induce iron limitation conditions in phytoplankton (*87*). In addition, Hutchins *et al* have shown that different groups of phytoplankton can tap different pools of organically complexed iron, with cyanobacteria being able to take up iron bound to various siderophores, but not porphyrin-bound iron. In contrast, diatoms show a preference for porphyrin-bound rather than siderophore-bound iron. This study suggests that cyanobacteria operate an iron uptake mechanism based on specific cell-surface receptors similar to heterotrophic bacteria, whereas diatoms are considered to use a non-specific, ferrireductase-like enzyme on the cell surface. (*88*). However, the relevance of such

studies is questionable since no evidence exists regarding the ecological availability of these particular microbial siderophores to marine phytoplankton in the natural environment (*89*). Recent advances in analytical techniques allowed the detection of natural siderophores in the North Atlantic, which has shown the availability of ferrioxamines E and G to be significant in the euphotic zone (*90*).

Most of the research on algal iron acquisition focused on direct algal uptake strategies via specific or non-specific transporters in diatoms. Although Fe(III) is more predominant in the ocean, research over the past 40 years has focused on clarifying the form of assimilated iron by diatom cells (*91-93*). It has been shown via radioisotope labeling and recently by genomic evidence that Fe(II) is the assimilated substrate while most of the Fe(III) available to algal cells is reduced via cell-surface reductase before being internalized (*94*, *95*). A study in the unicellular green alga *Chlamydomonas* shows the involvement of a Fe(III)-chelate reductase, similar to strategy I higher plants (*96*). Other common mechanisms of Fe(II) generation include photochemical reduction of organic ligands by sunlight and superoxide-mediated reduction of organically bound iron(*97-99*).

1.5. Phytoplankton blooms and associated bacterial siderophore production

Phytoplankton blooms, sometimes including toxic species such as the diatom genus *Pseudo-nitzschia* or the dinoflagellates *Gymnodinium catenatum* or *Alexandrium tamarense* are a frequent phenomenon in coastal and upwelling parts of the world's oceans. These blooms often have immediate acute effects on marine populations and their impact on public health and local economies is large and has been increasing (*100*). Through the last decade a relatively comprehensive catalogue of the microbial diversity of coastal and open-ocean regions has been achieved (*101*). Yet, how this biodiversity and its interactions therein structure the marine ecosystem is now a question of prime importance (*102*). The consequences of interactions

between heterotrophic bacterial activity and phytoplankton or harmful algal bloom (HAB) species within the backdrop of global climate change may have profound and unforeseen effects on global primary productivity and economics as well as ecosystem modification through the increased frequency of HAB events in coastal regions.

Bell & Mitchell first introduced the concept of the "phycosphere" to describe the zone around phytoplankton, under which influence, microbial activity is altered as compared to that of the surrounding seawater (*103*). Phytoplankton enrich this zone through active excretion of photosynthetically fixed carbon compounds which in turn attracts and maintains a specific microflora (*104*). This microflora may rapidly metabolize the excreted extracellular material, thus enriching the zone around the algal cell, and thereby potentially enhancing carbon fixation (*105*). Despite this work having been started over three decades ago, we still know very little about how the bacterial diversity directly functions within this zone.

The conventional view is that heterotrophic bacteria are consumers of primary production, and that the interactions between phytoplankton and heterotrophic bacteria are indirect. However, as recently noted, there is no *a priori* reason to exclude the possibility of direct interactions between heterotrophic bacteria and phytoplankton (*101*). There is a growing body of evidence to suggest that there are indeed direct interactions at the microscale between phytoplankton and heterotrophic bacteria, and that these interactions are likely to be quantitatively significant in terms of bacterial coupling to primary production (*106*). Bacteria have been observed to cluster around phytoplankton cells (*104*) and even to closely track motile algae (*107*). Some phytoplankton-bacteria associations appear to be species-specific (*108, 109*). The increasing incidence of harmful algal blooms (HABs) has sparked interest in the bacteria associated with toxic dinoflagellates (*110*). Recently, Green *et al* have identified a number of bacteria that can stimulate the growth of toxic and non-toxic dinoflagellates (*111, 112*). Various studies have discovered algicidal bacteria that kill marine microalgae (*113, 114*). Recently, it

was shown that some bacteria produce vitamin B_{12} in the presence of phytoplankton cells (*115*). Stimulation of axenic diatom growth by heterotrophic bacteria has also been reported (*116*) and an algal morphogenesis inducer of *Monostroma oxyspermum* has been found among the extracellular metabolites produced by an epiphytic bacterium strain (*117*).

1.6. Conclusion

While the uptake of iron-siderophore complexes by the bacterial strains producing these metal scavengers is well established, it is unclear to what extent other organisms of the plankton community can tap the pool of iron bound to microbial chelators. In particular it has not been investigated at all the extent of which a eukaryotic alga can make use of iron bound to the siderophores from *symbiotic bacteria.* The hypothesis that symbiotic or mutualistic bacteria can regulate the supply of iron to phytoplankton, including a bloom episode, is a very intriguing proposition, particularly with respect to identifying predictive model that enable forecasting of harmful algal blooms (HABs).

1.7. Acknowledgement

Parts of this chapter were published as: Carrano, C. J.; Schellenberg, S.; Amin, S. A.; Green, D. H.; Küpper, F. C. Boron and Marine Life: A New Look at an Enigmatic Bioelement. *Mar. Biotechnol.* **2009,** *11* (4), 431-440.

1.8. References

1. Wu, J., and Luther III, G. W. (1994) Size-fractionated iron concentrations in the water column of the western North Atlantic ocean, *Limnol. Oceanogr. 39*, 1119-1129.

2. Bruland, K. W., Donat, J. R., and Hutchins, D. A. (1991) Interactive influences of bioactive trace metals on biological production in oceanic waters, *Limnol. Oceanogr. 36*, 1555-1577.

3. Martin, J. H., and Fitzwater, S. E. (1988) Iron deficiency limits phytoplankton growth in the north-east Pacific subarctic, *Nature 331*, 341-343.

4. Wu, J., and Luther, G. W. (1995) Complexation of Fe(III) by natural organic ligands in the Northwest Atlantic Ocean by a competitive ligand equilibration method and a kinetic approach, *Mar. Chem. 50*, 159-177.

5. Rue, E. L., and Bruland, K. W. (1995) Complexation of iron(III) by natural organic ligands in the Central North Pacific as determined by a new competitive ligand equilibration/adsorptive cathodic stripping voltammetric method, *Mar. Chem. 50*, 117-138.

6. Boyd, P. W., Watson, A. J., Law, C. S., Abraham, E. R., Trull, T., Murdoch, R., Bakker, D. C. E., Bowie, A. R., Buesseler, K. O., Chang, H., Charette, M., Croot, P., Downing, K., Frew, R., Gall, M., Hadfield, M., Hall, J., Harvey, M., Jameson, G., LaRoche, J., Liddicoat, M., Ling, R., Maldonado, M. T., McKay, R. M., Nodder, S., Pickmere, S., Pridmore, R., Rintoul, S., Safi, K., Sutton, P., Strzepek, R., Tanneberger, K., Turner, S., Waite, A., and Zeldis, J. (2000) A mesoscale phytoplankton bloom in the polar Southern Ocean stimulated by iron fertilization, *Nature 407*, 695-702.

7. Martin, J. H., Coale, K. H., Johnson, K. S., Fitzwater, S. E., Gordon, R. M., Tanner, S. J., Hunter, C. N., Elrod, V. A., Nowicki, J. L., Coley, T. L., Barber, R. T., Lindley, S., Watson, A. J., Van Scoy, K., Law, C. S., Liddicoat, M. I., Ling, R., Stanton, T., Stockel, J., Collins, C., Anderson, A., Bidigare, R., Ondrusek, M., Latasa, M., Millero, F. J., Lee, K., Yao, W., Zhang, J. Z., Friederich, G., Sakamoto, C., Chavez, F., Buck, K., Kolber, Z., Greene, R., Falkowski, P., Chisholm, S. W., Hoge, F., Swift, R., Yungel, J., Turner, S., Nightingale, P., Hatton, A., Liss, P., and Tindale, N. W. (1994) Testing the iron hypothesis in ecosystems of the equatorial Pacific Ocean, *Nature 371*, 123-129.

8. Coale, K. H., Johnson, K. S., Fitzwater, S. E., Gordon, R. M., Tanner, S., Chavez, F. P., Ferioli, L., Sakamoto, C., Rogers, P., Millero, F., Steinberg, P., Nightingale, P., Cooper, D., Cochlan, W. P., Landry, M. R., Constantinou, J., Rollwagen, G., Trasvina, A., and Kudela, R. (1996) A massive phytoplankton bloom induced by an ecosystem-scale iron fertilization experiment in the equatorial Pacific Ocean, *Nature 383*, 495-501.

9. Winkelmann, G. (1991) *CRC handbook of microbial iron chelates*, CRC Press, Boca Raton.

10. Vraspir, J. M., and Butler, A. (2009) Chemistry of marine ligands and siderophores, *Annu. Rev. Mar. Sci. 1*, 43-63.

11. Winkelmann, G., and Carrano, C. J. (1997) *Transition metals in microbial metabolism*, Harwood Academic Publishers, Amsterdam.

12. Raymond, K. N. (1994) Recognition and transport of natural and synthetic siderophores by microbes, *Pure Appl. Chem. 66*, 773-781.

13. Sandy, M., and Butler, A. (2009) Microbial iron acquisition: marine and terrestrial siderophores, *Chem. Rev. 109*, 4580-4595.

14. Butler, A. (2005) Marine siderophores and microbial iron mobilization, *BioMetals 18*, 369-374.

15. Barbeau, K. (2006) Photochemistry of organic iron(III) complexing ligands in oceanic systems, *Photochem. Photobiol. 82*, 1505-1516.

16. Martin, J., Ito, Y., Homann, V., Haygood, M., and Butler, A. (2006) Structure and membrane affinity of new amphiphilic siderophores produced by *Ochrobactrum* sp. SP18, *J. Biol. Inorg. Chem. 11*, 633-641.

17. Martinez, J. S., Carter-Franklin, J. N., Mann, E. L., Martin, J. D., Haygood, M. G., and Butler, A. (2003) Structure and membrane affinity of a suite of amphiphilic siderophores produced by a marine bacterium, *Proc. Natl. Acad. Sci. U. S. A. 100*, 3754-3759.

18. Xu, G., Martinez, J. S., Groves, J. T., and Butler, A. (2002) Membrane affinity of the amphiphilic marinobactin siderophores, *J. Am. Chem. Soc. 124*, 13408-13415.

19. Martinez, J. S., Zhang, G. P., Holt, P. D., Jung, H. T., Carrano, C. J., Haygood, M. G., and Butler, A. (2000) Self-assembling amphiphilic siderophores from marine bacteria, *Science 287*, 1245-1247.

20. Homann, V. V., Sandy, M., Tincu, J. A., Templeton, A. S., Tebo, B. M., and Butler, A. (2009) Loihichelins A−F, a suite of amphiphilic siderophores produced by the marine bacterium *Halomonas* LOB-5, *J. Nat. Prod. 72*, 884-888.

21. Martinez, J. S., and Butler, A. (2007) Marine amphiphilic siderophores: marinobactin structure, uptake, and microbial partitioning, *J. Inorg. Biochem. 101*, 1692-1698.

22. Barbeau, K., Rue, E. L., Bruland, K. W., and Butler, A. (2001) Photochemical cycling of iron in the surface ocean mediated by microbial iron(III)-binding ligands, *Nature 413*, 409-413.

23. Barbeau, K., Zhang, G., Live, D. H., and Butler, A. (2002) Petrobactin, a photoreactive siderophore produced by the oil-degrading marine bacterium *Marinobacter hydrocarbonoclasticus*, *J. Am. Chem. Soc. 124*, 378-379.

24. Barbeau, K., Rue, E. L., Trick, C. G., Bruland, K. W., and Butler, A. (2003) Photochemical reactivity of siderophores produced by marine heterotrophic bacteria

and cyanobacteria based on characteristic Fe(III) binding groups, *Limnol. Oceanogr. 48*, 1069-1078.

25. Küpper, F. C., Carrano, C. J., Kuhn, J.-U., and Butler, A. (2006) Photoreactivity of iron(III)-aerobactin: photoproduct structure and iron(III) coordination, *Inorg. Chem. 45*, 6028-6033.

26. Abergel, R. J., Zawadzka, A. M., and Raymond, K. N. (2008) Petrobactin-mediated iron transport in pathogenic bacteria: coordination chemistry of an unusual 3,4-catecholate/citrate siderophore, *J. Am. Chem. Soc. 130*, 2124-2125.

27. Duckworth, O. W., Bargar, J. R., Jarzecki, A. A., Oyerinde, O., Spiro, T. G., and Sposito, G. (2009) The exceptionally stable cobalt(III)-desferrioxamine B complex, *Mar. Chem. 113*, 114-122.

28. Wichard, T., Bellenger, J.-P., Morel, F. o. M. M., and Kraepiel, A. M. L. (2009) Role of the siderophore azotobactin in the bacterial acquisition of nitrogenase metal cofactors, *Environ. Sci. Technol. 43*, 7218-7224.

29. Bellenger, J. P., Wichard, T., Kustka, A. B., and Kraepiel, A. M. L. (2008) Uptake of molybdenum and vanadium by a nitrogen-fixing soil bacterium using siderophores, *Nat. Geosci. 1*, 243-246.

30. Bellenger, J.-P., Arnaud-Neu, F., Asfari, Z., Myneni, S., Stiefel, E., and Kraepiel, A. (2007) Complexation of oxoanions and cationic metals by the biscatecholate siderophore azotochelin, *J. Biol. Inorg. Chem. 12*, 367-376.

31. Reading, N. C., and Sperandio, V. (2006) Quorum sensing: the many languages of bacteria, *FEMS Microbiol. Lett. 254*, 1-11.

32. Fong, K. P., Gao, L., and Demuth, D. R. (2003) *luxS* and *arcB* control aerobic growth of *Actinobacillus actinomycetemcomitans* under iron limitation, *Infect. Immun. 71*, 298-308.

33. Guan, L. L., and Kamino, K. (2001) Bacterial response to siderophore and quorum-sensing chemical signals in the seawater microbial community, *BMC Microbiol. 1*, 27.

34. Diggle, S. P., Matthijs, S., Wright, V. J., Fletcher, M. P., Chhabra, S. R., Lamont, I. L., Kong, X., Hider, R. C., Cornelis, P., Camara, M., and Williams, P. (2007) The *Pseudomonas aeruginosa* 4-quinolone signal molecules HHQ and PQS play multifunctional roles in quorum sensing and iron entrapment, *Chemistry & Biology 14*, 87-96.

35. Kaufmann, G. F., Sartorio, R., Lee, S.-H., Rogers, C. J., Meijler, M. M., Moss, J. A., Clapham, B., Brogan, A. P., Dickerson, T. J., and Janda, K. D. (2005) Revisiting quorum sensing: Discovery of additional chemical and biological functions for 3-oxo-N-acylhomoserine lactones, *Proc. Natl. Acad. Sci. U. S. A. 102*, 309-314.

36. Lamont, I. L., Beare, P. A., Ochsner, U., Vasil, A. I., and Vasil, M. L. (2002) Siderophore-mediated signaling regulates virulence factor production in *Pseudomonas aeruginosa*, *Proc. Natl. Acad. Sci. U. S. A. 99*, 7072-7077.

37. Guan, L. L., Kanoh, K., and Kamino, K. (2001) Effect of exogenous siderophores on iron uptake activity of marine bacteria under iron-limited conditions, *Appl. Environ. Microbiol. 67*, 1710-1717.

38. Hense, B. A., Kuttler, C., Muller, J., Rothballer, M., Hartmann, A., and Kreft, J.-U. (2007) Does efficiency sensing unify diffusion and quorum sensing?, *Nat. Rev. Microbiol. 5*, 230-239.

39. Redfield, R. J. (2002) Is quorum sensing a side effect of diffusion sensing?, *Trends Microbiol. 10*, 365-370.

40. Davy, H. (1808) Electro-chemical researches, on the decomposition of the earths with observations on the metals obtained from the alkaline rarths; and on the amalgam procured from ammonia, *Philos. Trans. R. Soc. London 98*, 333-370.

41. Gay-Lusac, J. L., and Thenard, L. J. (1808) Sur la décomposition et la recomposition de l'acide boracique, *Annales de Chimie et de Physique [Series 1] 68*, 167-174.

42. Goldbach, H. E., Rerkasem, B., Wimmer, M. A., Brown, P. H., Thellier, M., and Bell, R. W. (2001) *Boron in Plant and Animal Nutrition*, Kluwer Academic/Plenum Publishers, New York.

43. Warington, K. (1923) The effect of boric acid and borax on the broad bean and certain other plants, *Annals of Botany 27*, 629-672.

44. Tanaka, M., and Fujiwara, T. (2008) Physiological roles and transport mechanisms of boron: perspectives from plants, *Pflügers Archiv - European Journal of Physiology 456*, 671–677.

45. Yau, S. K., Nachit, M. M., Hamblin, J., and Ryan, J. (1995) Phenotypic variation in boron-toxicity tolerance at seedling stage in durum wheat (*Triticum durum*), *Euphytica 83*, 185–191.

46. Öztürk, N., Kavak, D., and Köse, T. E. (2008) Boron removal from aqueous solution by reverse osmosis, *Desalination 223*, 1-9.

47. Sverdrup, H. U., Johnson, M. W., and Fleming, R. H. (1942) *The Oceans. Their physics, chemistry and general biology.*, Prentice-Hall, New York.

48. Hunt, C. D. (2001) In *Boron in Plant and Animal Nutrition* (Goldbach, H. E., Rerkasem, B., Wimmer, M. A., Brown, P. H., Thellier, M., and Bell, R. W., Eds.), Kluwer Academic/Plenum Publishers, New York.

49. Rietjens, M., and Steenbergen, P. A. (2005) Crosslinking Mechanism of Boric Acid with Diols Revisited, *Eur. J. Inorg. Chem. 2005*, 1162-1174.

50. Bishop, M., Shahid, N., Yang, J. Z., and Barron, A. R. (2004) Determination of the mode and efficacy of the cross-linking of guar by borate using MAS B-11 NMR of borate cross-linked guar in combination with solution B-11 NMR of model systems, *Dalton Trans.*, 2621-2634.

51. Henkel, R. (1952) Ernährungsphysiologische Untersuchungen an Meeresalgen, insbesondere an *Bangia pumila*, *Kieler Meeresforschungen 8*, 192-211.

52. McIlrath, W. J., and Skok, J. (1958) Boron requirement of *Chlorella vulgaris*, *Botanical Gazette 119*, 231-233.

53. Eyster, C. (1952) Necessity of boron for *Nostoc muscorum*, *Nature 170*, 755.

54. Spector, W. S. e. (1956) *Handbook of Biological Data*, W.B. Saunders Co., Philadelphia, PA.

55. Lewin, J. (1966) Boron as a growth requirement for diatoms, *J. Phycol. 2*, 160-163.

56. Lewin, J., and Chen, C. (1976) Effects of boron deficiency on the chemical composition of a marie diatom., *J. Exp. Bot. 27*, 916-921.

57. Lewin, J. C. (1965) The boron requirement of a marine diatom, *Naturwissenschaften 52*, 70.

58. Lewin, J. C. (1966) Physiological studies of the boron requirement of the diatom, *Cylindrotheca fusiformis* Reimann and Lewin, *J. Exp. Bot. 17*, 473-479.

59. McLachlan, J. (1977) Effects of Nutrients on Growth and Development of Embryos of Fucus-Edentatus-Pyl (Phaeophyceae, Fucales), *Phycologia 16*, 329-338.

60. Motomura, T., and Sakai, Y. (1984) Regulation of gametogenesis of *Laminaria* and *Desmarestia* (Phaeophyta) by iron and boron, *Jap. J. Phycol. (Sorui) 32*, 209-215.

61. Amin, S. A., Küpper, F. C., Green, D. H., Harris, W. R., and Carrano, C. J. (2007) Boron binding by a siderophore isolated from marine bacteria associated with the toxic dinoflagellate *Gymnodinium catenatum*, *J. Am. Chem. Soc. 129*, 478-479.

62. Harris, W. R., Amin, S. A., Küpper, F. C., Green, D. H., and Carrano, C. J. (2007) Borate binding to siderophores: structure and stability, *J. Am. Chem. Soc. 129*, 12263-12271.

63. Black, W. A. P., and Mitchell, R. L. (1952) Trace elements in the common brown algae and in sea water, *Journal of the Marine Biological Association of the United Kingdom 30*, 575-584.

64. Kobayashi, M., Matoh, T., and Azuma, J. (1996) Two chains of rhamnogalacturonan II are cross-linked by borate-diol ester bonds in higher plant cell walls. , *Plant Physiol. 110*, 1017-1020.

65. Matoh, T., and Kobayashi, M. (2001) In *Boron in Plant and Animal Nutrition* (Goldbach, H. E., Rerkasem, B., Wimmer, M. A., Brown, P. H., Thellier, M., and Bell, R. W., Eds.), Kluwer Academic/Plenum Publishers, New York.

66. Haug, A. (1976) The influence of borate and calcium on the gel formation of a sulfated polysaccharide from *Ulva lactuca*, *Acta Chemica Scandinavica B 30*, 562-566.

67. Chuda, Y., Ohnishi-Kameyama, M., and Nagata, T. (1997) Identification of the forms of boron in seaweed by ^{11}B NMR, *Phytochemistry 46*, 209-213.

68. Raven, J. A. (1980) Short- and long-distance transport of boric acid in plants. , *New Phytologist 84*, 231-249.

69. Frommer, W. B., and von Wiren, N. (2002) Plant biology: Ping-pong with boron, *Nature 420*, 282-283.

70. Takano, J., Noguchi, K., Yasumori, M., Kobayashi, M., Gajdos, Z., Miwa, K., Hayashi, H., Yoneyama, T., and Fujiwara, T. (2002) *Arabidopsis* boron transporter for xylem loading, *Nature 420*, 337-340.

71. Takano, J., Wada, M., Ludewig, U., Schaaf, G., von Wiren, N., and Fujiwara, T. (2006) The *Arabidopsis* major intrinsic protein NIP5;1 is essential for efficient boron uptake and plant development under boron limitation., *Plant Cell 18*, 1498-1509.

72. Marsh, W., Dunitz, J. D., and White, D. N. J. (1974) Structure of a boron-free hydrolysis product from boromycin, *Helvetica Chimica Acta 57*, 10-17.

73. Dunitz, J. D., Hawley, D. M., Miklos, D., White, D. N. J., Berlin, Y., Marusic, R., and Prelog, V. (1971) Metabolic products of microorganisms. 95. Structure of boromycin, *Helvetica Chimica Acta 54*, 1709-&.

74. Hütter, R., Keller-Schierlein, W., Knüsel, F., Prelog, V., Rodgers Jr., G. C., Suter, P., Vogel, G., Voser, W., and Zähner, H. (1967) 159. Stoffwechselprodukte von Mikroorganismen. 57. Boromycin, *Helvetica Chimica Acta 50*, 158-159.

75. Okami, Y., Okazaki, T., Kitahara, T., and Umezawa, H. (1976) Studies on marine microorganisms. 5. New antibiotic, aplasmomycin, produced by a streptomycete isolated from shallow sea mud, *Journal of Antibiotics 29*, 1019-1025.

76. Chen, X., Schauder, S., Potier, N., Van Dorsselaer, A., Pelczer, I., Bassler, B. L., and Hughson, F. M. (2002) Structural identification of a bacterial quorum-sensing signal containing boron, *Nature 415*, 545-549.

77. Miller, M. B., and Bassler, B. L. (2001) Quorum sensing in bacteria, *Annual Review of Microbiology 55*, 165-199.

78. Miller, S. T., Xavier, K. B., Campagna, S. R., Taga, M. E., Semmelhack, M. F., Bassler, B. L., and Hughson, F. M. (2004) *Salmonella typhimurium* recognizes a chemically distinct form of the bacterial quorum-sensing signal Al-2, *Molecular Cell 15*, 677-687.

79. Moog, P. R., and Bruggemann, W. (1994) Iron Reductase Systems on the Plant Plasma-Membrane - a Review, *Plant and Soil 165*, 241-260.

80. Robinson, N. J., Procter, C. M., Connolly, E. L., and Guerinot, M. L. (1999) A ferric-chelate reductase for iron uptake from soils, *Nature 397*, 694-697.

81. Naito, K., Suzuki, M., Mito, S., Hasegawa, H., Imai, I., Sohrin, Y., and Matsui, M. (2001) The pursuit of siderophore secreted by marine phytoplankton *Rhodomonas ovalis*, *Anal. Sci. Suppl. 17*, 817-819.

82. Trick, C. G., Andersen, R. J., Price, N. M., Gillam, A., and Harrison, P. J. (1983) Examination of hydroxamate-siderophore production by neritic eukaryotic marine phytoplankton, *Mar. Biol. 75*, 9-17.

83. Maranger, R., Bird, D. F., and Price, N. M. (1998) Iron acquisition by photosynthetic marine phytoplankton from ingested bacteria, *Nature 396*, 248-251.

84. Castruita, M., Shaked, Y., Elmegreen, L. A., Stiefel, E. I., and Morel, F. M. M. (2008) Availability of iron from iron-storage proteins to marine phytoplankton, *Limnol. Oceanogr. 53*, 890-899.

85. Soria-Dengg, S., Reissbrodt, R., and Horstmann, U. (2001) Siderophores in marine coastal waters and their relevance for iron uptake by phytoplankton: experiments with the diatom Phaeodactylum tricornutum, *Mar. Ecol. Prog. Ser. 220*, 73-82.

86. Soria-Dengg, S., and Horstmann, U. (1995) Ferrioxamines B and E as iron sources for the marine diatom Phaeodactylum tricornutum, *Mar. Ecol. Prog. Ser. 127*, 269-277.

87. Hutchins, D. A., Franck, V. M., Brzezinski, M. A., and Bruland, K. W. (1999) Inducing Phytoplankton Iron Limitation in Iron-Replete Coastal Waters with a Strong Chelating Ligand, *Limnol. Oceanogr. 44*, 1009-1018.

88. Hutchins, D. A., Witter, A. E., Butler, A., and Luther, G. W., III. (1999) Competition among marine phytoplankton for different chelated iron species, *Nature 400*, 858-861.

89. Hopkinson, B., and Morel, F. (2009) The role of siderophores in iron acquisition by photosynthetic marine microorganisms, *BioMetals 22*, 659-669.

90. Mawji, E., Gledhill, M., Milton, J. A., Tarran, G. A., Ussher, S., Thompson, A., Wolff, G. A., Worsfold, P. J., and Achterberg, E. P. (2008) Hydroxamate Siderophores: Occurrence and Importance in the Atlantic Ocean, *Environ. Sci. Technol. 42*, 8675-8680.

91. Salmon, T. P., Rose, A. L., Neilan, B. A., and Waite, T. D. (2006) The FeL model of iron acquisition: nondissociative reduction of ferric complexes in the marine environment, *Limnol. Oceanogr. 51*, 1744-1754.

92. Morel, F. M. M., Kustka, A. B., and Shaked, Y. (2008) The role of unchelated Fe in the iron nutrition of phytoplankton, *Limnol. Oceanogr. 53*, 400-404.

93. Shaked, Y., Kustka, A. B., and Morel, F. M. M. (2005) A general kinetic model for iron acquisition by eukaryotic phytoplankton, *Limnol. Oceanogr. 50*, 872-882.

94. Anderson, M. A., and Morel, F. M. M. (1982) The influence of aqueous iron chemistry on the uptake of iron by the coastal diatom *Thalassiosira weissflogii*, *Limnol. Oceanogr. 27*, 789-813.

95. Kustka, A. B., Allen, A. E., and Morel, F. M. M. (2007) Sequence analysis and transcriptional regulation of Iron acquisition genes in two marine diatoms, *J. Phycol. 43*, 715-729.

96. Eckhardt, U., and Buckhout, T. J. (1998) Iron assimilation in *Chlamydomonas reinhardtii* involves ferric reduction and is similar to Strategy I higher plants, *J. Exp. Bot. 49*, 1219-1226.

97. Maldonado, M. T., Strzepek, R. F., Sander, S., and Boyd, P. W. (2005) Acquisition of iron bound to strong organic complexes, with different Fe binding groups and photochemical reactivities, by plankton communities in Fe-limited subantartic waters, *Global Biogeochem. Cycles 19*.

98. Kustka, A. B., Shaked, Y., Milligan, A. J., King, D. W., and Morel, F. M. M. (2005) Extracellular production of superoxide by marine diatoms: contrasting effects on iron redox chemistry and bioavailability, *Limnol. Oceanogr. 50*, 1172-1180.

99. Rose, A. L., and Waite, T. D. (2005) Reduction of Organically Complexed Ferric Iron by Superoxide in a Simulated Natural Water, *Environ. Sci. Technol. 39*, 2645-2650.

100. Hallegraeff, G. M. (2003) Harmful algal blooms: a global overview., In *Manual on Harmful Marine Microalgae.* (Hallegraeff, G. M., Anderson, D. M., and Cembella, A. D., Eds.), pp 25-49, UNESCO, Paris.

101. Giovannoni, S. J., and Rappé, M. S. (2000) Evolution, diversity, and molecular ecology of marine prokaryotes, In *Microbial ecology of the oceans* (Kirchman, D. L., Ed.), pp 47-84, Wiley.

102. Azam, F., and Worden, A. Z. (2004) OCEANOGRAPHY: Microbes, Molecules, and Marine Ecosystems, *Science 303*, 1622-1624.

103. Bell, W. H., and Mitchell, R. (1972) Chemotactic and growth responses of marine bacteria to algal extracellular products., *Biological Bulletin Woods Hole 143*.

104. Bell, W. H., Lang, J. M., and Mitchell, R. (1974) Selective stimulation of marine bacteria by algal extracellular products., *Limnology & Oceanography 19*, 833-839.

105. Azam, F. (1998) Microbial control of oceanic carbon flux: the plot thickens. , *Science 3*, 380-396.

106. Azam, F., and Malfatti, F. (2007) Microbial structuring of marine ecosystems, *Nat Rev Microbiol 5*, 782-791.

107. Barbara, G. M., and Mitchell, J. G. (2003) Bacterial tracking of motile algae, *FEMS Microbiol. Ecol. 44*, 79-87.

108. Rooney-Varga, J. N., Giewat, M. W., Savin, M. C., Sood, S., LeGresley, M., and Martin, J. L. (2005) Links between phytoplankton and bacterial community dynamics in a coastal marine environment, *Microb. Ecol. 49*, 163-175.

109. Sapp, M., Schwaderer, A. S., Wiltshire, K. H., Hoppe, H. G., Gerdts, G., and Wichels, A. (2007) Species-specific bacterial communities in the phycosphere of microalgae?, *Microb. Ecol. 53*, 683-699.

110. Doucette, G. J., Kodama, M., Franca, S., and Gallacher, S. (1998) Bacterial interactions with harmful algal bloom species: bloom ecology, toxigenesis, and cytology., In *Physiological ecology of harmful algal blooms* (Anderson, D. M., Cembella, A. D., and Hallegraeff, G. M., Eds.), pp 619-647, Springer, Berlin.

111. Bolch, C. J. S., Vincent, B., Blackburn, S. I., and Green, D. H. (2004) Host-symbiont range of growth stimulating bacteria associated with *Gymnodinium catenatum*. , In *XIth International Conference on Harmful Algal Blooms*, Cape Town, South Africa.

112. Green, D. H., Negri, A. P., Geier, S., Llewellyn, L., Blackburn, S., and Bolch, C. J. (2004) The role of bacteria in the growth and toxicity of *Gymnodinium catenatum*. , In *XIth International Conference on Harmful Algal Blooms*, Cape Town, South Africa.

113. Mayali, X., and Doucette, G. J. (2002) Microbial community interactions and population dynamics of an algicidal bacterium active against *Karenia brevis* (Dinophyceae), *Harmful Algae 1*, 277-293.

114. Mayali, X., Franks, P. J. S., and Azam, F. (2008) Cultivation and ecosystem role of a marine *Roseobacter* clade-affiliated cluster bacterium, *Appl. Environ. Microbiol. 74*, 2595-2603.

115. Croft, M. T., Lawrence, A. D., Raux-Deery, E., Warren, M. J., and Smith, A. G. (2005) Algae acquire vitamin B-12 through a symbiotic relationship with bacteria, *Nature 438*, 90-93.

116. Grossart, H. P. (1999) Interactions between marine bacteria and axenic diatoms (*Cylindrotheca fusiformis*, *Nitzschia laevis*, and *Thalassiosira weissflogii*) incubated under various conditions in the lab., *Aquatic Microbial Ecology 19*, 1-11.

117. Matsuo, Y., Imagawa, H., Nishizawa, M., and Shizuri, Y. (2005) Isolation of an algal morphogenesis inducer from a marine bacterium, *Science 307*, 1598-1598.

2. Boron binding by the marine siderophore vibrioferrin isolated from marine bacteria associated with the toxic dinoflagellate *Gymnodinium catenatum*

2.1. Introduction

Phytoplankton blooms, including toxic species such as the diatom *Pseudo-nitzschia* or the dinoflagellate *Gymnodinium catenatum*, are a characteristic phenomenon in coastal and upwelling regions of the world's oceans. Blooms of harmful algal species have deleterious effects on marine ecosystems, and their impact on public health and local economies can be large and has been increasing globally (*1*). This increasing incidence has sparked interest in species of bacteria closely associated with toxic algal species. Thus, axenic (bacteria-free) dinoflagellate cultures often cannot be established, and even when they can, they require the addition of vitamins and artificial metal complexes for satisfactory viability (*2*). It can be inferred that under natural conditions, these heterotrophic bacteria contribute some critical factor(s) to the nutrition of the relevant marine algae.

A broad hypothesis that links these bacterial "symbionts" to the growth of toxic dinoflagellates is in their control of the supply of iron since this element, while the fourth most abundant in the Earth's crust, is present under aerobic conditions at neutral pH only in the form of extremely insoluble minerals that severely restrict its bioavailability. The iron level in open ocean waters is even lower than in most terrestrial environments (*3, 4*). While the iron uptake systems of phytoplankton are largely unknown, bacteria on the other hand have evolved sophisticated systems based on high-affinity iron specific binding compounds called siderophores to acquire, transport, and process this essential metal ion. Several hundred siderophores, whose biosyntheses are repressed by high iron levels, are known, and extensive studies of their isolation, structure, transport, and molecular genetics have been undertaken in the last two decades (*5*). The structural variety of siderophores, both terrestrial and marine, has been comprehensively reviewed (*6, 7*). Considered essential to their role as iron transporters is the fact that siderophores have both high affinity and high specificity for Fe(III) over other biologically significant cations.

2.2. Results and Discussion

In the process of searching for new siderophores from *Marinobacter* sp. DG870, 893, and 979, marine bacteria associated with *G. catenatum* (*2*), we isolated by BioGel *P*2 size exclusion chromatography from extracts of spent culture medium, one CAS positive fraction (*8*). Negative ion ESI-MS revealed two major mass peaks in this fraction near 400 amu. Further purification via reversed phase HPLC followed by a second round of HPLC produced two clean fractions, one with a mass of 433 amu that was CAS positive and a second with mass 441 amu

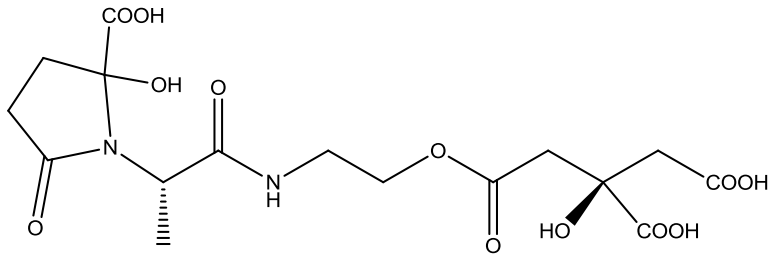

Figure 2.1. Structure of the siderophore vibrioferrin.

that was CAS negative. Subsequent high-resolution MS and a variety of 1 and 2-D NMR experiments unequivocally demonstrated that the CAS positive, 433 amu, fraction was the known siderophore vibrioferrin (VF; Fig. 2.1). Vibrioferrin is a member of the carboxylate class of siderophores and contains two α-hydroxy acid groups. It was previously isolated from *Vibrio parahemeolyticus*, an enteropathogenic estuarine bacterium often associated with seafood-borne gastroenteritis and has been extensively studied by Yamamoto et al (*9-16*). Because of its close association with the CAS positive fraction, we also investigated the nature of the CAS negative compound with molecular mass 441 amu. A curious isotope distribution pattern suggested the presence of an element other than the expected C, H, N, or O. In fact a search through the periodic table produced a match only for the unexpected element boron. The presence of boron was rapidly confirmed by ^{11}B NMR and this, coupled with high-resolution MS and a variety of other 1-and 2-D ^{1}H and ^{13}C NMR experiments, revealed that the CAS negative, 441 amu,

fraction is boronylated vibrioferrin. Since boron was not a component of the artificial seawater media used in culturing the bacteria (see Methods), the boron incorporated into VF could only have been derived from the borosilicate glass flasks, suggesting a strong sequestering ability of VF for boron. Indeed when we added boric acid to the media in the concentration reported to be present in seawater, 0.4 mM (*17*), boronylated vibrioferrin was the predominant species observed. A comparison between the ^{13}C NMR peaks of free VF and its boronylated analogue reveal significant coordination induced shifts (CIS) only for the carbon atoms assigned to the two hydroxyl acid groups demonstrating that the binding of boron by VF is through those four oxygens (Table 2.1). This was confirmed by the position of the peak in the ^{11}B NMR at 8.5 ppm that is consistent with a spiro-borate diester ((*18*). The structure of a variety of salts of borodicitrate have been reported where the boron is bound in a tetrahedral fashion through the carboxylate and α-hydroxyl groups from each of two citrates exactly as predicted from the CIS NMR data for B-VF (*19*).

Using the structural data for borocitrate binding from the crystal structures as a starting point, we determined the ten lowest energy conformers of the complex using Merck Molecular Force Field (MMFF) conformational searching algorithms as implemented in Spartan 2000. The four lowest energy conformers were then geometry-optimized at the DFT (B3LYP) level using Jaguar (Schrödinger), the lowest energy structure of which is shown (Fig. 2.2). It is clear from this structure that it is easy for VF to bind to a tetrahedral borate through the citrate groups in a strain-free way. The presence of several internal hydrogen bonds also appears to stabilize the structure. Further experiments show that some, (i.e., rhizoferrin and petrobactin), but not all (i.e., any of the hydroxamate) siderophores also bind boron to varying degrees (data not shown). The proposed structure of B-VF and its NMR assignments are presented below in Figure 2.3 and Table 2.2.

Table 2.1. ^{13}C Coordination Induced Shifts in B-VF compared to VF.

Assignment	Vibrioferrin[a,b] δ_C (in Acetone-d_6)	Boronylated Vibrioferrin[c] δ_C (in DMSO-d_6)	*Difference (ppm)*[d]
3”	14.3	13.2	-1.1
3”’	~ 29[e]	28.5	~ 0.5
4”’	33.0	32.4	-0.6
2’	39.0	37.6	-1.4
2	43.4	42.4	-1.0
4	44.2	43.3	-0.9
2”	52.5	53.4	+0.9
1’	63.9	62.1	-1.8
3	73.6	77.6	+4.0
5”’	90.7	91.9	+1.2
1	170.0	169.2	-0.8
5	171.6	170.1	-1.5
1”	171.9	172.1	+0.2
6”’	173.0	176.7	+3.7
6	175.4	177.0	+1.6
2”’	175.6	174.4	-1.2

[a] Only the major ring closed form of Vibrioferrin was taken into account since it is believed to be the only form capable of effective boron chelation.
[b] Values were taken from Yamamoto et al. 1994b.
[c] This work.
[d] Small (ca. 1 ppm) negative shifts are due to difference in solvents, significant positive shifts are coordination induced shifts.
[e] Estimate, partially obscured by solvent.

While boron is a known dietary requirement for various phytoplankton (*20*-*23*), structurally characterized boron-containing natural products are confined to just a few macrolide antibiotics (*24*-*26*) and a bacterial quorum-sensing molecule (*27*). The latter observation opens many intriguing possibilities. Quorum sensing molecules have been reported to be involved in siderophore production in some species (*28, 29*) and a naturally occurring derivative of a non-boron containing quorum-sensing molecule has been reported to possess siderophore-like iron binding abilities (*30*). Conversely, there is evidence that siderophores, in addition to their iron binding role, may function as signaling molecules (*28*). These observations suggest a role for siderophores in inter and/or intraspecies communication and growth control. Another possibility is that VF could be functioning as a “boronophore”, that is, a boron-scavenging molecule for the phytoplankton. The presence of a high concentration of boron in

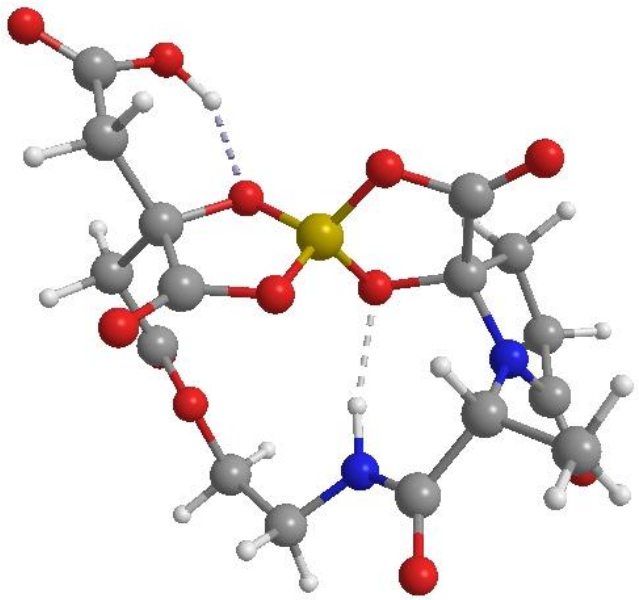

Figure 2.2. The DFT geometry-optimized structure of the lowest energy MMFF derived conformer of boron-vibrioferrin.

seawater does not *a priori* eliminate the need for an extracellular transporter. Indeed membrane-associated boron transporters have recently been described in plants although an extracellular boron scavenger is unknown (*31*). The details of these intriguing and potentially highly significant findings await further investigation, but it is now clear, in the marine environment at least where the concentration of boron is high, that the role of siderophores functioning exclusively as iron binding agents for their producing bacteria has to be reconsidered.

Despite the fact that VF has been extensively studied from a biological perspective (*11-13, 15, 32, 33*), its metal binding characteristics remain largely unknown. Although we have not yet measured accurate Fe binding constants there is evidence that the interaction is weaker than for most other siderophores. Attempts to determine the overall formation constant by EDTA competition at near neutral pH, as is standard methodology for siderophores, failed in the case of VF as a single equivalent of EDTA effectively removes all of the Fe from Fe-VF. This sets an upper limit of $10^{23\text{-}25}$ for K_{ML}. This relatively weak iron binding is not entirely unexpected as VF has only five potential donor groups, insufficient to satisfy the six coordination desired by

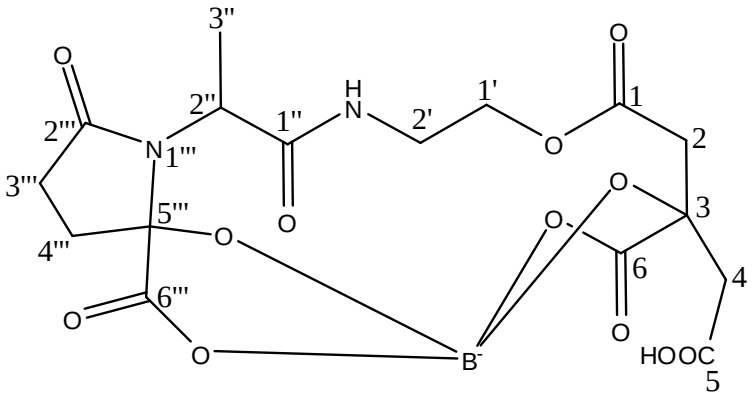

Figure 2.3. Proposed structure of B-VF.

Table 2.2. ^{1}H NMR assignments for B-VF in DMSO-d_6.

Chemical Shift (ppm)	Assignment
1.25 (d)	3”
1.89-2.03 (m)	4”’A
2.15-2.25 (m)	4”’B
2.26-2.39 (m)	3”’A
2.40-2.50 (m)	3”’B
2.52 (d)	4A*
2.62 (d)	2A*
2.64 (d)	4B*
2.68 (d)	2B*
2.90-3.0 (m)	2’A
3.57-3.68 (m)	2’B
3.80-3.89 (m)	1’A
4.20-4.28 (m)	1’B
4.40 (q)	2”
8.08 (dd)	-NH

* Assignment of H-2 and H-4 maybe interchanged.

Fe(III). The low binding constant also suggests a less negative reduction potential for the iron complex as there is typically a strong correlation between redox potential and the Fe(III) binding constant. Such a redox potential would likely be well within the range of cell surface reductases reported to be present in some phytoplankton (*34*). In addition to its unexpected property of binding boron and its relatively weak iron binding, vibrioferrin, when complexed with Fe, is like other marine siderophores that contain an α-hydroxy acid moiety,

photoreactive (*35*). However despite these properties, bioassays in media rendered iron limiting by the presence of chelators, 2,2'-bipyridyl and EDDHA, revealed that VF is able to relieve iron induced growth inhibition in DG870, 893, and 979 as expected of a true siderophore.

Marine bacteria, including DG870, 893, and 979, specifically associated with toxic, bloom-forming dinoflagellates, represent a unique subset of marine bacteria which share the ability to produce and use vibrioferrin unlike numerous closely related organisms. This functional conservation is interpreted as indicating that there are specific selective processes operating between the bacteria and the dinoflagellates (*36*). Why are dinoflagellates selecting for such a phylogenetically and functionally specific group of marine bacteria? The unique features of vibrioferrin may provide important clues about the nature of this relationship and related algal-bacterial interactions.

2.3. Methods

2.3.1. Bacterial Culture. All chemicals (A.C.S. grade or better) were purchased from Fisher Scientific unless otherwise indicated. Strains were cultured in on a broth consisting of 0.5 g Bacto Peptone (Difco), 0.1 g Yeast Extract (Difco), 750 ml GFC filtered open ocean seawater, 250 ml dH_2O per liter with the pH adjusted to 7.5. Working agar plates were made with the same media in addition to 1.5 % agar. Large scale cultures (2 L) for VF isolation utilized a chemically defined media containing per liter: 15 g NaCl, 0.75 g KCl, 3 g $CaCl_2 \cdot 2H_2O$, 1 g NH_4Cl, 5 g Succinic acid, 12.4 g $MgSO_4 \cdot 7H_2O$, and 0.1 g β-glycerophosphoric acid (Aldrich) and the pH adjusted to 7.5. Cultures were grown at room temperature with constant shaking at 160 rpm for 7 days in sterilized 4L flasks that were pre-washed with 6 M HCl to eliminate residual iron.

2.3.2. Siderophore Growth Bioassay. DG870 and DG979 were grown in separate agar plates with supplemented seawater that was rendered iron-deficient by the addition of 150 μM

EDDHA and 150 μM 2,2'-bipyridyl to the agar broth prior to autoclaving. 200 μL aliquots of bacterial solution broth cultures were added to the plates prior to agar solidification. Sterile filter disks were then impregnated with 20 μL of 250 μM solutions of VF, BVF, water (as negative control) and iron citrate (as positive control) and various known siderophores (*e.g.* aerobactin, petrobactin and desferrioxamine E) and dried. Filter disks were then placed on the agar plates, which were then incubated at 28^{o}C overnight. A positive response (siderophore utilization) was indicated by a halo of growth around the disk.

2.3.3. Vibrioferrin and Boron-Vibrioferrin Purification. The supernatant was isolated from bacterial cells by centrifugation at 5000 rpm for 25 min at 4^{o}C using Sorvall RC5C+ centrifuge and acidified to pH 2.5. Amberlite XAD-2 resin, (ca. 100 g/L, Supelco), was added to the supernatant and the suspension shaken for 12 hours. Subsequently, the resin was poured into a column, washed with several bed volumes of Milli-Q water and finally eluted with methanol. Concentration of the methanol eluant by rotary evaporation yielded crude culture extracts. Vibrioferrin was isolated from the extracts by purification on a size exclusion column (Biogel P-2, BioRad). Siderophore-containing fractions were identified via the Chrome azurol S (CAS) assay described by Schwyn and Neilands, combined and repurified using semipreparative reversed phase HPLC. A Phenomenex Synergi-Hydro C18 column was used with the following gradient: (A = 0.1% TFA in water, B = 0.1% TFA in Acetonitrile) 0-15% B in 30 min, 15-95% B in 15 min, 95% B for 5 min, and 95-0% B in 10 min at a flow rate of 6 mL/min and monitoring of the eluant at 220 nm. The B-VF and apo-VF containing fractions were separated at this point. The B-VF containing fractions were identified by negative ion mode ESI-MS (441 amu) while the VF fractions were determined by the CAS assay. The VF-containing fractions were further purified on a Phenomenex Luna C18 column with the following gradient: 0-3% B in 5 min, 3-12% B in 5 min, 12-15% B in 5 min, 15% B for 2 min,

and 15-0% B in 5 min at a flow rate of 5 mL/min. The appropriate fractions were then pooled and lyophilized.

2.3.4. B-VF and VF Characterization. The identity of VF was confirmed by high resolution MS, ^{1}H, ^{13}C, and gCOSY NMR. The identity of B-VF was confirmed by all the previous experiments in addition to TOCSY, HMQC, HMBC, DEPT, NOESY and ^{11}B NMR (Figures 2.3-2.6 and Table 2.2).

High-resolution mass spectra were obtained on a Micromass (Manchester, UK) QTOF-2 time of flight mass spectrometer (made available to us at UCSB by the courtesy of Prof. Alison Butler) with electrospray ionization source. Samples (in aqueous solution, 30 mM NH4HCO3 buffer or methanol) were injected by a Harvard Apparatus (Holliston, Massachusetts 01746, USA) infusion pump at a speed of 5 μL/min. For exact mass measurements an internal standard of known mass (H9985, an octapeptide with m/z = 829.5393), was co-infused with the VF or BVF. The exact mass measured for the parent peak of BVF in positive ion mode of 440.0971 agrees within 4.1 ppm with that calculated for C16H1810BN2O12 (440.0989). Routine ESI-MS and MSn spectra were obtained on a Finnigan LCQ ion-trap mass spectrometer equipped with an ESI source (Finnigan MAT, San Jose, CA). MS/MS spectra were obtained utilizing a collision voltage between 20-50 V and argon as the collision gas. Isotope distribution patterns were simulated using the program IsoPro 3.0

All 1- and 2-D NMR experiments were carried out on a Varian 500MHz instrument using standard pulse sequences available on the instrument. ^{11}B NMR spectra were acquired using quartz NMR tubes to reduce the broad borosilicate background of glass tubes and referenced to boric acid at pH 2.

2.3.5. EDTA Binding Competition. Solutions contained 1:1, 1:5, and 1:10 VF to EDTA ratios with the pH fixed at 7.90 using 50 mM Bicine buffer. In addition, ionic strength was

fixed by maintaining a NaCl concentration of 0.25 M. Iron was added in a 1:1 ratio with respect to VF in the form of standard atomic absorption solution purchased from Fisher. Solutions were left to equilibrate for 5 days and monitored at 330 nm (the absorption maximum of FeVF using a Cary 50 UV-Visible spectrophotometer.

2.4. Appendix

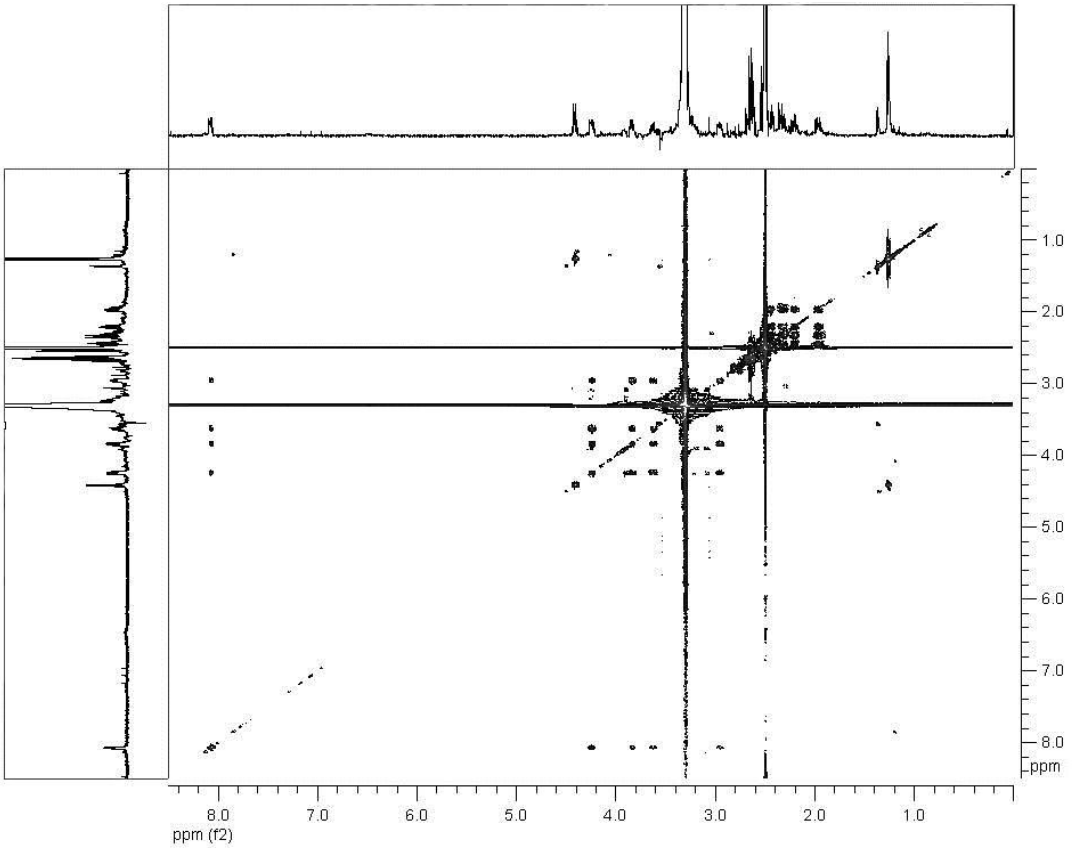

Figure 2.4. TOCSY spectrum of B-VF in DMSO-d_6.

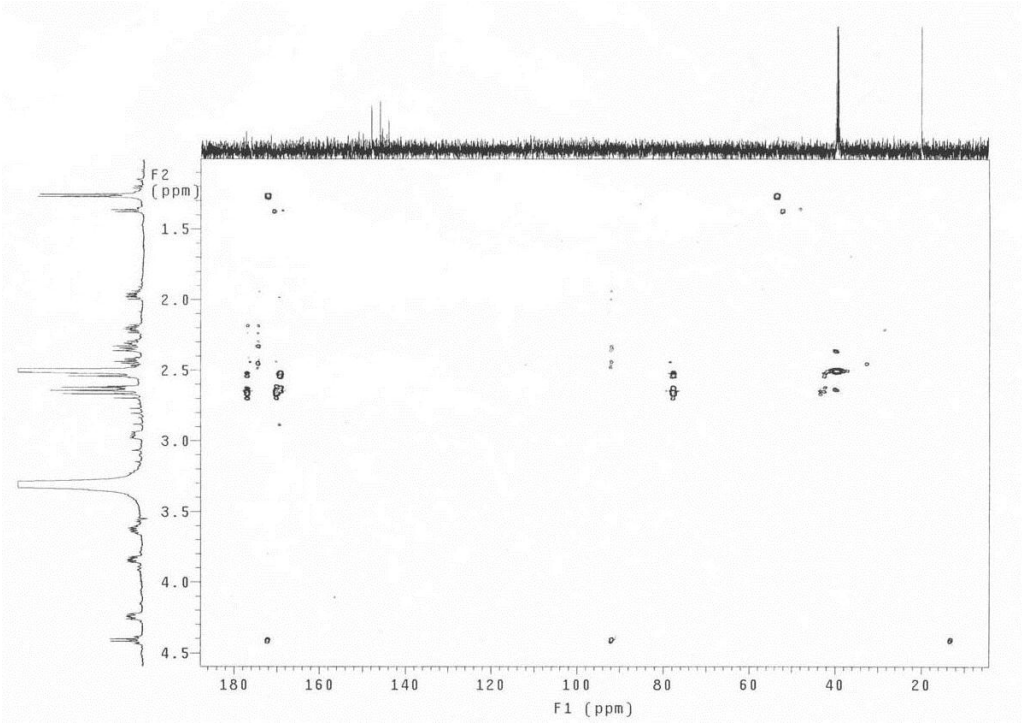

Figure 2.5. HMBC spectrum of B-VF in DMSO-d_6.

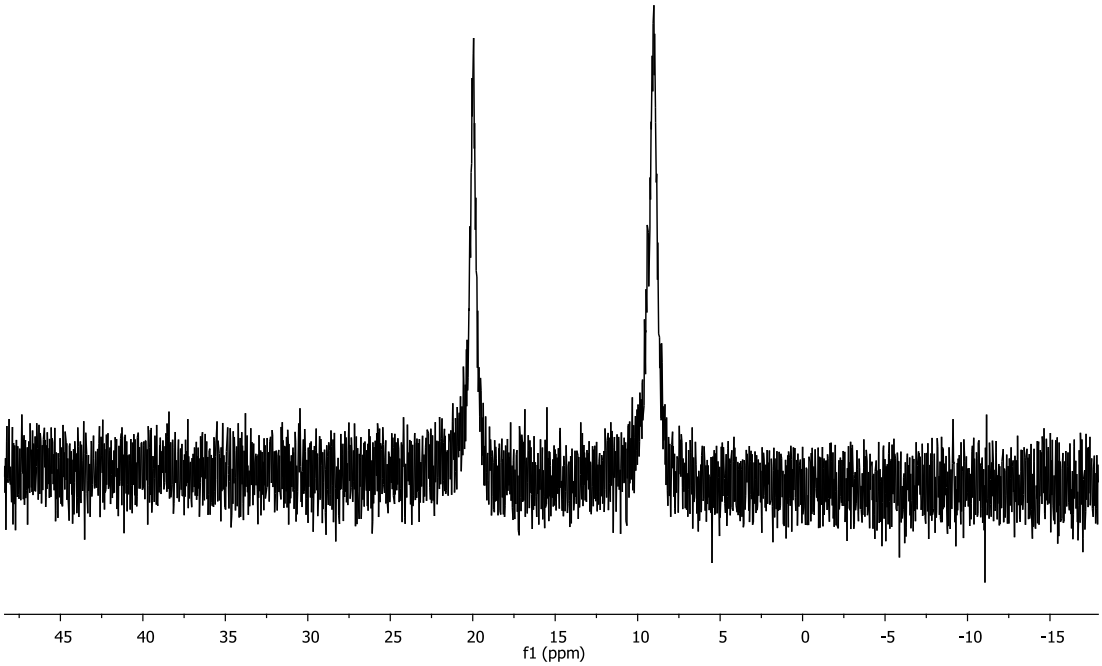

Figure 2.6. ^{11}B NMR spectrum of B-VF in D_2O. Spectrum was referenced relative to an external standard of 4 mM boric acid (pH 2.0) at 20 ppm. The peak at 8.5 ppm is due to the coordination of the boron to VF, while the peak at 20 ppm is unbound boric acid.

2.5. Acknowledgements

This work was supported by California SeaGrant #020-C-N. The authors thank Günther Winkelmann, at the University of Tübingen for a sample of rhizoferrin, Alison Butler at UCSB, for a sample of petrobactin and Susan Blackburn (CSIRO, Australia) for contributing strains of *G. catenatum*. This chapter was previously published as: Amin, S. A., Küpper, F. C., Green, D. H., Harris, W. R., and Carrano, C. J. (2007) Boron binding by a siderophore isolated from marine bacteria associated with the toxic dinoflagellate *Gymnodinium catenatum*, *J. Am. Chem. Soc. 129*, 478-479.

2.6. References

1. Hallegraeff, G. M., Anderson, D. M., and Cembella, A. D., (Eds.) (2003) *Manual on harmful marine microalgae*, Vol. 11, UNESCO, Paris.

2. Green, D. H., Llewellyn, L. E., Negri, A. P., Blackburn, S. I., and Bolch, C. J. S. (2004) Phylogenetic and functional diversity of the cultivable bacterial community associated with the paralytic shellfish poisoning dinoflagellate *Gymnodinium catenatum*, *FEMS Microbiol. Ecol. 47*, 345-357.

3. Martin, J. H., and Fitzwater, S. E. (1988) Iron deficiency limits phytoplankton growth in the north-east Pacific subarctic, *Nature 331*, 341-343.

4. Wu, J., and Luther III, G. W. (1994) Size-fractionated iron concentrations in the water column of the western North Atlantic ocean, *Limnol. Oceanogr. 39*, 1119-1129.

5. Winkelmann, G., and Carrano, C. J., (Eds.) (1997) *Transition metals in microbial metabolism*, Harwood Academic Pub., Amsterdam, The Netherlands.

6. Butler, A. (2005) Marine siderophores and microbial iron mobilization, *BioMetals 18*, 369-374.

7. Raymond, K. N. (1994) Recognition and transport of natural and synthetic siderophores by microbes, *Pure Appl. Chem. 66*, 773-781.

8. Schwyn, B., and Neilands, J. B. (1987) Universal chemical assay for the detection and determination of siderophores, *Anal. Biochem. 160*, 47-56.

9. Takeuchi, Y., Akiyama, T., and Harayama, T. (1999) Total synthesis of the siderophore vibrioferrin, *Chem. Pharm. Bull. (Tokyo) 47*, 459-460.

10. Takeuchi, Y., Nagao, Y., Toma, K., Yoshikawa, Y., Akiyama, T., Nishioka, H., Abe, H., Harayama, T., and Yamamoto, S. (1999) Synthesis and siderophore activity of vibrioferrin and one of its diastereomeric isomers, *Chem. Pharm. Bull. (Tokyo) 47*, 1284-1287.

11. Tanabe, T., Funahashi, T., Nakao, H., Miyoshi, S.-I., Shinoda, S., and Yamamoto, S. (2003) Identification and characterization of genes required for biosynthesis and transport of the siderophore vibrioferrin in *Vibrio parahaemolyticus*, *J. Bacteriol. 185*, 6938-6949.

12. Tanabe, T., Nakao, H., Kuroda, T., Tsuchiya, T., and Yamamoto, S. (2006) Involvement of the *Vibrio parahaemolyticus pvsC* gene in export of the siderophore vibrioferrin, *Microbiol. Immunol. 50*, 871-876.

13. Yamamoto, S., Akiyama, T., Okujo, N., Matsu-ura, S., and Shinoda, S. (1995) Demonstration of a ferric vibrioferrin-binding protein in the outer membrane of *Vibrio parahaemolyticus*, *Microbiol. Immunol. 39*, 759-766.

14. Yamamoto, S., Fujita, Y., Okujo, N., Minami, C., Matsuura, S., and Shinoda, S. (1992) Isolation and partial characterization of a compound with siderophore activity from *Vibrio parahaemolyticus*, *FEMS Microbiol. Lett. 94*, 181-186.

15. Yamamoto, S., Okujo, N., Matsuura, S., Fujiwara, I., Fujita, Y., and Shinoda, S. (1994) Siderophore-mediated utilization of iron bound to transferrin by *Vibrio parahaemolyticus*, *Microbiol. Immunol. 38*, 687-693.

16. Yamamoto, S., Okujo, N., Yoshida, T., Matsuura, S., and Shinoda, S. (1994) Structure and iron transport activity of vibrioferrin, a new siderophore of *Vibrio parahaemolyticus*, *J. Biochem., Tokyo 115*, 868-874.

17. Bowen, H. J. M. (1966) *Trace elements in biochemistry*, Academic Press, London, New York,.

18. Semmelhack, M. F., Campagna, S. R., Hwa, C., Federle, M. J., and Bassler, B. L. (2004) Boron binding with the quorum sensing signal AI-2 and analogues, *Org. Lett. 6*, 2635-2637.

19. Zviedre, I., Fundamenskii, V. S., Krasnikov, V. V., and Kolesnikova, G. P. (1984) Crystal structure of potassium borodicitrate (dicitratoborate) ($K[(C_6H_6O_7)_2B]\cdot 2H_2O$, *Zhurnal Strukturnoi Khimii 25*, 95-101.

20. Lewin, J., and Chen, C.-H. (1976) Effects of boron deficiency on the chemical composition of a marine diatom, *J. Exp. Bot. 27*, 916-921.

21. Hunt, D. C. (2003) Dietary boron: An overview of the evidence for its role in immune function, *The J. Trace Elements Exp. Med. 16*, 291-306.

22. Bonilla, I., Garcia-Gonzalez, M., and Mateo, P. (1990) Boron Requirement in Cyanobacteria : Its Possible Role in the Early Evolution of Photosynthetic Organisms, *Plant Physiol. 94*, 1554-1560.

23. Lewin, J. (1966) Boron as a growth requirement for diatoms, *J. Phycol. 2*, 160-163.

24. Pache, W., and Zahner, H. (1969) Metabolic products of microorganisms. 77. Studies on the mechanism of action of boromycin, *Arch. Mikrobiol. 67*, 156-165.

25. Schummer, D., Irschik, H., Reichenbach, H., and Höfle, G. (1994) Antibiotics from gliding bacteria, LVII. Tartrolons: new boron-containing macrodiolides from *Soragnium cellulosum*., *Liebigs Ann Chem*, 283-289.

26. Nakamura, H., and Iitaka, Y. (1977) Structure of aplasmomycin, *J. Antibiot. 30*, 714-719.

27. Chen, X., Schauder, S., Potier, N., Van Dorsselaer, A., Pelczer, I., Bassler, B. L., and Hughson, F. M. (2002) Structural identification of a bacterial quorum-sensing signal containing boron, *Nature 415*, 545-549.

28. Guan, L. L., and Kamino, K. (2001) Bacterial response to siderophore and quorum-sensing chemical signals in the seawater microbial community, *BMC Microbiol. 1*, 27.

29. Fong, K. P., Gao, L., and Demuth, D. R. (2003) *luxS* and *arcB* control aerobic growth of *Actinobacillus actinomycetemcomitans* under iron limitation, *Infect. Immun. 71*, 298-308.

30. Diggle, S. P., Matthijs, S., Wright, V. J., Fletcher, M. P., Chhabra, S. R., Lamont, I. L., Kong, X., Hider, R. C., Cornelis, P., Camara, M., and Williams, P. (2007) The *Pseudomonas aeruginosa* 4-quinolone signal molecules HHQ and PQS play multifunctional roles in quorum sensing and iron entrapment, *Chemistry & Biology 14*, 87-96.

31. Takano, J., Noguchi, K., Yasumori, M., Kobayashi, M., Gajdos, Z., Miwa, K., Hayashi, H., Yoneyama, T., and Fujiwara, T. (2002) *Arabidopsis* boron transporter for xylem loading, *Nature 420*, 337-340.

32. Funahashi, T., Fujiwara, C., Okada, M., Miyoshi, S.-I., Shinoda, S., Narimatsu, S., and Yamamoto, S. (2000) Characterization of *Vibrio parahaemolyticus* manganese-resistant mutants in reference to the function of the ferric uptake regulatory protein, *Microbiol. Immunol. 44*, 963-970.

33. Funahashi, T., Moriya, K., Uemura, S., Miyoshi, S.-I., Shinoda, S., Narimatsu, S., and Yamamoto, S. (2002) Identification and characterization of *pvuA*, a gene encoding the ferric vibrioferrin receptor protein in *Vibrio parahaemolyticus*, *J. Bacteriol. 184*, 936-946.

34. Jones, G. J., Palenik, B. P., and Morel, F. M. M. (1987) Trace metal reduction by phytoplankton: the role of plasmalemma redox enzymes, *J. Phycol. 23*, 237-244.

35. Barbeau, K. (2006) Photochemistry of organic iron(III) complexing ligands in oceanic systems, *Photochem. Photobiol. 82*, 1505-1516.

36. Kodama, M., Doucette, G., and Green, D. (2006) Relationships Between Bacteria and Harmful Algae, In *Ecology of Harmful Algae* (Granéli, E., and Turner, J. T., Eds.), pp 243-255, Springer-Verlag, Heidelberg.

3. Borate binding to siderophores: structure and stability

3.1. Introduction

Iron is an essential element for all living organisms due to its ubiquitous role in redox enzymes, especially in the context of respiration and photosynthesis, and marine organisms are no exception to this (*1*). Although iron is the fourth most abundant element in the Earth's crust, it is present under aerobic conditions at neutral pH only in the form of extremely insoluble minerals that severely restrict its bioavailability. The iron level in open ocean waters is even lower than in most terrestrial environments (*2-4*), since a large fraction of the limited iron available in the ocean appears to be already tightly complexed (*6, 7*). Marine bacteria, like their terrestrial counterparts, have evolved sophisticated systems based on high-affinity iron-specific binding compounds called siderophores to acquire, transport and process this essential, but biologically unavailable, metal ion. Their major role is the extracellular solubilization of iron from minerals and/or organic substrates and its specific transport into microbial cells. Several hundred siderophores, including some from the marine environment are known, and extensive studies of their isolation, structure, transport and molecular genetics have been undertaken in the last four decades (*8-12*). The structural variety of siderophores has been comprehensively reviewed and they can be generally divided into three groups depending on the iron chelating ligands (*13, 14*). Thus there are hydroxamate, catecholate and carboxylate type siderophores, as well as those that use some combination of these three functional groups.

Considered essential to their role as iron transporters is the fact that siderophores have both high affinity and high specificity for Fe(III) over other biologically significant cations. We have recently reported the unrecognized binding of borate to the siderophore vibrioferrin isolated from cultures of a marine bacterium (*15*). Here we follow up on that work and show, using a combination of ESI-MS, heteronuclear NMR, as well as potentiometric and NMR titrations, that certain well-established siderophores have an unexpectedly high affinity for

boron, an element found in high concentrations in seawater (*16*), which may be significant for siderophore chemistry under the prevailing chemical conditions in the ocean.

3.2. Results

3.2.1. Boron Binding to Vibrioferrin. In the process of searching for new siderophores from *Marinobacter* sp. DG870, 893 and 979, species of marine bacteria associated with the toxic dinoflagellate *Gymnodinium catenatum*, we isolated by HPLC from XAD extracts of spent

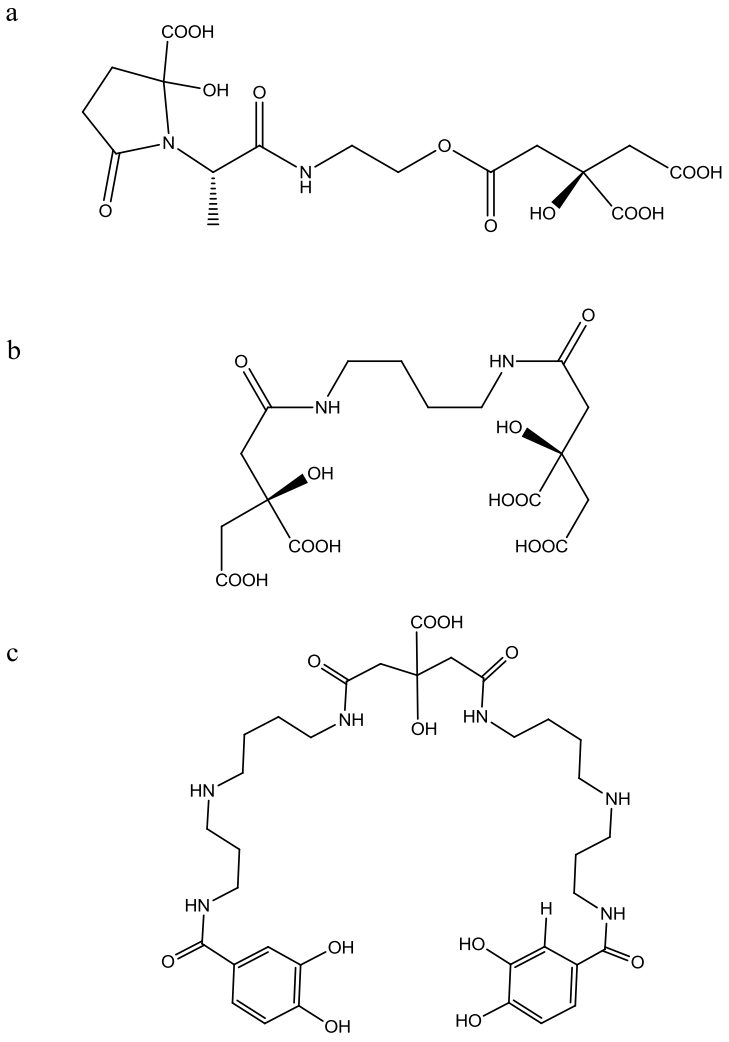

Figure 3.1. The structure of the siderophores used in this study. Vibrioferrin in its predominant closed chain form (a), rhizoferrin (b), petrobactin (c).

culture medium a species that we identified as the boron complex of the known carboxylate siderophore vibrioferrin (VF; Fig. 3.1a) (*15*). Since boron was not a component of the artificial seawater media used in culturing the bacteria, the boron incorporated into VF could only have been derived from the borosilicate glass flasks, suggesting a strong sequestering ability of VF for boron.

Based on ^{13}C and ^{11}B NMR shifts, we have shown in a preliminary communication that the reaction of vibrioferrin with borate involves the two α-hydroxycarboxylate functional groups of the ligand (*15*). Each of these groups interacts in a bidentate fashion, binding to boron via one carboxylate oxygen and a deprotonated α-hydroxy group. By utilizing both functional groups, vibrioferrin displaces the OH^- groups from boric acid and forms a stable tetrahedral complex with boron.

Addition of increments of boric acid to a solution of VF at around pD 2.6 revealed changes in the ^1H and ^{11}B NMR spectra indicative of a mixture of free boric acid and the boron-VF complex (B-VF) in slow exchange on the NMR timescale (Figs. 3.16, 3.17). Since water is an expected product of the reaction between borate and VF (*vide infra*), it is not surprising that the degree of borate binding is highly solvent dependent. Thus while a mixture of equimolar borate and VF in water shows peaks in the ^{11}B NMR spectrum corresponding to free and bound borate of approximately equal intensity, the free borate peak is much smaller in acetonitrile and unobservable in DMSO (Figure 3.2).

Figure 3.3 shows a plot of [BVF] formed in D_2O vs. equivalents of boric acid added that indicates the formation of a 1:1 B-VF complex. The curvature of the plot suggests a modest overall stability constant. Formal metal-ligand stability constants are defined as

$$\beta_{ijk} = \frac{[M_i L_j H_k]}{[M]^i [L]^j [H^+]^k} \qquad (1)$$

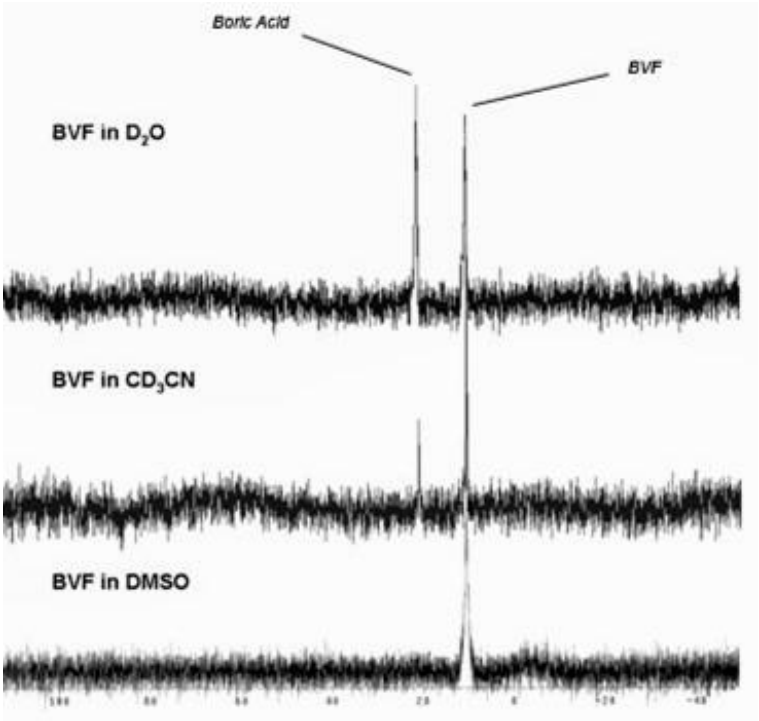

Figure 3.2. ^{11}B spectra of a mixture of boric acid and vibrioferrin in D_2O, acetonitrile-d_3, and DMSO-d_6. The peak near 20 ppm corresponds to free boric acid, while the peak at 8.5 ppm represents a boron-vibrioferrin complex.

Formal binding constants are typically expressed using the fully deprotonated form of the free ligand. Ligand deprotonation constants have been measured by potentiometric titration with standardized KOH. The only groups that are deprotonated over the pH range of 2-12 are the three carboxylic acid groups. The analysis of the potentiometric data gave successive pK_a values of 5.13, 3.60, and 2.71.

In this study, boric acid is treated as the free metal ion, and the equilibrium expression for boron binding to VF is thus

$$H^+ + B(OH)_3 + VF^{3-} \rightleftharpoons B(H_{-2}VF)^{2-} + 3\,H_2O \qquad (2)$$

The formation of the tetrahedral boron-VF complex involves the displacement of the three -OH groups from the boric acid as three water molecules, which requires the addition of three protons. Two of these protons are generated internally by the deprotonation of the α-hydroxyl

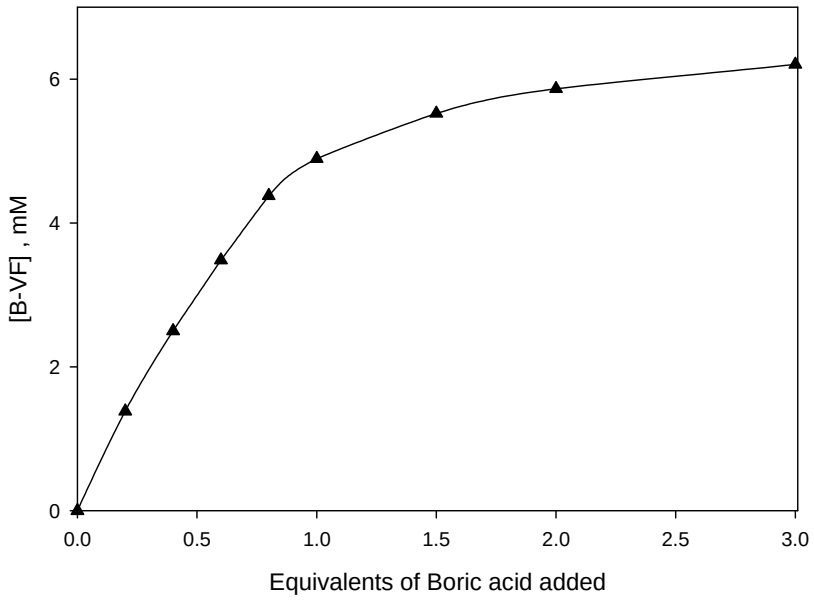

Figure 3.3. Titration of 6.4 mM vibrioferrin with boric acid at pD 2.6 showing the concentration of the borate-vibrioferrin complex as a function of added boric acid.

groups of vibrioferrin, thus the complexed form of vibrioferrin is shown as $H_{-2}VF$. The third proton comes from the solution and is shown as a reactant in eqn 2. Based on the formalism defined in eqn (1), the equilibrium shown in eqn (2) corresponds to the binding constant

$$\beta_{111} = \frac{[B(H_{-2}VF)^{2-}]}{[B(OH)_3][VF^{3-}][H^+]} \qquad (3)$$

This expression can be rearranged to define an effective binding constant that is valid at a specific pH as in eqn 4,

$$K_{eff} = \beta_{111}[H^+] = \frac{[B(H_{-2}VF)^{2-}]}{[B(OH)_3][VF^{3-}]} \qquad (4)$$

Values of K_{eff}^{D} have been obtained from NMR data at a series of pD values, which were obtained from the measured pH electrode readings as described in the methods. Based on eqn (4) we expected that a plot of log K_{eff} vs. pD would be linear with a slope equal to -1 and an

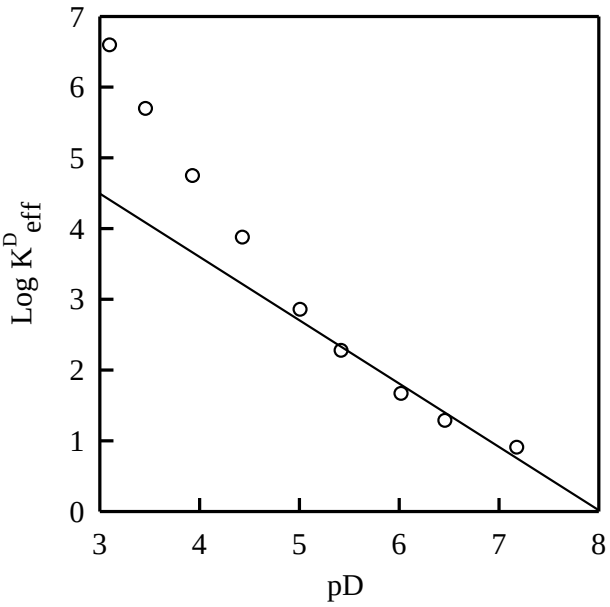

Figure 3.4. Plot of Log K^{D}_{eff} for the formation of borate-vibrioferrin complexes vs the solution pD.

intercept equal to the log of the overall binding constant β_{111}. A plot of log K^{D}_{eff} vs pD is shown in Figure 3.4. Clearly the plot is not linear over the entire pD range. The segment of the plot from pD 5.0 to 7.2 is linear with the expected slope of n = -0.9 $\pm$ 0.10. However, it is clear that log K^{D}_{eff} has a steeper pD-dependence as the pD decreases below 5. We interpret these data as indicating that the $B(H_{-2}VF)^{2-}$ complex undergoes an additional protonation at the lower pD values. Thus the equilibrium model was expanded to include the species $B(H_{-1}VF)^{1-}$. Formation of such a species would require two protons as reactants in order to release three water molecules from $B(OH)_3$ and would be described by the formation constant β_{112} based on the formalism defined in eqn 1. The ^{11}B NMR experiments only show signals for bound and free boron and do not distinguish between $B(H_{-2}VF)^{2-}$ and $B(H_{-1}VF)^{-}$. Therefore an analysis of the NMR data directly yields an effective binding constant defined as

$$K^{D}_{eff} = \frac{([B(H_{-2}VF^{2-}]+[B(H_{-1}VF)^{-}])}{[B(OH)_3][VF^{3-}]} \qquad (5)$$

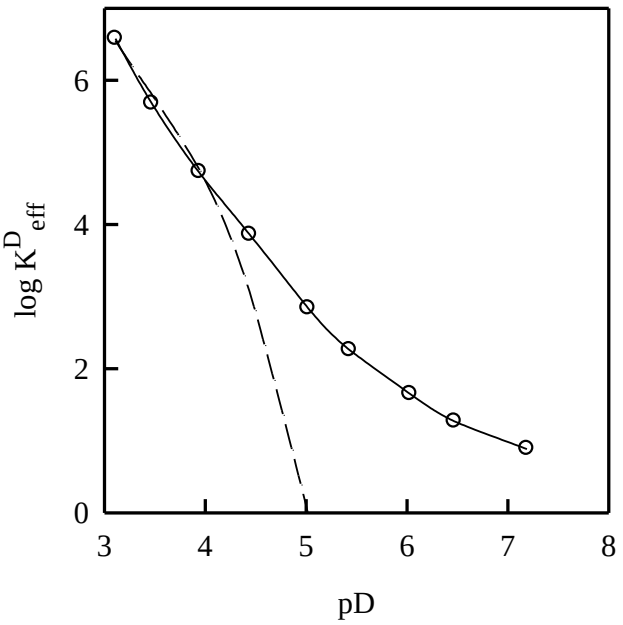

Figure 3.5. Plot of Log K^D_{eff} vs pD for the binding of borate by vibrioferrin. The solid line shows the calculated plot from a least squares fit of the data to eqn (7), while the dashes line shows the calculated plot from a least squared fit of the data to eqn (6).

This K^D_{eff} is related to formal binding constants by the equation

$$K^D_{eff} = \beta^D_{111}[D^+] + \beta^D_{112}[D^+]^2 \qquad (6)$$

We attempted to calculate values for β^D_{111} and β^D_{112} from a least squares fit of K_{eff} vs [D] using eqn (6) and the commercial software package TableCurve (*17*). The calculation included a (1/y) weighting factor to prevent the fit from being completely dominated by the larger K^D_{eff} values. There was a reasonably good fit to the data, but the calculation resulted in a physically meaningless negative value for β^D_{111}. The equilibrium model was then expanded to include a third species, such that K^D_{eff} was defined as

$$K^D_{eff} = \beta^D_{111}[D^+] + \beta^D_{112}[D^+]^2 + \beta^D_{113}[D^+]^3 \qquad (7)$$

Values of K^D_{eff} vs $[D^+]$ were then fitted to eqn 7. The use of eqn (7) gave an improvement in the least-squares fit that was highly significant as judged from the F_{stat} parameter calculated by TableCurve™. To illustrate the improvement in the fit, Figure 3.5

Table 3.1. Formal binding constants, β_{ijk}, for boron complexes with vibrioferrin and petrobactin

Species	i	j	k	Log β_{ijk}	Complex pK_a
$B(H_{-2}VF)^{2-}$	1	1	1	7.34 ± 0.10	—
$B(H_{-1}VF)^{1-}$	1	1	2	11.21 ± 0.04	3.87
B(VF)	1	1	3	14.10 ± 0.02	2.89
$B(H_{-3}PB)^{-}$	1	1	0	5.04 ± 0.07	—
$B(H_{-2}PB)$	1	1	1	11.54 ± 0.16	6.5

shows the original data from Figure 3.4 along with the calculated lines associated with eqns (6) and (7). The plot clearly shows that the data conform to eqn (7). Thus, three β^{D}_{ijk} values were calculated from the fit to eqn (7) and corrected to H_2O solution using eqn 1. These corrected values for β_{ijk} are listed in Table 3.1.

The borate titration data shown in Figure 3.3 were collected at pD 2.60. The predominant boron containing species at this pD would be the B-VF complex described by the binding constant β_{113}. An effective binding constant for pD 2.60 based on eqn (7) would be log K^{D}_{eff} = 8.0. The effective binding constant calculated from the data in Figure 3.3 is log K^{D}_{eff} = 8.25 ± 0.09.

3.2.2. Boron Binding to Rhizoferrin. Although we have not analyzed it in the same detail as for VF, we note that the related dicitrate siderophore rhizoferrin (RF; Fig. 3.1b), also binds borate as determined by HPLC, ESI-MS, ^{11}B, ^{1}H and ^{13}C NMR (Fig. 3.18, Tables 3.2, 3.3 and 3.4). The ^{1}H NMR spectrum of free RF and RF in the presence of borate at pD 2.48 is shown in Figure 3.6. The ^{13}C NMR spectrum indicates that the RF molecule retains its two-fold symmetry when bound to boron as only eight resonances are observed. Again the only significant coordination induced shifts were for carbons 3, 13, 6 and 16 indicating binding of

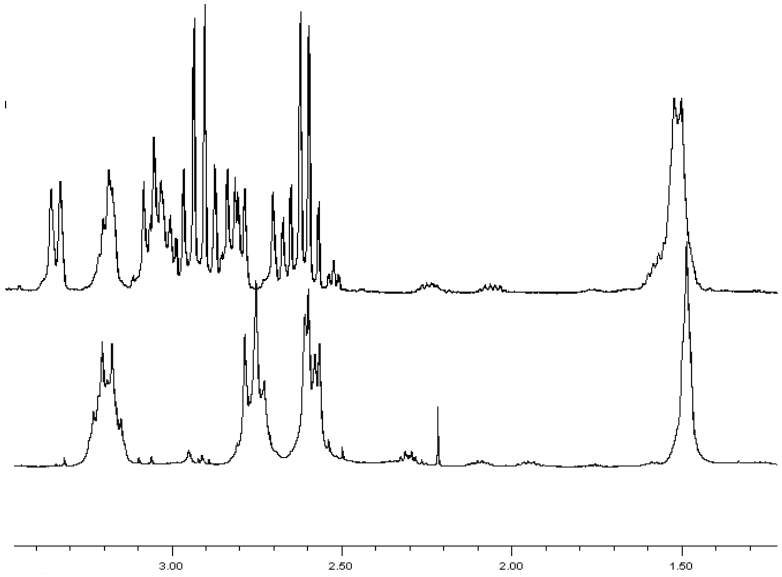

Figure 3.6. ^{1}H NMR spectra for rhizoferrin in the presence (upper) and absence (lower) of one equivalent of boric acid at pD 2.48.

the boron through the two citrate moieties (Fig. 3.18, Table 3.2). The ^{11}B peak at 9.5 ppm is close to that observed for VF providing further evidence that the binding mode is similar for both. ESI-MS of a solution of B-RF shows a peak cluster at 443 amu with the appropriate isotope pattern indicative of a 1:1 borate complex (Table 3.4). To evaluate the possible structure of such a 1:1 borate-RF complex we used the ten lowest energy conformers of the complex obtained from MMFF conformational searching algorithms as implemented in Spartan '02 (*18*) followed by geometry optimization at the DFT level (B3LYP) using Jaguar™ (Schroedinger). The resulting lowest energy structure is shown in Figure 3.7. The overall structure is very similar to that proposed for the $B(H_{-1}VF)^{1-}$ complex and is stabilized by a number of internal hydrogen bonds. The effective boron affinity of RF, log K^{D}_{eff} = 10.6 at pD 2.48, as determined by ^{11}B NMR titration, is significantly larger than the effective binding constant of VF of log K^{D}_{eff} = 8.32 as calculated for this pD from eqn (7).

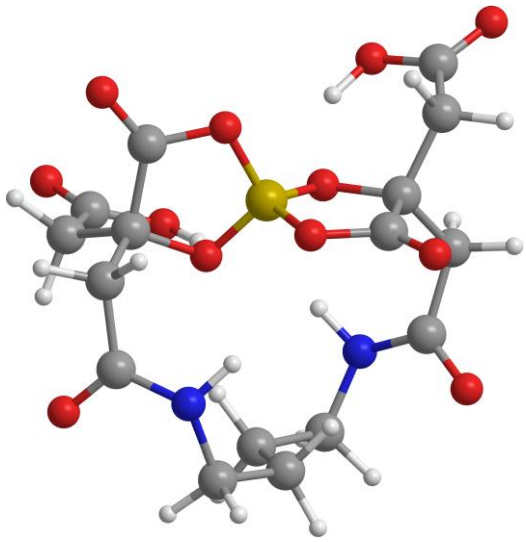

Figure 3.7. Geometry optimized structure (DFT) of the lowest energy conformer of boron-rhizoferrin.

3.2.3. Boron Binding to Petrobactin. Having established that simple dicitrate-type siderophores such as VF and RF both have significant affinity for boron, the question arises whether this is an unrecognized property of all classes of siderophores. To examine this issue we looked at petrobactin (PB), a siderophore with mixed carboxylate-catecholate functionality (Fig. 3.1c). Since PB contains both citrate and catecholate groups either of which, in principle, could bind to boron (*19, 20*) we conducted ^{1}H NMR titrations that clearly reveal that the binding of petrobactin to boron is not through the citrate group as in vibrioferrin but rather through the two catecholate functionalities (Fig. 3.8). The sharp ^{1}H NMR peaks of B-PB are suggestive of a well-defined structure. The ^{11}B NMR spectrum reveals a peak at 8.8 ppm, very close to that found for the spiro-diester formed by VF (*21, 22*). Using the structural data gleaned from the ^{1}H and ^{11}B NMR, we again determined the ten lowest energy conformers of the complex using MMFF conformational searching algorithms. Several of the lowest energy conformers were then geometry optimized at the DFT level (B3LYP) the lowest energy structure of which is shown in Figure 3.9.

Quantitative boron binding experiments were conducted next. There are seven potentially dissociable protons in the ligand, two phenolic protons from each of the two catechol

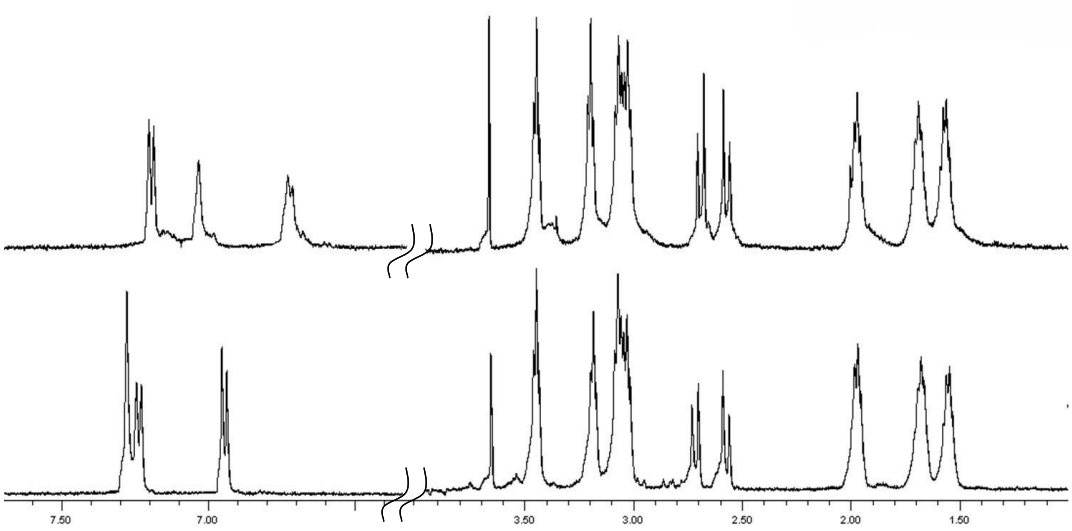

Figure 3.8. ^{1}H NMR spectra of petrobactin in the presence (upper) and absence (lower) of one equivalent of boric acid at pD 8.49.

groups, two protonated secondary amines, and the central carboxylic acid. However, the reported potentiometric titration of petrobactin detects the dissociation of only three groups, with successive pK_a values of 9.77, 7.95, and 3.13 (*23*). The pK_a value of 3.13 can be assigned to the single carboxylate group. It is more difficult to assign the two higher pK_a values to specific functional groups, since the intrinsic pK_a values of secondary amines and catechol groups overlap. However, it is not necessary to assign the macroscopic pK_a values to specific functional groups in order to measure the boron-PB binding constants.

Since we can only measure pK_a values for the loss of three protons from fully protonated H_7PB^{2+}, it is necessary to redefine the "fully-deprotonated" form of the ligand as the monoanion. As noted above, the precise location of the remaining four dissociable protons on the ligand is not known, but for convenience we will assume that the amines are deprotonated and that all four of the catechol oxygens are protonated.

Effective binding constants for the boron-PB complex have been determined from both ^{1}H and ^{11}B NMR data collected over the pD range of 6.8 to 9.4. The calculations of K_{eff}^{D}

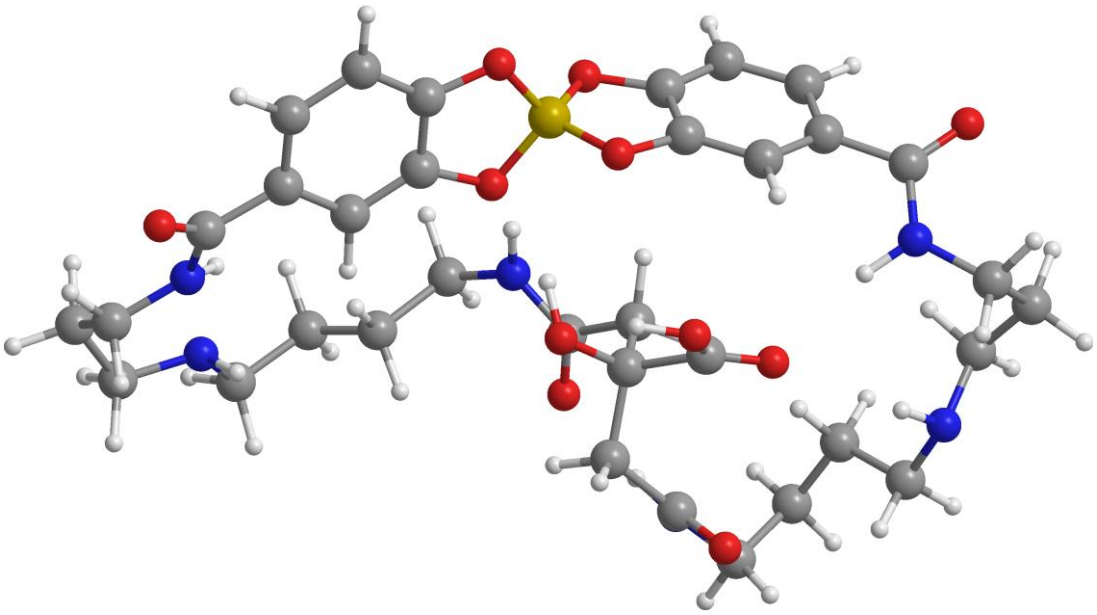

Figure 3.9. Geometry optimized structure (DFT) of the lowest energy conformer of boron-petrobactin.

incorporated both the ligand pK_a^D values and a pK_a^D of 9.63 for boric acid. Based on the interactions of borate with catechol and the NMR titrations, we had expected that petrobactin would coordinate boron through all four of the phenolic groups in the ligand. The equilibrium for this reaction would then be

$$B(OH)_3 + PB^{1-} \overset{\beta_{11-1}}{\rightleftharpoons} B(H_{-4}PB)^{2-} + H^+ \qquad (8)$$

where the three water molecules produced in the forward reaction have been omitted for clarity.

The description of the bound ligand as $H_{-4}PB^{5-}$ reflects the loss of four protons in addition to the three protons for which we have measured pK_a values. If eqn 8 accurately described the binding reaction, we would define the effective binding constant as $K_{eff} = \frac{\beta_{11-1}}{[H^+]}$, and we would expect that a plot of log K_{eff}^D vs pD would have a slope of 1. Instead, the plot of K_{eff}^D vs pD between pD 6 and 9 shown in Figure 3.10 has a slope of -0.2 $\pm$ 0.04. Such a small slope indicates that borate binding in this system consists primarily of the reaction

$$B(OH)_3 + PB^{1-} \overset{\beta_{110}}{\rightleftharpoons} B(H_{-3}PB)^{1-} \qquad (9)$$

where the three water molecules produced in the forward reaction here and in the subsequent equation have again been omitted for clarity.

If one ignores the pD dependence and simply calculates a simple mean value for the

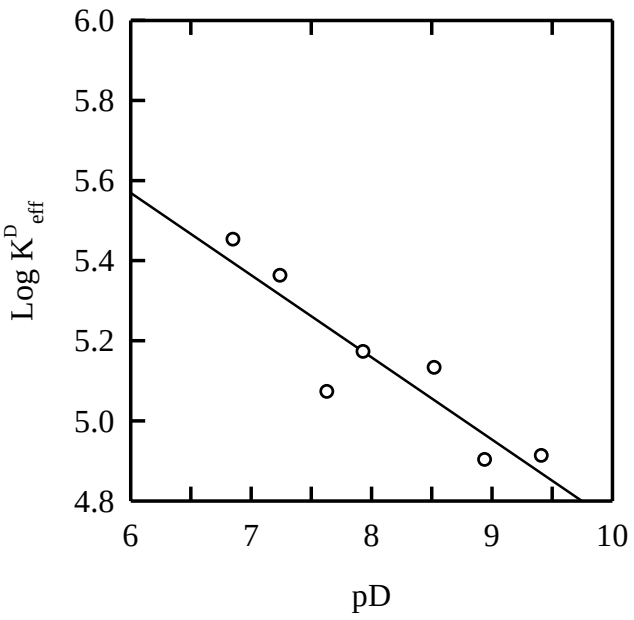

Figure 3.10. Plot of log K^D_{eff} vs pD for the binding of borate to petrobactin.

binding constant, the result is that log $K^D_{eff} = 5.1 \pm 0.2$ for eqn (9).

Although the pH dependence of the B-PB binding is small, it is still statistically significant. To account for the negative slope of the plot in Figure 3.10, it is necessary to include the equilibrium

$$B(OH)_3 + PB^{1-} + H^+ \overset{\beta_{111}}{\rightleftharpoons} B(H_{-2}PB) \qquad (10)$$

Based on eqns (9) and (10), the pH dependence of K_{eff} would be

$$K_{eff} = \beta_{110} + \beta_{111}[H^+] \quad (11)$$

A fit of K_{eff}^{D} vs $[D^+]$ to eqn (11) was used to determine β_{110}^{D} and β_{111}^{D}. The expression for β_{110} contains no protons, therefore the equilibrium for H_2O is the same as that for D_2O, i.e. $\beta_{110} = \beta_{110}^{D}$. The pK_a^D for the protonated complex was corrected using eqn (14) in the methods. The corrected values for β_{110} and β_{111} are listed in Table 1.

The final equilibrium model for PB is summarized in Figure 3.11. Given the inherently high pK_a's of the catechol groups in petrobactin, it is not necessarily surprising that protons are retained in the boron complex. In Figure 3.11 these protons have been arbitrarily placed on the secondary amines. A speciation diagram for the B-PB system for the conditions of the NMR titrations is shown in Figure 3.12. Because of the higher basicity of the ligand functional groups, there is virtually no boron binding at low pH, where the ligand is highly protonated. However, as the pH increases to approximately 7, the higher binding affinity of the catecholate groups results in the conversion of a large percentage of the petrobactin into the $B(H_{-3}PB)^{1-}$ complex. In order to produce a significant binding of borate to PB, the pH must be above the pK_a of 6.5 for the $B(H_{-2}PB)$ complex. As a result, the $B(H_{-2}PB)$ complex accumulates to a maximum of only about 3%. Because of the low degree of formation of this complex, there is less confidence in the value reported for log β_{111}.

3.2.4. Boron Binding to Aerobactin. Given the boron affinity that we have observed for the dicarboxylate siderophores VF and RF, and the catecholate petrobactin, we also examined the boron binding affinity of the other major siderophore class that has been found in marine microbes - the hydroxamates (*24, 25*). The hydroxamates constitute the longest-known and largest group of siderophores. We have therefore examined the ability of the dihydroxamate siderophore aerobactin, which has been isolated both from terrestrial sources (*26*) and from several marine *Vibrio* species (*25*), to bind boron. Using a combination of HPLC, ESI-MS and

NMR, we could find no evidence for boron binding by aerobactin at any pH between 2 and 9. No boron binding was evident even in more nonpolar solvents such as DMSO, where the binding of boron to VF was shown to be essentially complete and irreversible. Indeed no boron binding was detected for any of the hydroxamate siderophores we tested (data not shown).

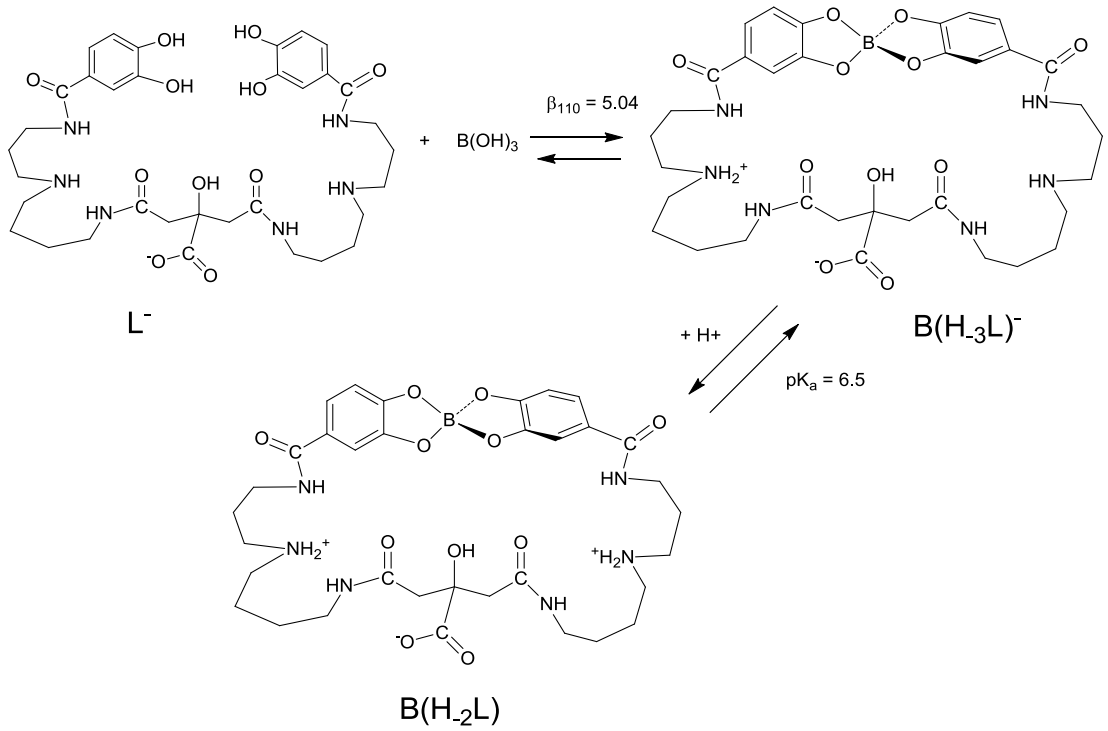

Figure 3.11. Proposed equilibrium model for the borate-PB system.

3.3. Discussion

3.3.1. α-Hydroxy Acid Binding. The α-hydroxy acid moiety has long been known to bind significantly to borate. Indeed the structure of a variety of salts of "borodicitrate" have been reported where the boron is bound in a tetrahedral fashion through the carboxylate and deprotonated α-hydroxyl groups from each of two citrates (*27*). Such a binding mode was also confirmed for VF whose ^{13}C coordination-induced shifts and position of the peak in the ^{11}B

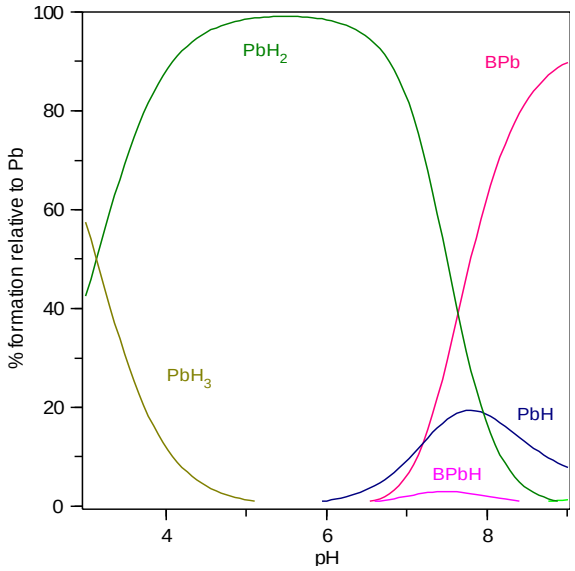

Figure 3.12. Speciation diagram for a mixture of 3.5 mM petrobactin and 3.9 mM borate as a function of pH.

NMR at 8.5 ppm are completely consistent with a spiro-borate diester structurally analogous to borodicitrate (*15*). Mass spectrometry, ^{11}B and ^{1}H NMR also suggest a similar mode of binding for another dicitrate siderophore, rhizoferrin.

The pH-dependence of boron binding by VF represents a complex balancing of factors. Increasing the pH decreases the effective binding constants, since the formal binding constants include protons as reactants. Conversely, increasing the pH up to approximately pH 6 increases the fraction of the unbound ligand in the deprotonated form, which increases the effective binding constant. In the pH range from 2 to 5 these factors largely offset one another and the percentage of boric acid bound to VF is relatively constant. However, once all the ligand has been converted to the deprotonated VF^{3-} form, further increases in pH results in a sharp decrease in the effective binding constant. This behavior is illustrated by the speciation diagram shown in Figure 3.13.

3.3.2. Catechol Binding. Martell & Smith list two binding constants for the reaction of catechol with boric acid (*28*). The 1:1 and 2:1 complexes are described respectively by the constants

$$\beta_{11-1} = \frac{[L-B(OH)_2][H^+]}{[B(OH)_3][H_2L]} = 10^{-5.13} \qquad (12)$$

$$\beta_{12-1} = \frac{[B(L)_2][H^+]}{[B(OH)_3][H_2L]^2} = 10^{-4.84} \qquad (13)$$

The value for $\beta_{12\text{-}1}$ for catechol corresponds to an effective binding constant $\beta_2^* = 10^{3.16}$ at pH 8. The effective binding constant for PB at this pH is $10^{5.04}$. Thus there appears to be a significant chelate effect associated with the binding to PB. Since the catecholate groups in PB are so widely separated in the ligand structure, the magnitude of the chelate effect suggests that the complex is stabilized by internal hydrogen bonding interactions.

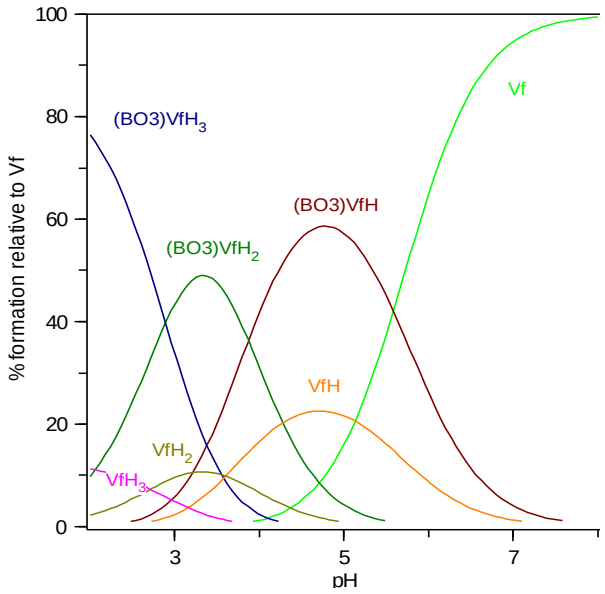

Figure 3.13. Speciation diagram for a mixture of 6.0 mM vibrioferrin and 20 mM boric acid as a function of pH.

3.3.3. Hydroxamate "binding". Siderophores have been divided into three major groups depending on the donor atoms utilized in iron binding, i.e. the catecholate, hydroxamate and carboxylate classes. Mixed siderophores are also well known. We have shown here that boron binding is significant for some, but not all, of these siderophore classes. The notable exceptions are the hydroxamates, which, although the largest class of siderophores, do not show

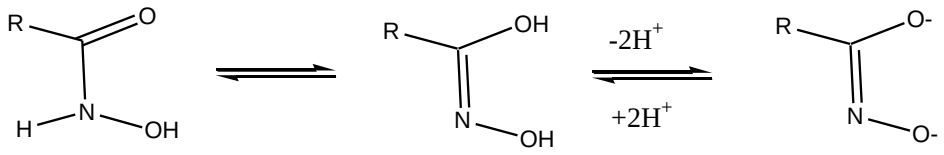

Figure 3.14. Resonance forms of hydroximates.

boron binding at any pH. Previous reports in the literature indicate that simple hydrox*i*mates but not hydrox*a*mates are capable of binding boron (*29*). This has been further confirmed by our work. The relevant criterion appears to be a vicinal dianionic dioxygen binding group (i.e. citrate or catecholate). Hydrox*i*mates have a resonance structure (Figure 3.14) that allows this while the N-substituted hydroxamates that make up all known siderophores of this class do not.

3.3.4. Biological Implications. Given the binding constants and other properties we have described here, what might be the biological implications (if any) of the ability of some siderophores to bind boron? Curiously, the first borate-siderophore complex, B-vibrioferrin, was isolated from the culture media of a bacterial "symbiont" of a toxic marine dinoflagellate, suggesting that it may have a biological function for the algal partner of the symbiosis (*15*). Despite the fact that boron is an essential trace element for various species of phytoplankton (*30-32*), these calculations suggest it is less likely that VF has a direct role in boron uptake either to the producing bacteria or the dinoflagellate partner at pH 8.0 typical of seawater. However, boron binding to VF is strongly enhanced at lower pH and in solvents other than water as shown by the fact that boron binding to VF is essentially complete and irreversible in DMSO as compared to H_2O. Thus in either an acidic or less polar microenvironment, such as in

a membrane or vesicle, boron binding by VF could be greatly enhanced. Membrane associated boron transporters have recently been described in both plants and animals although an extracellular boron scavenger is unknown (*33-35*).

The calculated binding of boron to PB under marine environmental conditions is much more significant than is the case for VF. Nevertheless, bacteria are not known to have an absolute dietary requirement for boron suggesting that its primary purpose is not to bind and transport boron. If a direct uptake and transport role for boron is less likely, the question remains as to what its biological significance may be.

While siderophores are known to primarily function to bind and transport iron from the environment into microbial cells, increasing evidence suggests that they may also play another significant role as signaling molecules. "Quorum sensing" is the term used to describe the cell density-dependent regulation of bacterial physiology, including gene expression (*36, 37*). Quorum sensing bacteria excrete low molecular weight chemical "messenger" molecules into the environment, which when a critical concentration is reached, trigger a signal transduction cascade. This signal cascade results in an alteration of gene expression, ostensibly in a population dependent manner. Siderophore production and other iron transport genes are among those long reported to be under "quorum sensing" control (*38, 39*). An additional link between quorum sensing and iron regulation has been uncovered with the observation that certain quorum sensing molecules also possess the ability to bind iron and thus influence siderophore production and use (*40*). Of more direct relevance are the numerous recent reports that siderophores themselves can have a cell signaling function in addition to their iron uptake and transport roles. For example pyoverdin is reported to regulate not only its own production but also that of several other secreted virulence factor proteins in *Pseudomonas aeruginosa (41)*. Siderophores produced by one species of marine bacteria have also been reported to induce production of siderophores from a previously nonproducing and unrelated bacterium (*42, 43*).

Simplistically, a quorum sensing role for siderophores might provide a convenient rationale for what has long been an enigma in the area of marine siderophores: namely, why should free living marine bacteria produce and excrete a metabolically expensive molecule such as a siderophore if there is such a low probability of its recapture and uptake into the cell, as would be the case in an open aqueous environment. What however if there were a reasonable chance for recapture and uptake, such as would be present when there were a large number of bacteria in a small space such as a biofilm or other micro-niche? From this point of view it would be reasonable for siderophores to be produced in large amounts when conditions for successful recapture exist i.e. under a type of quorum sensing control. Indeed an alternative view of the whole quorum sensing concept is that it is rather a diffusion sensing instead of a direct population sensing (*44, 45*). If we accept for the moment the concept of siderophores as quorum sensing molecules, what then is the relationship to boron binding?

Structurally characterized boron-containing natural products are confined to just a few macrolide antibiotics and a bacterial quorum-sensing molecule known as AI-2 (*46, 47*). We believe that it is highly significant that virtually all of these molecules originate from marine organisms. Most telling is that AI-2 functions as a signal molecule in its boronylated form in marine environments but in its unboronylated form in terrestrial ones (*48*). The observed affinity of certain siderophores for borate, a common chemical species in the marine but not the terrestrial environment, allows for significant concentrations of B-siderophore to exist even at oceanic pH. These concentrations, though small, could be sufficient for them to function as signaling molecules. Binding of the tetrahedral boron to these siderophores will also result in a conformation that is different from either the free siderophore or the iron complex, allowing a distinction to be made between its iron uptake and any cell signaling roles. Experimental work designed to address these issues is underway.

3.4. Methods

3.4.1. Siderophore isolation. Vibrioferrin isolation from *Marinobacter spp.* DG870 and DG979 was described previously (*15*). A sample of petrobactin was kindly provided by Prof. Alison Butler (UCSB) and a sample of rhizoferrin by Prof. Günther Winkelmann (University of Tübingen).

3.4.2. Potentiometric Titrations. Standard carbonate-free solutions of NaOH were prepared from Dilut-it™ ampules (Baker) using doubly deionized boiled water and stored under argon, which had been passed over Ascarite™. Base solutions were standardized with KHP to the phenolphthalein end point. The absence of carbonate was confirmed by Gran's plot (*49*). The potentiometric titrations were performed on a Mettler-Toledo DL50 instrument. The hydrogen ion concentration was measured using a Mettler-Toledo DG111-5C electrode, which was corrected to read the negative log of the hydrogen ion concentration directly using dilute HCl solution. The titrations were performed in a jacketed titration vessel connected to a constant-temperature water bath, which was kept at 25.00 ± 0.05^{o}C, and the ionic strength was fixed with 0.10 M NaCl. The solution was kept under an argon atmosphere throughout the titration. The ligand protonation constants were determined from nonlinear refinement of the data using the program BEST.[16]

3.4.3. NMR Titrations. All NMR experiments were carried out on a Varian 500 MHz instrument using standard pulse sequences for the ^{1}H and ^{11}B experiments. To eliminate the broad borosilicate background of glass, quartz NMR tubes were used in all titrations. A solution of boric acid at pH 2 was used as an external ^{11}B standard throughout the titrations. All boron complexes were obtained by the incremental addition of boric acid from a stock solution, which was prepared by dissolving a known, dried amount of boric acid in D_2O, to a 7 mM solution of siderophore in D_2O. The hydrogen (deuterium) ion concentration was measured using an Accumet AB15 pH meter with an Accumet MicroProbe pH electrode. The electrode was

calibrated using standard buffers in H_2O. The meter readings in D_2O were corrected by adding 0.44 to obtain values of pD (*50*). The pD titrations were carried out by the addition of NaOD solution, which was prepared by dissolving metallic sodium in a D_2O solution. The base was standardized by titration against potassium hydrogen phthalate to the phenolphthalein end point. The titration solutions were left to equilibrate for a minimum of 6 hours after each addition of NaOD or boric acid.

In the analyses of the NMR titration data, the pK_a values for VF measured in H_2O were corrected to pK_a^D values for use with D_2O solutions. Literature values of pK_a^D were used to prepare a plot of pK_a^D vs pK_a that contained 12 data points representing 8 different acids (*51-53*). There is an excellent linear correlation ($R^2 = 0.998$) between pK_a^D and pK_a that is described by the function

$$pK_a^D = (1.031 \pm 0.014)\,(pK_a) + (0.395 \pm 0.084) \qquad (14)$$

The calculations of effective boron binding constants from NMR data were based on pD and pK_a^D values. The effective binding constants were fitted to various functions of formal binding constants (β^D) and pD. Any values of β^D that involved deuterium ion as explicit reactant or product were then corrected to β values for H_2O by use of eqn (14). Since eqn (14) is based on pK_a's for monoprotic reactions (i.e stepwise pK_a values, rather than overall β values), the equilibrium constants measured for boron binding to siderophore were formulated as single-proton, stepwise constants, and then corrected to the appropriate value for H_2O solutions. Effective binding constants, for which the overall proton stoichiometry was not known, have not been corrected and are reported as K_{eff}^D values that are valid for D_2O solutions.

3.4.4. Electrospray-ionization Mass Spectrometry. High-resolution mass spectra were obtained on a Micromass (Manchester, UK) QTOF-2 time of flight mass spectrometer (made

available to us at UCSB by the courtesy of Prof. Alison Butler) with an electrospray ionization source. Samples (in aqueous solution, 30 mM NH_4HCO_3 buffer or methanol) were injected by a Harvard Apparatus (Holliston, Massachusetts 01746, USA) infusion pump at a rate of 5 μL/min. For exact mass measurements an internal standard of known mass (H9985, an octapeptide with m/z = 829.5393), was co-infused with the samples of free vibrioferrin (VF) or the borate-vibrioferrin complex (B-VF). The exact mass measured for the parent peak of B-VF in negative ion mode of 440.0971 agrees to within 4.1 ppm with that calculated for $C_{16}H_{18}{}^{10}BN_2O_{12}$ (440.0989). Routine ESI-MS and MS/MS spectra were obtained on a Finnigan LCQ ion-trap mass spectrometer equipped with an ESI source (Finnigan MAT, San Jose, CA). MS/MS spectra were obtained utilizing a collision voltage between 20-50 V and argon as the collision gas. Isotope distribution patterns were simulated using the program IsoPro 3.0

3.5. Appendix

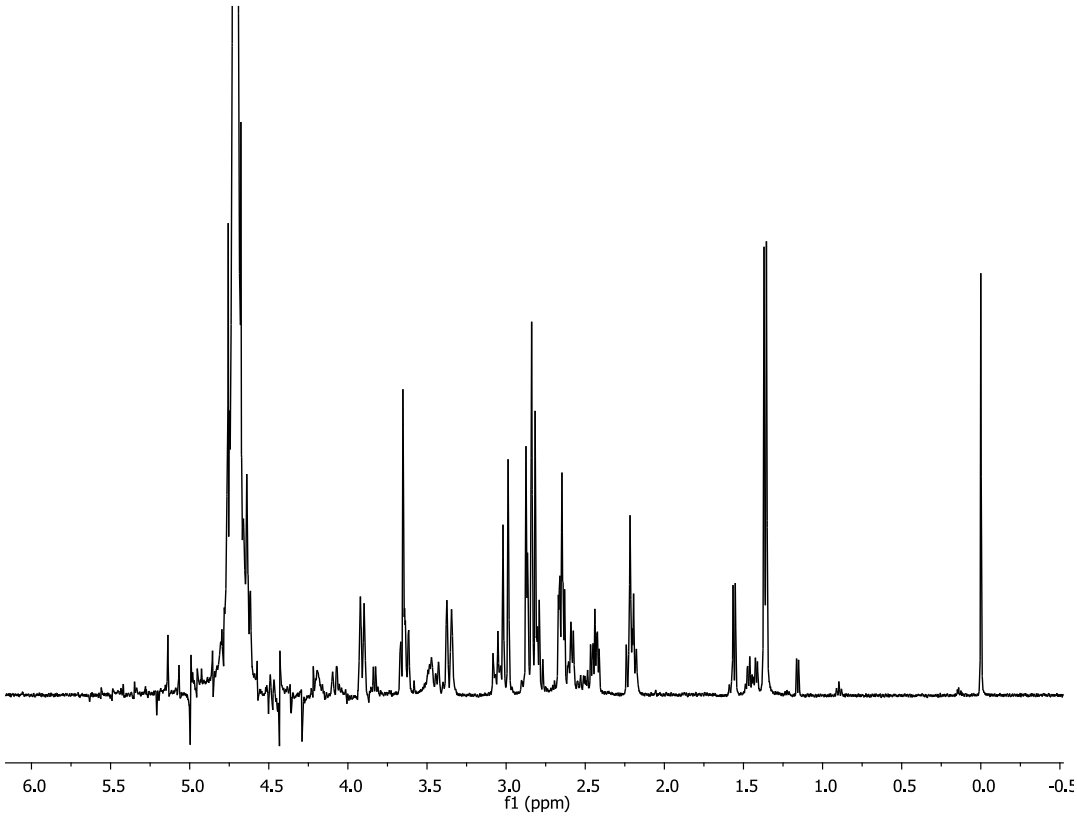

Figure 3.15. ^{1}H NMR spectrum of B-VF in D_2O. Boron was added as boric acid at pD 2.6 to reach a final equivalent of 3:1 boric acid to VF. At this ratio, no appreciable amounts of VF are present in solution. Spectrum was referenced to DSS at 0.0 ppm.

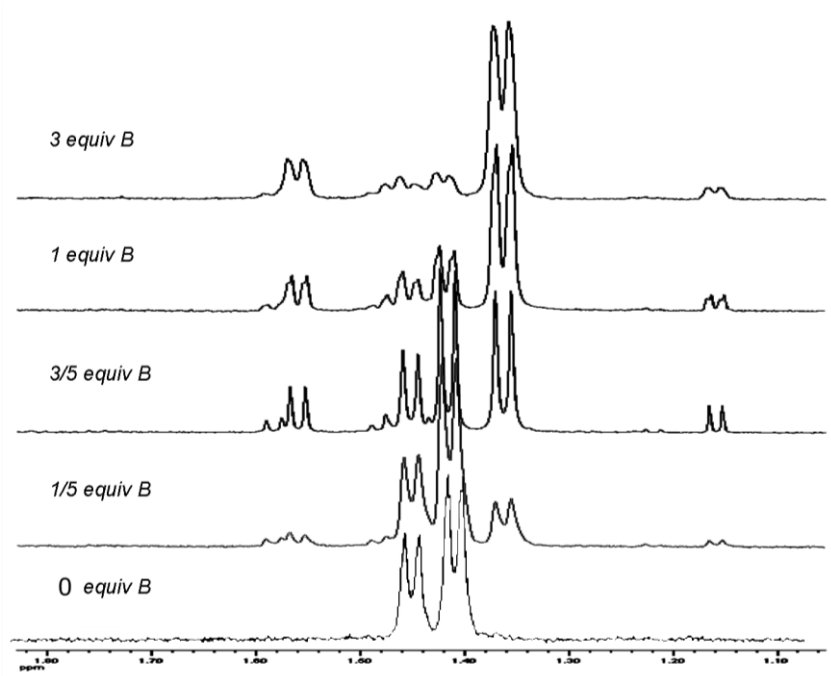

Figure 3.16. ^{1}H NMR titration of vibrioferrin with increments of boric acid. Only the resonance of the alanine's $-CH_3$ of VF are shown. At 0 equivalents of boron only the two doublets of the two forms of VF are visible at 1.41, and 1.45 ppm (*5*) but as more boric acid is added, new doublets belonging to B-VF arise at 1.36 and 1.56 ppm. Minor doublets visible elsewhere are presumably due to minor B-VF species that were thermodynamically less stable and eventually disappeared. Boric acid was prepared according to the Methods section and pD was maintained at 2.6.

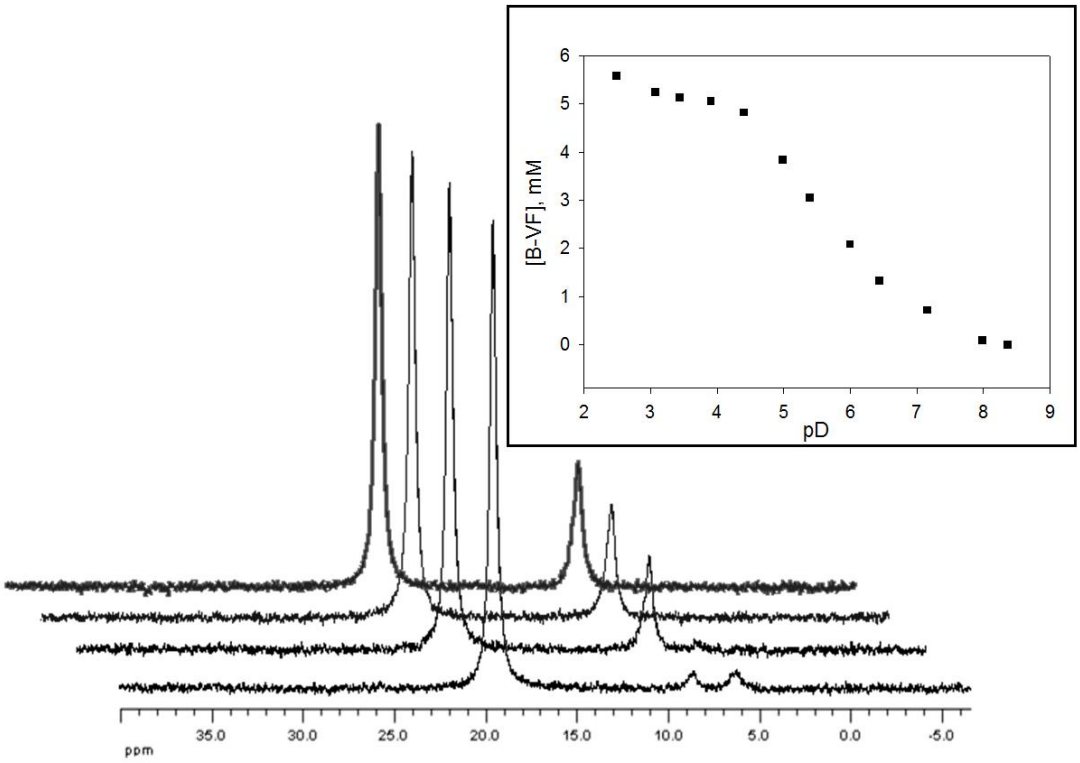

Figure 3.17. pD titration of B-VF monitored with ^{11}B NMR. Overlayed spectra represent pD values of 3.0, 4.9, 5.4, and 7.1 (top to bottom). Inset: plot of $[\text{B-VF}]_{\text{total}}$ calculated from B-VF peak at 8.5 ppm as a function of pD. Spectrum was referenced relative to an external standard of 4 mM boric acid (pH 2.0) at 20 ppm. pD was changed by adding known amounts of NaOD at 20°C, I = 0 M.

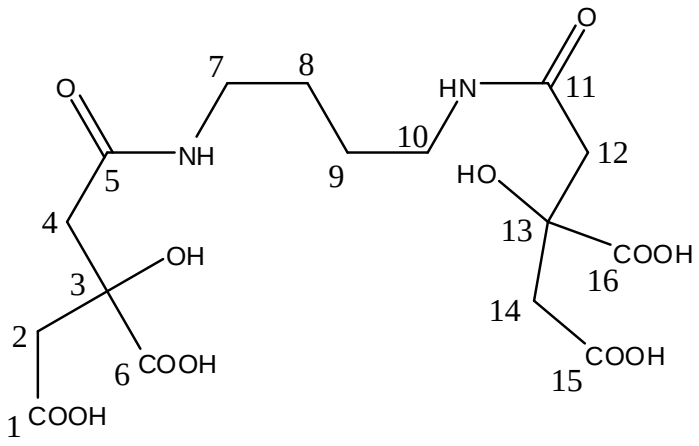

Figure 3.18. Structure and numbering scheme of rhizoferrin (RF).

Table 3.2. ^{13}C-NMR data of Rhizoferrin and boronylated Rhizoferrin in D_2O.

Assignment*	Rhizoferrin (ppm)	Boronylated Rhizoferrin (ppm)	Δ (ppm)
C8,C9	**28.3**	**28.9**	**- 0.6**
C7,C10	**41.5**	**41.2**	**0.3**
C2,C14	**45.8**	**44.6**	**1.2**
C4,C12	**47.3**	**46.9**	**0.4**
C3,C13	**76.3**	**81.2**	**- 4.9**
C5,C11	**173.6**	**173.2**	**0.4**
C1,C15	**176.2**	**175.7**	**0.5**
C6,C16	**179.3**	**184.1**	**- 4.8**

* Consult Fig. 3.18 for atom assignments.

Table 3.3. ^{1}H-NMR data of boronylated Rhizoferrin in D_2O.

Assignment*	***Boronylated Rhizoferrin (ppm)***
8A/9A	1.50 (d)
8B/9B	1.52 (dd)
7A	3.34 (d)
7B	3.03 (m)
10A	3.20 (m)
10B	3.03 (m)
4A/12A	2.62 (dd)
4B	2.68 (m)
12B	2.81 (m)
2A/14A	2.92 (dd)
2B	2.82 (m)
14B	3.06 (m)

* Consult Fig. 3.18 for atom assignments.

Table 3.4. Comparison between physical characterization parameters for B-RF and RF.

	Rhizoferrin	**Boronylated Rhizoferrin**
Calculated Mass	436.1	443.1
Observed Mass (negative ion)	435.1	443.1
^{11}B NMR δ (ppm)	—	9.5

3.6. Acknowledgments

This work was supported by California SeaGrant 020-C-N. The authors thank Günther Winkelmann at the University of Tübingen for a sample of rhizoferrin and Alison Butler at the University of California, Santa Barbara for a sample of petrobactin. This chapter has been previously published as Harris, W. R., Amin, S. A., Küpper, F. C., Green, D. H., and Carrano, C. J. (2007) Borate binding to siderophores: structure and stability, *J. Am. Chem. Soc. 129*, 12263-12271.

3.7. References

1. Black, K. D., and Shimmield, G. B. (2003) *Biogeochemistry of marine systems*, Blackwell Publishing, Oxford, UK.

2. Bruland, K. W., Donat, J. R., and Hutchins, D. A. (1991) Interactive influences of bioactive trace metals on biological production in oceanic waters, *Limnol. Oceanogr. 36*, 1555-1577.

3. Martin, J. H., and Fitzwater, S. E. (1988) Iron deficiency limits phytoplankton growth in the north-east Pacific subarctic, *Nature 331*, 341-343.

4. Wu, J., and Luther III, G. W. (1994) Size-fractionated iron concentrations in the water column of the western North Atlantic ocean, *Limnol. Oceanogr. 39*, 1119-1129.

5. Yamamoto, S., Okujo, N., Yoshida, T., Matsuura, S., and Shinoda, S. (1994) Structure and iron transport activity of vibrioferrin, a new siderophore of *Vibrio parahaemolyticus*, *J. Biochem., Tokyo 115*, 868-874.

6. Rue, E. L., and Bruland, K. W. (1995) Complexation of iron(III) by natural organic ligands in the Central North Pacific as determined by a new competitive ligand equilibration/adsorptive cathodic stripping voltammetric method, *Mar. Chem. 50*, 117-138.

7. van den Berg, C. M. G. (1995) Evidence for organic complexation of iron in seawater, *Mar. Chem. 50*, 139-157.

8. Winkelmann, G., and Carrano, C. J., (Eds.) (1997) *Transition metals in microbial metabolism*, Harwood Academic Pub., Amsterdam, The Netherlands.

9. Winkelmann, G. (1991) *CRC handbook of microbial iron chelates*, CRC Press, Boca Raton.

10. Raymond, K. N. (1994) Recognition and transport of natural and synthetic siderophores by microbes, *Pure Appl. Chem. 66*, 773-781.

11. Sandy, M., and Butler, A. (2009) Microbial iron acquisition: marine and terrestrial siderophores, *Chem. Rev. 109*, 4580-4595.

12. Raymond, K., Müller, G., and Matzanke, B. (1984) Complexation of iron by siderophores a review of their solution and structural chemistry and biological function, In *Struct. Chem.*, pp 49-102.

13. Butler, A. (2005) Marine siderophores and microbial iron mobilization, *BioMetals 18*, 369-374.

14. Vraspir, J. M., and Butler, A. (2009) Chemistry of marine ligands and siderophores, *Annu. Rev. Mar. Sci. 1*, 43-63.

15. Amin, S. A., Küpper, F. C., Green, D. H., Harris, W. R., and Carrano, C. J. (2007) Boron binding by a siderophore isolated from marine bacteria associated with the toxic dinoflagellate *Gymnodinium catenatum*, *J. Am. Chem. Soc. 129*, 478-479.

16. Bowen, H. J. M. (1966) *Trace elements in biochemistry*, Academic Press, London, New York,.

17. (2002) TableCurve 2D, SYSTAT Software, Inc., Richmond, CA.

18. (2002) Spartan '02, Wavefunction Inc., Irvine, CA.

19. Yoshino, K., Kotaka, M., Okamoto, M., and Kakihana, H. (1979) Boron-11 NMR study of the complex formation of borate with catechol and L-dopa, *Bull. Chem. Soc. Jpn. 52*, 3005-3009.

20. Barnes, H. H., and Ishimaru, C. A. (1999) Purification of catechol siderophores by boronate affinity chromatography: identification of chrysobactin from *Erwinia carotovora* subsp. carotovora, *BioMetals 12*, 83-87.

21. Pizer, R., and Ricatto, P. J. (2002) Ternary alkaline earth metal complex ions in the M^{2+}/borate/tartrate system as studied by ^{11}B NMR, *Inorg. Chem. 33*, 4985-4990.

22. Semmelhack, M. F., Campagna, S. R., Hwa, C., Federle, M. J., and Bassler, B. L. (2004) Boron binding with the quorum sensing signal AI-2 and analogues, *Org. Lett. 6*, 2635-2637.

23. Zhang, G., Amin, S. A., Küpper, F. C., Holt, P. D., Carrano, C. J., and Butler, A. (2009) Ferric stability constants of representative marine siderophores: marinobactins, aquachelins, and petrobactin, *Inorg. Chem. 48*, 11466-11473.

24. Martinez, J. S., Haygood, M. G., and Butler, A. (2001) Identification of a natural desferrioxamine siderophore produced by a marine bacterium, *Limnol. Oceanogr. 46*, 420-424.

25. Haygood, M. G., Holt, P. D., and Alison, B. (1993) Aerobactin production by a planktonic marine *Vibrio* sp., *Limnol. Oceanogr. 38*, 1091-1097.

26. Gibson, F., and Magrath, D. I. (1969) The isolation and characterization of a hydroxamic acid (aerobactin) formed by *Aerobacter aerogenes* 62-I, *Biochim Biophys Acta 192*, 175-184.

27. Zviedre, I. I., Fundamenskii, V. S., Krasnikov, V. V., and Kolesnikova, G. P. (1985) Crystal structure of potassium borodicitrate (dicitratoborate) $K[(C_6H_6O_7)_2B]\cdot 2H_2O$, *J. Struct. Chem. 25*, 593-599.

28. Martell, A. E., and Smith, R. M. (1974) *Critical stability constants*, Plenum Press, New York.

29. Fields, A. R., Daye, B. M., and Christian, R., Jr. (1966) Borate complexes of benzohydroxamic acid and some of its derivatives, *Talanta 13*, 929-937.

30. Lewin, J., and Chen, C.-H. (1976) Effects of boron deficiency on the chemical composition of a marine diatom, *J. Exp. Bot. 27*, 916-921.

31. Lewin, J. (1966) Boron as a growth requirement for diatoms, *J. Phycol. 2*, 160-163.

32. Eyster, C. (1952) Necessity of boron for *Nostoc muscorum*, *Nature 170*, 755.

33. Takano, J., Noguchi, K., Yasumori, M., Kobayashi, M., Gajdos, Z., Miwa, K., Hayashi, H., Yoneyama, T., and Fujiwara, T. (2002) *Arabidopsis* boron transporter for xylem loading, *Nature 420*, 337-340.

34. Takano, J., Miwa, K., Yuan, L., von Wiren, N., and Fujiwara, T. (2005) Endocytosis and degradation of BOR1, a boron transporter of *Arabidopsis thaliana*, regulated by boron availability, *Proc. Natl. Acad. Sci. U. S. A. 102*, 12276-12281.

35. Park, M., Li, Q., Shcheynikov, N., Zeng, W., and Muallem, S. (2004) NaBC1 is a ubiquitous electrogenic Na^+-coupled borate transporter essential for cellular boron homeostasis and cell growth and proliferation, *Mol. Cell 16*, 331-341.

36. Waters, C. M., and Bassler, B. L. (2005) Quorum sensing: cell-to-cell communication in bacteria, *Annu. Rev. Cell Dev. Biol. 21*, 319-346.

37. Reading, N. C., and Sperandio, V. (2006) Quorum sensing: the many languages of bacteria, *FEMS Microbiol. Lett. 254*, 1-11.

38. Guan, L. L., and Kamino, K. (2001) Bacterial response to siderophore and quorum-sensing chemical signals in the seawater microbial community, *BMC Microbiol. 1*, 27.

39. Fong, K. P., Gao, L., and Demuth, D. R. (2003) *luxS* and *arcB* control aerobic growth of *Actinobacillus actinomycetemcomitans* under iron limitation, *Infect. Immun. 71*, 298-308.

40. Diggle, S. P., Matthijs, S., Wright, V. J., Fletcher, M. P., Chhabra, S. R., Lamont, I. L., Kong, X., Hider, R. C., Cornelis, P., Camara, M., and Williams, P. (2007) The *Pseudomonas aeruginosa* 4-quinolone signal molecules HHQ and PQS play multifunctional roles in quorum sensing and iron entrapment, *Chemistry & Biology 14*, 87-96.

41. Lamont, I. L., Beare, P. A., Ochsner, U., Vasil, A. I., and Vasil, M. L. (2002) Siderophore-mediated signaling regulates virulence factor production in *Pseudomonas aeruginosa*, *Proc. Natl. Acad. Sci. U. S. A. 99*, 7072-7077.

42. Guan, L. L., Onuki, H., and Kamino, K. (2000) Bacterial growth stimulation with exogenous siderophore and synthetic N-acyl homoserine lactone autoinducers under iron-limited and low-nutrient conditions, *Appl. Environ. Microbiol. 66*, 2797-2803.

43. Guan, L. L., Kanoh, K., and Kamino, K. (2001) Effect of exogenous siderophores on iron uptake activity of marine bacteria under iron-limited conditions, *Appl. Environ. Microbiol. 67*, 1710-1717.

44. Redfield, R. J. (2002) Is quorum sensing a side effect of diffusion sensing?, *Trends Microbiol. 10*, 365-370.

45. Hense, B. A., Kuttler, C., Muller, J., Rothballer, M., Hartmann, A., and Kreft, J.-U. (2007) Does efficiency sensing unify diffusion and quorum sensing?, *Nat. Rev. Microbiol. 5*, 230-239.

46. Chen, X., Schauder, S., Potier, N., Van Dorsselaer, A., Pelczer, I., Bassler, B. L., and Hughson, F. M. (2002) Structural identification of a bacterial quorum-sensing signal containing boron, *Nature 415*, 545-549.

47. Pache, W., and Zahner, H. (1969) Metabolic products of microorganisms. 77. Studies on the mechanism of action of boromycin, *Arch. Mikrobiol. 67*, 156-165.

48. Miller, S. T., Xavier, K. B., Campagna, S. R., Taga, M. E., Semmelhack, M. F., Bassler, B. L., and Hughson, F. M. (2004) *Salmonella typhimurium* recognizes a chemically distinct form of the bacterial quorum-sensing signal AI-2, *Mol. Cell 15*, 677-687.

49. Gran, G. (1952) Determination of the equivalence point in potentiometric titrations. Part II, *Analyst 77*, 661-670.

50. Krezel, A., and Bal, W. (2004) A formula for correlating pKa values determined in D_2O and H_2O, *J. Inorg. Biochem. 98*, 161-166.

51. Covington, A. K., Paabo, M., Robinson, R. A., and Bates, R. G. (2002) Use of the glass electrode in deuterium oxide and the relation between the standardized pD (paD) scale and the operational pH in heavy water, *Anal. Chem. 40*, 700-706.

52. Glasoe, P. K., and Long, F. A. (2002) Use of glass electrodes to measure acidities in deuterium oxide, *The J. Phys. Chem. 64*, 188-190.

53. Gary, R., Bates, R. G., and Robinson, R. A. (2002) Second Dissociation Constant of Deuteriophosphoric Acid in Deuterium Oxide from 5 to 50°. Standardization of a pD Scale, *The J. Phys. Chem. 68*, 3806-3809.

4. Photolysis of iron-siderophore chelates promotes bacterial-algal mutualism

4.1. Introduction

The growth and species composition of microalgal communities in the ocean are often regulated by the micronutrient iron (*1*), which in turn influences climate by controlling biogenic calcification, oceanic sequestration of CO_2 and biological release of dimethylsulfide (*2, 3*). Iron may also influence blooms of toxic or harmful algae that have occurred with increasing frequency in recent decades, and have caused substantial ecological and economic damage worldwide (*4*). Many bloom-forming algal species, including climatically important dinoflagellates and coccolithophores (*2, 3*), are known to form beneficial or obligatory close associations with certain bacteria, but the reasons for these associations remain obscure (*5-8*). The bacteria that closely associate with phytoplankton are believed to be involved in a wide range of interactions including metabolite/nutrient uptake, provision and remineralization (*5, 6*), cell differentiation (*7*) as well as algicidal or bacterioprotective effects (*8, 9*). However, these interactions are poorly understood and only a few well-studied examples exist.

Among the most intriguing factors that may involve algal-bacterial interactions is iron acquisition. Iron is an essential element for photosynthesis and respiration and limits primary productivity and bacterial growth in much of the ocean due to its poor solubility and resultant exceedingly low concentration (*1, 10, 11*). To alleviate limitation of this key micronutrient, many marine heterotrophic bacteria and some cyanobacteria produce siderophores, small organic molecules that tightly bind iron and thereby increase its solubility (*12*). The bacteria then take up the siderophores via outer membrane transporters that are specific for different groups of siderophores. By contrast, eukaryotic phytoplankton are not known to produce siderophores or to directly take up bacterially derived Fe(III)-siderophore complexes. However, many eukaryotic phytoplankton are able to access iron from siderophores or other chelates via ferrireductases and adjacent Fe(II) transporters on their outer cell membranes for which genomic evidence exists in diatoms and green algae (*13*).

4.2. Results

We have previously observed that the bacterial community co-occurring with the toxic dinoflagellate *Gymnodinium catenatum* bears a remarkable similarity to the bacterial communities of other marine dinoflagellates from different algal collections (*14*). Among the most notable members of these communities were bacteria phylogenetically affiliated with the α-proteobacterial *Roseobacter* and the γ-proteobacterial *Marinobacter* clades. Here, examining a larger set of cultures, we find that members of the genus *Marinobacter* were detected in 83% of dinoflagellate and 87% of the coccolithophorid cultures we examined whereas *Marinobacter* spp. were found less frequently in diatom cultures (Tables 4.1). These closely related *Marinobacter* spp. have also been cultured from dinoflagellates by others, corroborating the idea that several species of *Marinobacter* are very frequently associated with dinoflagellates and coccolithophores (*15, 16*).

Table 4.1. *Marinobacter* spp. distribution among phytoplankton cultures examined.

Algal Lineage	**Cultures (n)**	***Marinobacter* (%)**
Diatoms	27	22
Dinoflagellates	18	83
Coccolithophores	8	87
Total	53	53

While these algal-associated species were closely related to other *Marinobacter* species (e.g. *M. hydrocarbonoclasticus* or *Marinobacter* sp. DS40M8), most of the tested strains did not produce the siderophores commonly produced by free-living members of the *Marinobacter* genus (e.g. petrobactin and the marinobactins; Fig. 4.1) (*12*). This observation prompted us to screen a larger number of *Marinobacter* isolates for their siderophore production using a

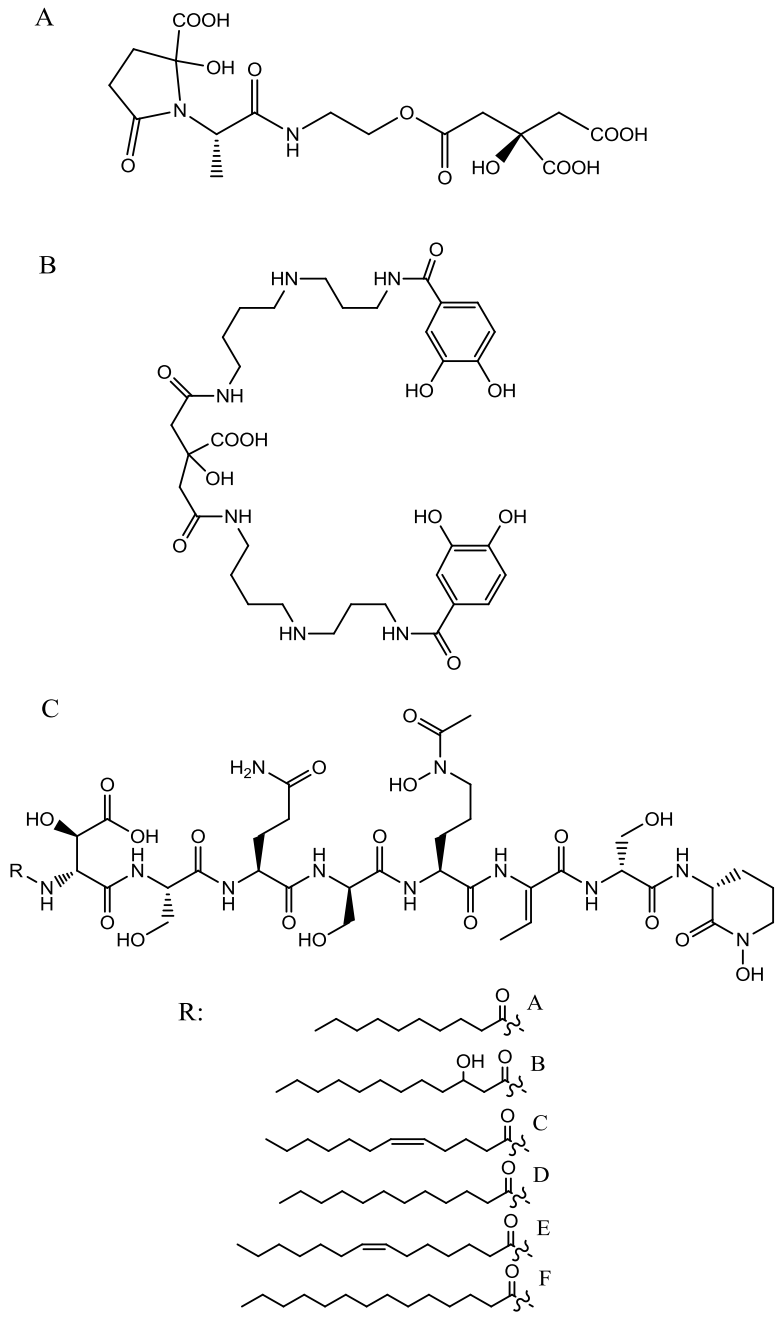

Figure 4.1. Structures of some of the siderophores produced by *Marinobacter* spp. Vibrioferrin (A), petrobactin (B), and the marinobactins (C).

combination of LC-MS, NMR, growth promotion assays and PCR of selected siderophore biosynthetic genes (Fig. 4.2). The known molecule vibrioferrin (VF; Fig. 4.1) was the only siderophore detected in two particular algal-associated subclades suggesting that: a) siderophore

production may be a useful chemotaxonomic marker for algal-associated *Marinobacter* species and b) there might be some unique functional significance for VF production (*17*, *18*).

Vibrioferrin is a member of the carboxylate class of siderophores containing two α-hydroxy acid groups. It was originally isolated from *Vibrio parahaemolyticus*, an estuarine enteropathogenic bacterium associated with seafood-borne gastroenteritis (*17*). We observed several unique features of vibrioferrin and its iron chemistry that differed substantially from most other siderophores produced by free living marine bacteria. The first was its only moderate affinity for binding iron (conditional stability constant in seawater relative to Fe', log $K^{cond}_{FeL,Fe'}$ = 10.93 ± 0.03) owing to the presence of only five iron-binding ligand groups and placing it on par with the weaker class of generic iron binding ligands found in the ocean (*19*). Most other marine siderophores contain six donor groups and hence form much more stable ferric chelates (*12*). However the most remarkable feature of VF is the striking sensitivity of its iron complex to light. Siderophores containing α or β-hydroxy acid moieties are known to undergo photochemical reactions involving the oxidative cleavage of a carboxylate group and the concomitant reduction of Fe(III) to Fe(II) (*20, 21*). The Fe(II) thus produced can then dissociate from the "degraded" siderophore, and be re-oxidized to soluble inorganic ferric hydrolysis species (designated Fe(III)'), which are highly bioavailable to algal cells (*22*, *23*). It has been shown that the photolysis of certain ferric chelates and the resultant production of dissolved Fe(II) and Fe(III)' species increases the uptake of iron by marine phytoplankton (*20, 22*). However, the efficiency of this mechanism in increasing the bioavailability of iron is open to question because of the unexpected observation that the photoproducts formed for many photoactive marine siderophores retain the ability to strongly coordinate Fe(III) (*20, 24, 25*). Indeed in some cases the photoproduct is actually a better Fe(III) chelator than the parent siderophore (*24*, *25*).

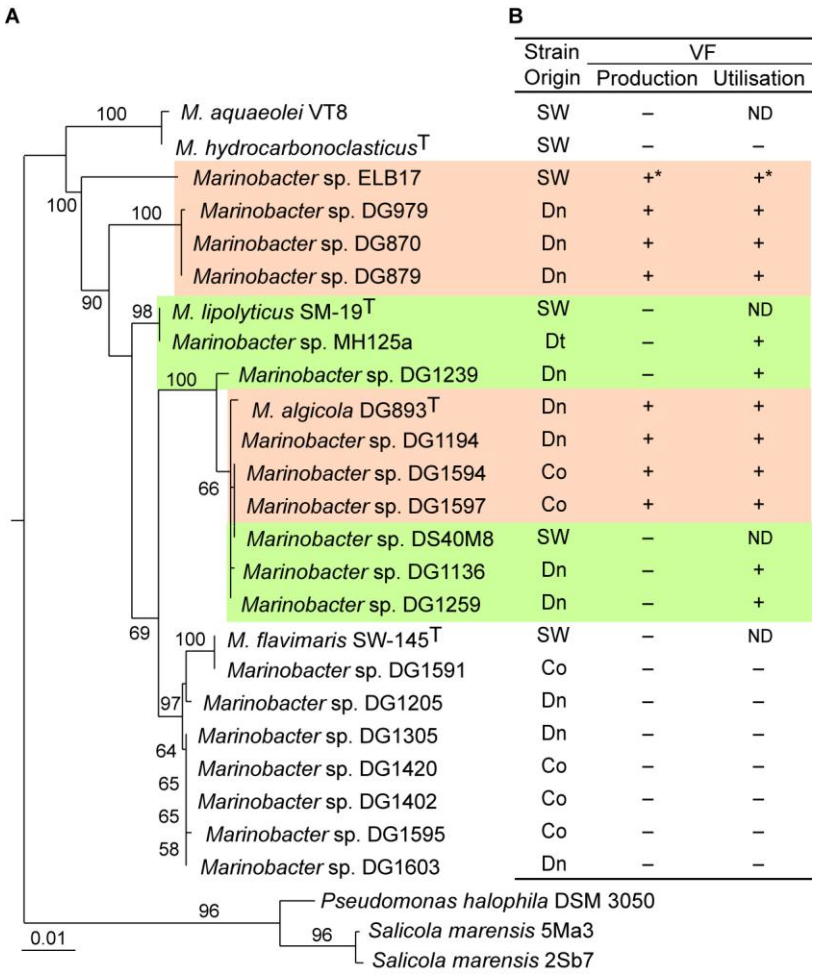

Figure 4.2. 16S rRNA gene phylogeny of the *Marinobacter* clade and VF production profile. (A) Maximum likelihood neighbor-joining tree with bootstrap support (≥50 %) of *Marinobacter* 16S rRNA genes. (B) Production and utilization of VF by *Marinobacter* for iron acquisition, as determined by LC-MS, NMR, PCR screening of VF biosynthetic genes and siderophore growth promotion assays. Seawater (SW), Dinoflagellate (Dn), Coccolithophore (Co), Diatoms (Dt), not determined (ND). Orange shading indicates those strains capable of VF production and uptake; green shading indicates VF uptake only. Bar denotes nucleotide substitutions per site. *Production and uptake were presumed based on the presence of close homologs of VF biosynthetic and uptake genes.

Because VF contains two α-hydroxy acid moieties, we anticipated that Fe(III)-VF chelates would be highly photolabile (Fig. 4.3) and indeed Fe(III)-VF demonstrated exceptional sensitivity to light. It underwent photolysis at a 10-20-fold higher rate than other photoactive siderophores such as petrobactin, marinobactin and aquachelin (Table 4.2). In addition, unlike any other marine siderophore examined thus far, the resulting photoproduct (VF^{*}) (Fig. 4.3) has

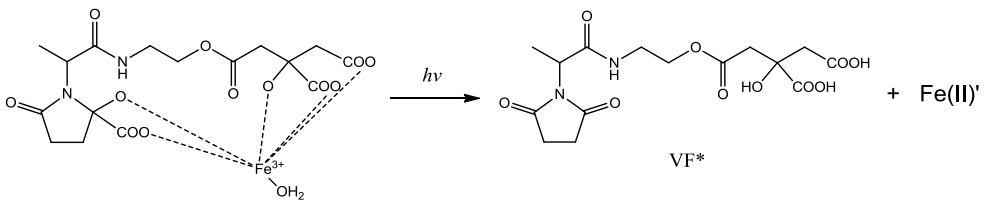

Figure 4.3. The photolysis of Fe(III)-VF in sunlight produces a photoproduct (VF*) and Fe(II)', which is quickly oxidized in seawater to Fe(III)'.

no significant affinity for iron (See Methods) which maximizes net Fe(III)' production compared to those siderophores whose photoproducts are still efficient ferric chelators. Thus the photochemistry of Fe(III)-VF is an irreversible process that leads to the destruction of the siderophore. Such a scenario would seem to be extremely disadvantageous for the producing bacterium, prompting us to examine the iron uptake kinetics of photolyzed and un-photolyzed Fe(III)-VF by *Marinobacter sp.* DG879, and its dinoflagellate host.

Growth promotion assays indicate that VF is a functional siderophore for *Marinobacter sp.* DG879 (Fig. 4.2) and ^{55}Fe-labelled VF chelates were taken up by the bacteria in a time- and concentration-dependent manner with a K_m of 17.6 μM. Fe(III)-VF uptake showed active transport behavior as indicated by its inhibition by an uncoupler of oxidative phosphorylation

Table 4.2. Rates of Fe(II) production during the photolysis of the ferric complexes of VF and other marine siderophores.

	Initial Specific Rate[a] (hr^{-1}) 2000 μEinstein m^{-2} s^{-1}	Rate of photolysis[b] (hr^{-1}) 80 μEinstein m^{-2} s^{-1}	References
Vibrioferrin	12.9 (0.017)	0.031	*this study*
Aquachelin C	0.6 (0.015)	-	*ref 20*
Petrobactin	—	0.003	*this study*
Marinobactin	—	< 0.001	*this study*

[a] Initial specific rates were determined by monitoring LMCT of $Fe^{2+}(BPDS)_3$ at 535 nm as described in the methods. Values in parentheses represent rates of Fe(II) production from dark controls. VF photolysis was conducted in natural sunlight attenuated by 75% to an intensity of 500 μEinstein m^{-2} s^{-1} and thus our measured rate was multiplied by a factor of four to give the full sunlight rate for comparison with aquachelin C.

[b] Rates were determined by monitoring changes in the LMCT bands at 330, 490 and 407 nm of the ferric complexes of VF, petrobactin and marinobactin respectively as described in the methods.

(CCCP) (Fig. 4.4). In experiments with Fe(III)-VF chelates photolyzed *in situ* with attenuated sunlight, ^{55}Fe was assimilated at a 70% higher rate than observed with un-photolyzed Fe(III)-VF (Fig. 4.4). Since the photolysis completely destroyed the VF, and VF* shows no significant affinity for either Fe(II) or Fe(III), the cells must have acquired iron from photochemically released inorganic Fe(II) or Fe(III). In addition to siderophore-mediated transport systems, many gram-negative bacteria possess siderophore-independent Fe(III) uptake systems such as the FbpABC transporter that utilizes dissolved ferric hydrolysis species, Fe(III)', and other partially chelated forms of ferric ion (*26*). Examination of the genome of the closely related VF-producer *M. algicola* DG893 reveals the presence of putative homologs to FbpA and FbpB containing the functionally important and universally conserved dityrosine unit in FbpA (Fig. 4.5) involved in the binding of ferric iron (*27*). We were not able to find homologs of specific Fe(II) transport systems indicating that the bacteria may not be able to assimilate ferrous iron. Indeed, bacterial ^{55}Fe uptake from photolyzed FeVF was diminished more than 4-fold in the presence of the reductant ascorbate, confirming that the bacteria are most likely assimilating photochemically produced ferric iron species (Fig. 4.4).

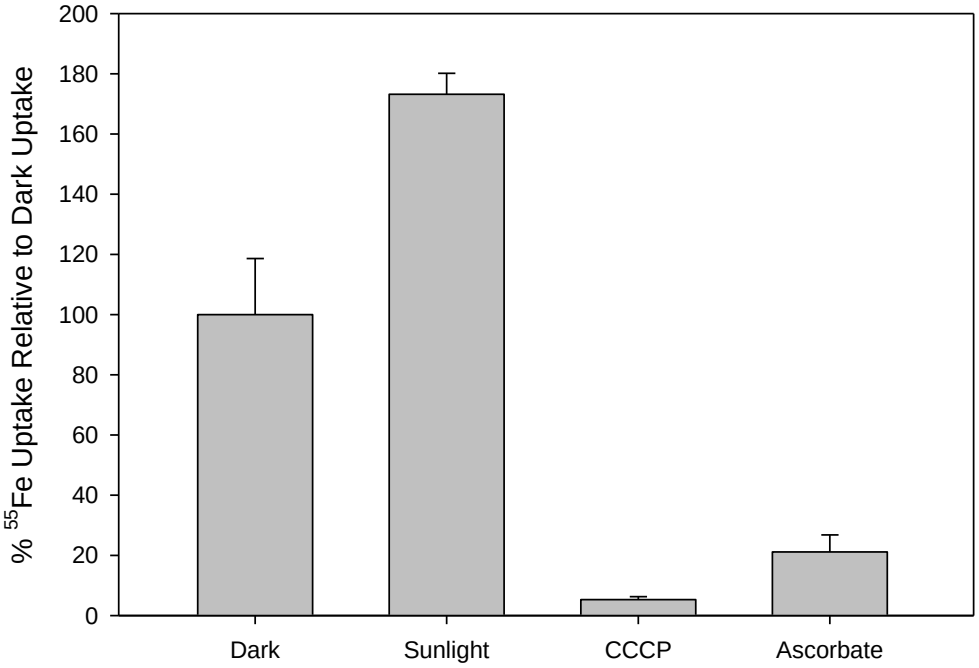

Figure 4.4. VF mediated iron uptake in *Marinobacter* sp. DG879 in the dark and in the presence of sunlight. ^{55}Fe uptake rates by *Marinobacter* sp. DG879 was performed using 1 μM Fe(III) and 3 μM total VF either in the dark or in attenuated natural sunlight (450 μEinstein m^{-2} s^{-1}) at 20°C. The uncoupler of oxidative phosphorylation, CCCP (carbonyl cyanide 3-chlorophenyhydrazone) was used as a metabolic inhibitor; incubations were carried out in the dark. The reductant ascorbate was used to prevent the oxidation of photochemically produced Fe(II) in bacteria exposed to light. Error bars represent s.d. of triplicate cultures.

While the uptake of iron from VF was expected for the producing bacteria, the question of its availability to a phytoplanktonic partner remained unresolved. For these studies we used axenic cultures of the bloom-forming dinoflagellate *Scrippsiella trochoidea* to eliminate complications that would arise in a mixed culture experiment. In the dark *S. trochoidea* assimilated iron from seawater media containing 50 nM Fe(III) and 500 nM VF at a rate of 0.74 amol Fe $cell^{-1}$ hr^{-1}. However, this rate increased more than 20-fold with *in situ* photolysis of Fe(III)-VF in the presence of attenuated sunlight (Fig. 4.6). The photolysis initially produces dissolved Fe(II), which at the pH of seawater, should have rapidly re-oxidized to dissolved Fe(III)' and colloidal ferric hydroxide particles. Thus, the enhanced uptake appeared to be linked to the much higher biological availability of these inorganic iron photolysis products, in

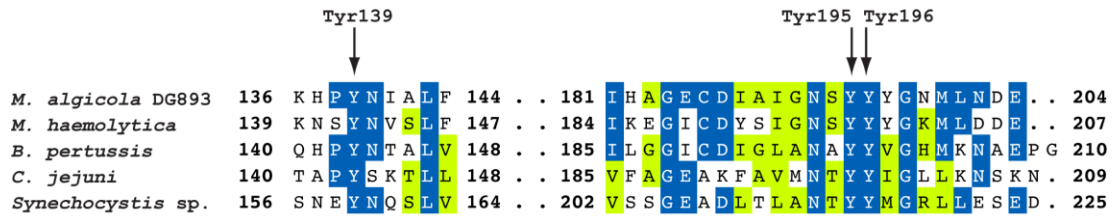

Figure 4.5. Partial predicted translation of *M. algicola* DG893 FbpA homolog aligned with known FbpA proteins. *M. algicola* DG893 accession No. EDM49388. Protein PDB ID No. are: *Mannheimia haemolytica* (1SI0), *Bordetella pertussis* (1Y9U), *Campylobacter jejuni* (1Y4T), *Synechocystis sp.* FutA1 (2PT2). Alignment was performed using Muscle as implemented in CLC Sequence Viewer (Vers. 6). Identical residues are depicted with blue shading and similar residues with green shading. Y195 and Y196 are universally conserved in FbpA proteins and are responsible for binding Fe^{3+}. Y139 is only found in a subset of FbpA proteins and is present in the coordination sphere of Fe^{3+} as well.

agreement with previous photolysis experiments with other ferric chelates (*20, 22*). Similar results were obtained when the FeVF complex was photolyzed separately and then added to cultures of *S. trochoidea* in the dark. The uptake of the photochemically produced Fe(III)' by *S. trochoidea* could involve a cell surface reductase/Fe(II) permease system similar to that described in diatoms and green algae (*13, 28*). Preliminary evidence showing such ferrireductase activity for *S. trochoidea* cells is consistent with this model (Fig. 4.7). Consequently, Fe(III)' acts as a convergence point from which both the bacteria and the algae utilize the newly "bioavailable" inorganic iron produced from photochemical redox cycling.

If it is evident from our data that phytoplankton stand to gain from this bacterial-algal interaction, what of the bacteria? Heterotrophic marine bacteria such as *Marinobacter* ultimately depend on organic matter produced by algae and other phototrophs for their growth and reproduction. However, our observations suggest that a more direct, mutualistic, relationship has evolved between the bacterial and algal partners. We have observed that *Marinobacter* spp. growth in binary dinoflagellate cultures with *S. trochoidea* is dependent on algal growth whereas the same bacterium growing in algal medium only (no algae present) shows by comparison only static growth (Fig. 4.8). Marine algae are known to release a complex array of organic compounds during growth, such as sugars, amino acids and lipids (*29*) and *Marinobacter* species are capable of using such compounds as sole carbon and energy

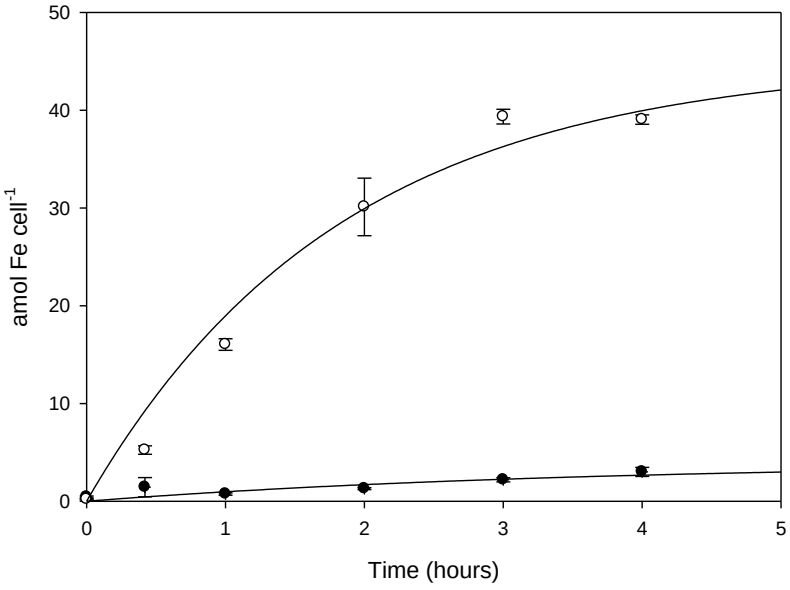

Figure 4.6. VF mediated iron uptake in the dinoflagellate *Scrippsiella trochoidea* in the dark and in the presence of sunlight. ^{55}Fe Uptake by axenic *S. trochoidea* cells was performed in trace metal- and EDTA-free Aquil using 50 nM Fe(III) and 500 nM VF either in the dark (filled circles) or in the presence of attenuated natural sunlight (open circles) as above. Error bars represent s.d. of triplicate cultures. Bars were not shown when smaller than the symbol.

sources (*14*). Genome data of the VF-producing *M. algicola* DG893 corroborates this apparent adaptation to the utilization of algal exudates, as a range of genes have been identified for sugar and amino acid transport and utilization as well as metabolism of glycolate, lipids, esters and aliphatics. This genome data also suggests an even more intimate relationship can exist between the bacterium and the algal host, as a number of 'eukaryotic-like' proteins and secretion systems more typically associated with bacterial pathogens or symbionts have also been identified in *M. algicola* DG893, and in the genomes of other bacteria associated with algae (*30*).

4.3. Discussion

The production of VF may be particularly well suited to the cellular characteristics and behavior of bloom-forming dinoflagellates, which may help explain why dinoflagellate-

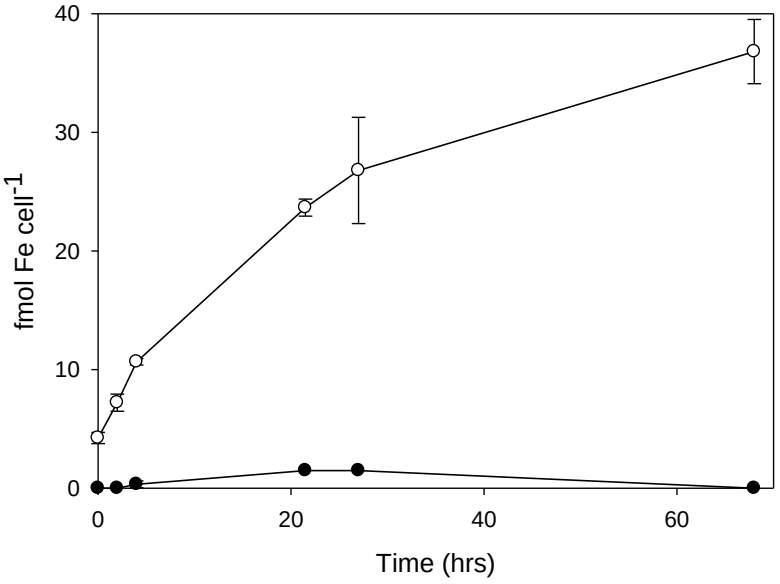

Figure 4.7. Ferrireductase assay of axenic cultures of *S. trochoidea*. Formation of Fe(II) as measured as its BPDS complex in the presence (open circles) or absence (closed circles) of *S. trochoidea* cells.

bacterial associations are so widespread. Dinoflagellates are large motile cells (ca. 10-100 μm in diameter), which often migrate vertically between sunlit, nutrient-depleted surface waters during the day and deeper, more nutrient-enriched waters at night (*31*). They are positively phototactic, which causes them to accumulate in dense aggregations at the sea surface during the day. In addition it has recently been shown that hydrodynamic effects also tend to force their accumulation into narrow concentrated subsurface layers (*32*). Such a dense accumulation of algal cells and associated bacteria should lead to more elevated concentrations of VF in the surrounding seawater than would occur if the cells were evenly distributed throughout the water column. This, taken together with the high photolysis rate constants of Fe-VF chelates, the lack of competing complexation by the photoproduct, and the accumulation of cells near the sea surface, should greatly enhance Fe(III)' production rates and lead to a highly efficient system for the formation of bioavailable iron. Finally, the large size of dinoflagellates causes a further increase in VF concentrations near the cell surface relative to that in the surrounding bulk

seawater owing to their thick surface diffusive boundary layers (*33*). The resulting high surface concentrations of VF would help overcome any negative effect of its lower stability constant on

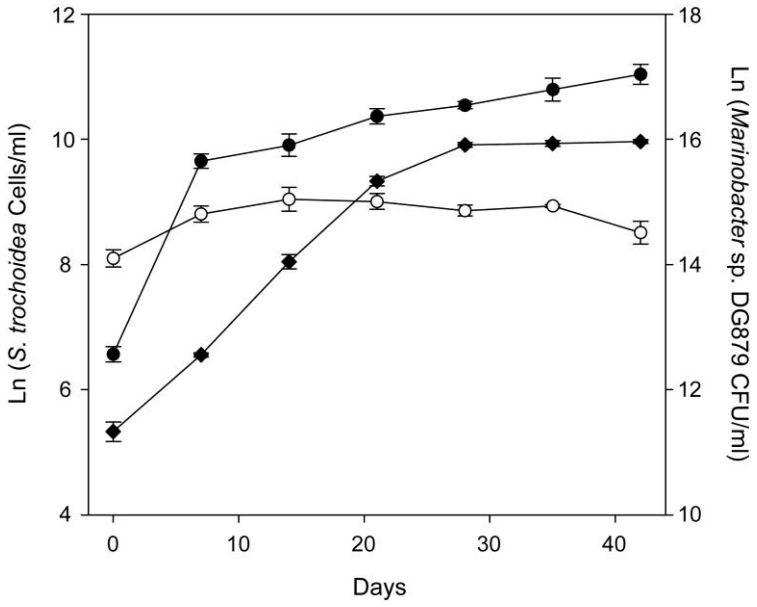

Figure 4.8. Growth pattern of a binary culture of the bloom-forming *S. trochoidea* and an associated vibrioferrin-producing *Marinobacter* strain (DG879) in f/2 medium. Growth of *S. trochoidea* (closed diamonds) in the presence of *Marinobacter* sp. DG879 (closed circles) is shown alongside *Marinobacter* sp. DG879 growing alone in f/2 medium (open circles). Error bars represent s.d. of cell counts from triplicate cultures.

its ability to solubilize iron oxides or to compete with the strong iron binding ligands found in seawater, whose conditional stability constants ($3x10^{11}$ to $1x10^{13}$ M^{-1}) are higher than those for vibrioferrin, but whose concentrations are extremely low (1-3 nM) (*19*).

It is likely that the low stability of ferric VF chelates is not an accident and has been favoured by natural selection to make the chelate more readily reducible, both in terms of photoreduction and bioreduction at cell surfaces, which in turn would increase the bioavailability of the iron to the host algal cells (*22, 23*). There is an inverse relationship between the stability of Fe(III) siderophore chelates and their ease of reduction because high chelate stability energetically favours the maintenance of the bound iron in the +3 oxidation state and discourages its reduction to Fe(II) (*34, 35*). Thus, weakly bound chelates may have

been selected evolutionarily in bacterial symbionts to favour iron reduction and iron availability to phytoplankton. There is a trade-off of course because if the Fe(III) binding is too weak, the chelators will not compete with the strong Fe-binding ligands in seawater or with the formation of Fe hydroxides. However as noted above, dinoflagellates and other algae may have found a way around this difficulty by increasing the ligand concentration in the vicinity of the cells through the formation of dense blooms and the limited diffusive flux of VF (and of photo-produced Fe(II)' and Fe(III)' species) in the cells' surface boundary layer.

Thus it is evident from our findings that both bacteria and their algal hosts stand to gain in evolutionary selection through close association with one another. The labile iron produced from photolysis of ferric chelates with VF provides iron to the phytoplankton, which need iron in large amounts to support the photosynthetic fixation of carbon. This fixed carbon subsequently fuels the growth and reproduction of both the phytoplankton and their bacterial associates and is ultimately used to synthesize the siderophore VF (Fig. 4.9). Such mutualistic sharing of fixed carbon and iron, some aspects of which have been noted earlier (*36*), has far reaching implication for the biogeochemical cycling of iron and carbon, and the overall influence of phytoplankton and bacteria on each others' evolution. We need a better understanding of these mutualistic interactions if we are to understand and predict the creation of algal blooms and the response of populations of marine algae and bacteria to changes in their environment. This is particularly true given the rapid changes now occurring with coastal eutrophication and current and future climate change.

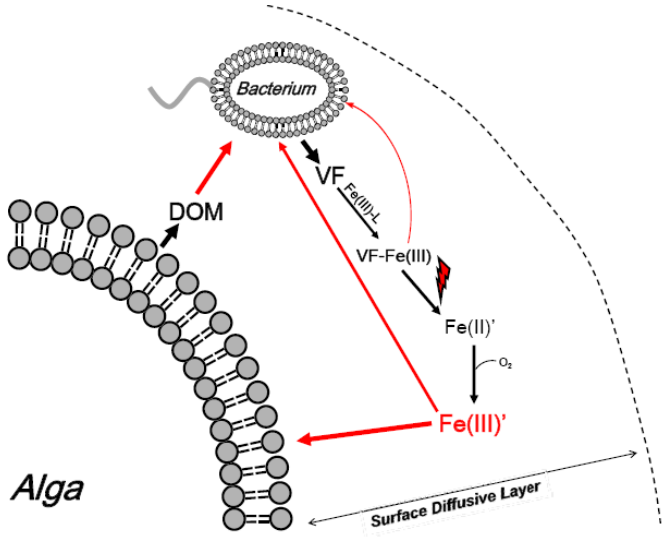

Figure 4.9. Bacterial-algal mutualism based on the photoreductive dissociation of Fe(III)-VF chelates. Upon binding iron in the light, Fe(III)-VF photolyzes to ultimately produce Fe(III)', which is then assimilated by both organisms. In the algae, the assimilated iron is needed in large amounts to support photosynthetic fixation of carbon. Some of this fixed carbon is excreted and used to support bacterial growth and VF production. Due to the thick boundary layer surrounding large algal cells such as dinoflagellates, diffusion of VF and excreted organic carbon away from the algal cell is highly diminished.

4.4. Methods

4.4.1. Bacterial isolation, culturing and growth. *Marinobacter* spp. were isolated from algal cultures by serial 10-fold dilution and spread-plating on either a low-strength modified Zobell's marine agar (ZM/10)(*14*) or artificial seawater (ASW) agar (ONR7a) (*37*) supplied with *n*-hexadecane (SigmaAldrich, UK) in the vapor phase as the sole carbon source. Incubation was at room temperature in the dark for 1-4 weeks. Routine culture of *Marinobacter* isolates was on marine agar (2216 or ZM/1) at 30˚C, and cultures were stored frozen at -80˚C in 20% glycerol.

4.4.2. Marinobacter phylogeny. Genomic DNA was extracted and the 16S rRNA gene amplified by PCR according to Green et al (*14*). Phylogenetic affiliation was established following automatic alignment by the NAST aligner (http://greengenes.lbl.gov) (*38*) and importation of the aligned sequences into ARB software using the ARB parsimony tool (*39*).

The alignment was refined and ambiguous positions were masked from the analysis. Phylogenetic inference of the masked alignment was based on maximum likelihood (PHYML) using the GTR model of nucleotide substitutions, with bootstrap support (100 re-samplings) for nodes, as implemented in ARB. Gamma-proteobacteria of the genus *Salicola* were used as an outgroup.

4.4.3. VF Production and Uptake. Vibrioferrin was isolated as previously described (*18*) and LC-MS spectra were obtained on a Finnigan LCQ ion-trap mass spectrometer equipped with an ESI source (Finnigan MAT, San Jose, CA). NMR characterization was carried out on a Varian 500 MHz instrument using standard pulse sequences. Siderophore growth bioassay was performed according to Amin et al (*18*).

4.4.4. Determination of the inability of the photoproduct to bind Fe. The inability of the photoproduct (VF^*) to coordinate iron was determined by five different methods: 1) the absence of any LMCT bands in the UV-visible region always observed for Fe(III)-siderophore complexes; 2) VF^* showed negative results in the universal CAS assay often used to test for siderophores in solution; 3) at seawater pH, VF^* failed to prevent the precipitation of an equimolar amount of Fe(III) as the hydroxide (added as $FeCl_3$ solution); 4) in growth promotion assays, VF^* failed to support the growth of the producing bacteria compared to an equimolar amount of VF indicating that VF^* is not used as an iron scavenger. 5) Solutions of Fe + VF^* produced by photolysis subjected to HPLC yielded only pure VF^* and not an $FeVF^*$ complex.

4.4.5. PCR amplification of vibrioferrin biosynthetic genes, pvsAB. Degenerate PCR primers were designed to amplify a region between the N-terminus of PvsA (PvsAf1: GARTGYGAYGTNTTYAAYCC) and C-terminus of the PvsB (PvsBr1: CCRTARAAYTTRTTDATRTC), two of the enzymes involved in vibrioferrin biosynthesis. PCR amplification used standard PCR buffer conditions with 1 µM of each primer and 2 mM Mg^{2+}. Cycling conditions used an initial denaturation step of 94˚C for 5 min, followed by 10

cycle step-down annealing profile starting at 58˚C, extension at 72˚C for 3 min and denaturation at 94˚C for 10 sec, then a further 30 cycles of annealing at 48˚C (30 sec), 72˚C for 3 min and 94˚C for 10 sec, and a final 72˚C for 10 min extension. The expected PCR product was ca. 3 kbp. PCR products were cloned into pGEM-TEasy (Promega, UK) according to the manufacturer's instructions and sequenced using the forward and reverse M13 sequencing primers and ver 1.1 BigDye terminator chemistry (Applied Biosystems, UK) and electropherograms obtained using on an ABI 3730xl (Applied Biosystems). Nucleotide sequences were deposited with GenBank under accession numbers EU241703- EU241707.

4.4.6. Axenic algal culture generation and growth. S. trochoidea cultures were maintained in f/2 medium prepared with seawater collected either from the Santa Barbara Pier or the seawater system at the Dunstaffnage Marine Laboratory in Oban and supplemented with selenium (*40*). They were grown either in borosilicate glass flasks or vented 25 cm^2 tissue culture flasks (Greiner Bio-One, UK and USA). Axenic *S. trochoidea* cultures were generated using a two-stage procedure. *Stage 1*: *S. trochoidea* CCAP 1134/1 was induced to form sexual resting cysts by growth in f/2 media deficient in nitrate and phosphate. Cysts were harvested by micropipette, washed in sterile f/2 medium and surface-sterilized using 0.1% H_2O_2. The cysts were then washed with sterile f/2 medium to remove residual H_2O_2. The cysts were added to sterile f/2 in Petri dishes (Nunc, UK) to which ca. 1 x 10^4 CFU ml^{-1} of *Marinobacter* sp. DG879 was added, and were allowed to germinate and grow-out under standard light and temperatures regimes suitable for *Scrippsiella*. *Stage 2*: ca. 1 ml of viable vegetative culture was added to 100 ml f/2 medium in glass flasks and amended with streptomycin sulphate (30 µg ml^{-1}; SigmaAldrich, UK) and the culture was grown through to stationary phase. Bacterial presence was monitored weekly by spread-plate technique using ZM/10 agar. Cultures from which bacteria had been eliminated were sub-cultured by adding 1 ml of the axenic culture 100 ml of sterile f/2 medium containing streptomycin (30 µg ml^{-1}) and the culture was again grown

through to stationary phase. Bacterial contamination was then monitored using agar culture and absence of bacterial PCR amplicon amplified using the universal bacterial primer pair 27f and 1492r (*41*).

All cultures were grown in a Thermo-818 Illuminated incubator at 18^{o}C with 14:10 light/dark cycle at a photon flux density of 80 µE m^{-2} s^{-1}. Algal cell counts were routinely monitored using a Trilogy fluorometer (Turner Designs 7200) or using a Sedgwick-Rafter counting slide.

4.4.7. Algal-bacterial binary culture growth. *S. trochoidea* and *Marinobacter* sp. DG879 binary cultures, or *Marinobacter* sp. DG879 alone, were grown in triplicate 100 ml flasks containing f/2 medium prepared with natural seawater and amended with selenium (*40*). The *Marinobacter* only flasks were inoculated with a suspension of DG879 prepared by resuspending several colonies of DG879 in sterile f/2 medium. *S. trochoidea* and DG879 binary culture flasks were inoculated with 1 ml of stationary phase binary culture. Growth was at 15˚C with a 12:12 light/dark cycle at a photon flux density of ca. 80 µE m^{-2} s^{-1}. All flasks were sampled weekly. Lugol's fixed *S. trochoidea* cell numbers were enumerated using a Sedgewick Rafter chamber. Bacterial colony forming units (CFU) were determined by spread-plating 10-fold serial dilutions of *Marinobacter* on ZM/1 agar (*14*).

4.4.8. ^{55}Fe Uptake by S. trochoidea and Marinobacter* sp. *DG879. ^{55}Fe-VF complex was prepared by adding a standard solution of $FeCl_3 \cdot 6H_2O$ (Aldrich; 1 mg/mL) and $^{55}FeCl_3$ (1522 MBq/mL; Perkin-Elmer) to VF (final Fe:ligand = 1:10 for algal uptake and 1:3 for bacterial uptake; final $FeCl_3$:^{55}Fe = 1:0.1) in the dark. The complex was allowed to equilibrate for at least 24 hrs in the dark prior to use.

For bacterial iron uptake, cells were grown in ASW (*18*) with the final pH adjusted to 8.0. The ASW was passed through Chelex-100 resin (BioRad) to remove trace metals and supplemented with 100 nM $FeCl_3$. Cultures were harvested at mid-exponential growth phase by

centrifuging at 6000 rpm for 20 minutes using Sorvall RC5C+ centrifuge followed by washing 3 times with iron-free ASW. The harvested cells were then diluted with ASW to an optical density at 600 nm of 0.4 and incubated at 4^{o}C until further use (*24*). Prior to the start of the uptake, cells were shaken at 130 rpm and 20^{o}C for 30 minutes after which the experiment was started by adding a 1 µM final ^{55}FeVF concentration. Ascorbate (10 mM) and CCCP (30 µM) were added 1 hour prior to adding ^{55}FeVF. Uptake experiments in the presence of CCCP were kept in the dark and maintained at 20^{o}C. Uptake in the presence of the reductant ascorbate was performed by photolyzing the required amount of ^{55}FeVF using a mercury vapor lamp (175W) for 30 minutes at acidic pH and in the presence of 10 mM ascorbate prior to addition to the culture. Cultures not kept in the dark were exposed to attenuated sunlight (450 µEinstein m^{-2} s^{-1}) and maintained at 20^{o}C using a refrigerated circulating water bath (Neslab). Aliquots were withdrawn at each time point and filtered using a Millipore 1225 sampling vacuum manifold onto 0.6 µm-pore size polycarbonate filters (Millipore). Filtered cells were washed with 5 mL ASW followed by 5 mL Ti(III)-citrate-EDTA reagent (*42*) and a final 5 mL rinse with ASW to reductively remove iron oxides and iron bound to cell surfaces. ^{55}Fe cellular uptake was measured using a Beckman-Coulter LS6500 liquid scintillation counter.

Axenic *S. trochoidea* cultures used in iron uptake experiments were grown in Aquil (*43*) (886 µM NO_3^-, 36.3 µM PO_4^{3-}, 100 µM EDTA, 100 nM Fe supplemented as FeEDTA). All cultures were grown in a Thermo-818 Illuminated incubator at 18^{o}C with 14:10 light/dark cycle at a photon flux density of 80 µEinstein m^{-2} s^{-1}. Exponentially growing cells were harvested by gravity filtration into Aquil medium containing no EDTA, vitamins, iron, or other trace metal additions. To do this the culture sample was concentrated by passage of ~90% of the culture medium through a 1.2 µm-pore polycarbonate filter [(Millipore) housed in an acid-washed Nalgene polysulfone filter holder] followed by redilution of the culture with EDTA and trace metal free Aquil medium. This procedure was repeated at least 4 more times to free the culture

of residual EDTA. The final diluted culture contained ca. 10^4 algal cells mL^{-1}. ^{55}FeVF was then added as previously described for the bacteria and cultures were either kept in the dark or exposed to attenuated sunlight (450 µEinstein m^{-2} s^{-1}). Both cultures were maintained at 20°C. Aliquots were withdrawn at each time point and filtered onto 3 µm-pore size polycarbonate filters (Millipore). Sample washings and counts were done as previously described.

4.4.9. Determination of the conditional stability constant of VF in seawater. To determine the conditional stability constant of vibrioferrin in seawater, 10 ml subsamples of open-ocean surface seawater that had been UV-irradiated for 8 hours and "chelexed", were aliquoted into acid cleaned Teflon cups. 1 nM vibrioferrin was then added to each cup, followed by boric acid buffer (pH 8), and iron additions ranging from 0-6 nM. Subsamples were allowed to equilibrate for two hours before adding 10 µM salicylaldoxime (SA). After equilibrating for 15 minutes with SA, samples were then analyzed (3 independent titrations) by competitive ligand-exchange adsorptive cathodic stripping voltammetry (CLE-ACSV) according to Buck et al (*44*). All titrations were done in the dark to prevent photodegradation of vibrioferrin. The total dissolved iron concentration in the chelexed, UV-irradiated seawater (0.1 nM) was determined via ACSV with SA (*44*).

4.4.10. Photolysis of Fe(III)-chelates. Fe(III)-VF (5, 10, and 15 µM, 3 replicates each) solutions containing a 10-fold molar excess of total VF were irradiated in the presence of 20, 40, and 45 µM ferrous trapping agent, BPDS (Bathophenanthrolinedisulfonic acid, Fluka), respectively. The solutions contained 5 mM HEPES buffer (pH 8.1) and were made up in Aquil (without nutrients, trace metals, EDTA or vitamins). One set of solutions were exposed to attenuated sunlight (500 µEinstein m^{-2} s^{-1}) at 20°C while a set of control samples were kept in the dark. Initial rates of Fe(II) production were measured by monitoring $Fe(BPDS)_3^{2+}$ LMCT band at 535 nm (22140 M^{-1} cm^{-1}). For the low light flux experiment, 0.1 mM ferric complexes of vibrioferrin, petrobactin and marinobactin solutions were exposed to a fluorescent lamp (80

µEinstein m^{-2} s^{-1}, Sylvania Ecologic Cool White, 34W) at 20°C in the presence of 50 mM HEPES buffer (pH 8.2) and 0.7 M NaCl. UV-Visible spectra were recorded using a Cary 50 spectrophotometer.

4.4.11. Ferrireductase assay. Axenic *S. trochoidea* was grown in acid-washed 250 ml Erlenmeyer flasks in f/2 supplemented with 10^{-5} M Fe. Late log phase cells were harvested by gentle filtration onto 10 µm-pore polycarbonate membranes, washed twice with equal volumes of sterile natural seawater and finally suspended in an equal volume of sterile natural seawater. Triplicate *S. trochoidea* cell suspensions were incubated at 21˚C in the dark in the presence of 130 µM HEPES buffer (pH 8.1), 10 µM Fe (chelated with 10-fold excess EDTA) and 100 µM of the Fe(II) chelator BPDS (bathophenanthrolinedisulfonate). Sterile natural seawater was used as a background control. Ferrireductase activity was measured by pelleting the algal cells by centrifugation and measuring the absorbance of Fe(II)BPDS chelates in the supernatant at a wavelength of 535 nm.

4.5. Appendix

Table 4.3. List and origin of *Marinobacter* strains isolated and examined in this study.[a]

	Algal-Associated *Marinobacter*		*Marinobacter* Affiliation		
Bacterial Strain	Accession No.	Algal Host	Closest Relative (Type Strain)	Accession No.	ID (%)
Dinoflagellate					
DG870	AY258106	*Gymnodinium catenatum* GCHU11	*Marinobacter sediminum* R65	AJ609270	99
DG879	AY258107	*G. catenatum* GCDE08	*M. sediminum* R65	AJ609270	99
DG979	AY258112	*G. catenatum* GCTRA14	*M. sediminum* R65	AJ609270	99
CAWD101_Q*	AY701428	*G. catenatum* CAWD101	*M. sediminum* R65	AJ609270	99
DG893	AY258110	*G. catenatum* YC499B15	*Marinobacter algicola* DG893	AY258110	100
DG1136	AY258116	*G. catenatum* GC21V	*M. algicola* DG893	AY258110	99
DG1194	EF140746	*Amphidinium carterae* CCAP1102/7	*M. algicola* DG893	AY258110	99
DG1197	EF140747	*Alexandrium tamarense* CCAP 1119/4	*M. algicola* DG893	AY258110	99
DG1239	DQ486486	*Scrippsiella trochoidea* CCAP 1134/1	*M. algicola* DG893	AY258110	99
DG1259	DQ486497	*Lingulodinium polyedrum* CCAP 1121/2	*M. algicola* DG893	AY258110	99
DG1191	EU052752	*A. carterae* CCAP1102/7	*Marinobacter flavimaris* SW-145	AY517632	99
DG1205	EF140748	*Gymnodinium microreticulatum* I011	*M. flavimaris* SW-145	AY517632	99
DG1305	DQ486512	*Scrippsiella* sp. CCMP 1073	*M. flavimaris* SW-145	AY517632	99
DG1603	DQ660886	*G. catenatum* GCJP01	*M. flavimaris* SW-145	AY517632	99
MH197	EU052740	*Alexandrium ostenfeldii* CCMP 1773	*M. flavimaris* SW-145	AY517632	98
MH199	EU052741	*Prorocentrum minimum* CCMP 1529	*M. flavimaris* SW-145	AY517632	98
Coccolithophore					
DG1594	EF140750	*Emiliania huxleyi* AC475	*M. algicola* DG893	AY258110	99
DG1597	EF140753	*Coccolithus braarudii* AC400	*M. algicola* DG893	AY258110	99
DG1556	EU732746	*C. braarudii* AC392	*Marinobacter* sp. NT N125	AB167040	99
DG1402	EF140754	*E. huxleyi* CCAP920/8	*M. flavimaris* SW-145	AY517632	99
DG1420	EF140749	*E. huxleyi* CCAP 920/10	*M. flavimaris* SW-145	AY517632	99
DG1591	EF140752	*E. huxleyi* AC472	*M. flavimaris* SW-145	AY517632	100
DG1595	EF140751	*E. huxleyi* AC475	*M. flavimaris* SW-145	AY517632	99
MH204	EU052744	*E. huxleyi* CCMP 1516	*M. flavimaris* SW-145	AY517632	98
Diatom					
DG1618	EU052770	*Pseudo-nitzschia* sp. RUS	*Marinobacter* sp. NT N125	AB167040	99
MH125a	EF140755	*Achnanthes* sp. CCAP 1095/1	*Marinobacter lipolyticus* SM19	AY147906	99
MH171	EU052727	*Thalassosira pseudonana* CCAP 1085/12	*M. algicola* DG893	AY258110	99
CB22	EU052697	*Asterionellopsis glacialis* CSIRO CS-372	*M. flavimaris* SW-145	AY517632	99
CB42	EU052699	*Fallacia carpentariae* CSIRO CS-346	*M. sediminum* R65	AJ609270	97
TG365	EU732745	*Skeletonema costatum* CCAP1077/7	*M. algicola* DG893	AY258110	99

[a] Orange shading denotes strains tested for VF production and utilization.

4.6. Acknowledgments

This work was supported by NOAA Grants #NA04OAR4170038 and NA08OAR4170669, California Sea Grant College Program Project numbers R/CZ-198 and R/CONT-205. D.H.G. was supported in part by a New Zealand FRST postdoctoral fellowship. DNA sequencing was supported by a NERC Molecular Genetics Facility grant to D.H.G (MGF 122). The authors thank C. Bolch and T. Gutierrez for access to additional bacteria isolated from algae. Particular thanks go to Prof. Kathy Barbeau and Randelle M. Bundy, Scripps Institute of Oceanography, for the measurement of the conditional stability constant of VF in seawater. Genome sequencing of *M. algicola* DG893 was funded by the Gordon and Betty Moore Foundation. This chapter has been previously published as Amin, S. A., Green, D. H., Hart, M. C., Küpper, F. C., Sunda, W. G., and Carrano, C. J. (2009) Photolysis of iron–siderophore chelates promotes bacterial–algal mutualism, *Proceedings of the National Academy of Sciences 106*, 17071-17076.

4.7. References

1. Coale, K. H., Johnson, K. S., Fitzwater, S. E., Gordon, R. M., Tanner, S., Chavez, F. P., Ferioli, L., Sakamoto, C., Rogers, P., Millero, F., Steinberg, P., Nightingale, P., Cooper, D., Cochlan, W. P., Landry, M. R., Constantinou, J., Rollwagen, G., Trasvina, A., and Kudela, R. (1996) A massive phytoplankton bloom induced by an ecosystem-scale iron fertilization experiment in the equatorial Pacific Ocean, *Nature 383*, 495-501.

2. Dymond, J., and Lyle, M. (1985) Flux comparisons between sediments and sediment traps in the eastern tropical Pacific: implications for atmospheric CO_2 variations during the Pleistocene, *Limnol. Oceanogr. 30*, 699-712.

3. Keller, M. D., Bellows, W. K., and Guillard, R. R. L. (1989a) Dimethyl sulfide production in marine phytoplankton, In *Biogenic sulfur in the environment* (Saltzman, E. S., and Cooper, W. J., Eds.), pp 167-182, American Chemical Society, Washington D.C.

4. Cloern, J. E. (2001) Our evolving conceptual model of the coastal eutrophication problem, *Mar. Ecol. Prog. Ser. 210*, 223-253.

5. Cho, B. C., and Azam, F. (1988) Major role of bacteria in biogeochemical fluxes in the ocean's interior, *Nature 332*, 441-443.

6. Croft, M. T., Lawrence, A. D., Raux-Deery, E., Warren, M. J., and Smith, A. G. (2005) Algae acquire vitamin B_{12} through a symbiotic relationship with bacteria, *Nature 438*, 90-93.

7. Matsuo, Y., Imagawa, H., Nishizawa, M., and Shizuri, Y. (2005) Isolation of an algal morphogenesis inducer from a marine bacterium, *Science 307*, 1598.

8. Mayali, X., Franks, P. J. S., and Azam, F. (2008) Cultivation and ecosystem role of a marine *Roseobacter* clade-affiliated cluster bacterium, *Appl. Environ. Microbiol. 74*, 2595-2603.

9. Mayali, X., and Doucette, G. J. (2002) Microbial community interactions and population dynamics of an algicidal bacterium active against *Karenia brevis* (Dinophyceae), *Harmful Algae 1*, 277-293.

10. Bruland, K. W., Donat, J. R., and Hutchins, D. A. (1991) Interactive influences of bioactive trace metals on biological production in oceanic waters, *Limnol. Oceanogr. 36*, 1555-1577.

11. Tortell, P. D., Maldonado, M. T., Granger, J., and Price, N. M. (1999) Marine bacteria and biogeochemical cycling of iron in the oceans, *FEMS Microbiol. Ecol. 29*, 1-11.

12. Vraspir, J. M., and Butler, A. (2009) Chemistry of marine ligands and siderophores, *Annu. Rev. Mar. Sci. 1*, 43-63.

13. Kustka, A. B., Allen, A. E., and Morel, F. M. M. (2007) Sequence analysis and

transcriptional regulation of Iron acquisition genes in two marine diatoms, *J. Phycol. 43*, 715-729.

14. Green, D. H., Llewellyn, L. E., Negri, A. P., Blackburn, S. I., and Bolch, C. J. S. (2004) Phylogenetic and functional diversity of the cultivable bacterial community associated with the paralytic shellfish poisoning dinoflagellate *Gymnodinium catenatum*, *FEMS Microbiol. Ecol. 47*, 345-357.

15. Alavi, M., Miller, T., Erlandson, K., Schneider, R., and Belas, R. (2001) Bacterial community associated with *Pfiesteria*-like dinoflagellate cultures, *Environ. Microbiol. 3*, 380-396.

16. Hold, G. L., Smith, E. A., Rappé, M. S., Maas, E. W., Moore, E. R. B., Stroempl, C., Stephen, J. R., Prosser, J. I., Birkbeck, T. H., and Gallacher, S. (2001) Characterisation of bacterial communities associated with toxic and non-toxic dinoflagellates: *Alexandrium* spp. and *Scrippsiella trochoidea*, *FEMS Microbiol. Ecol. 37*, 161-173.

17. Yamamoto, S., Okujo, N., Yoshida, T., Matsuura, S., and Shinoda, S. (1994) Structure and iron transport activity of vibrioferrin, a new siderophore of *Vibrio parahaemolyticus*, *J. Biochem. (Tokyo, Japan) 115*, 868-874.

18. Amin, S. A., Küpper, F. C., Green, D. H., Harris, W. R., and Carrano, C. J. (2007) Boron binding by a siderophore isolated from marine bacteria associated with the toxic dinoflagellate *Gymnodinium catenatum*, *J. Am. Chem. Soc. 129*, 478-479.

19. Rue, E. L., and Bruland, K. W. (1995) Complexation of iron(III) by natural organic ligands in the Central North Pacific as determined by a new competitive ligand equilibration/adsorptive cathodic stripping voltammetric method, *Mar. Chem. 50*, 117-138.

20. Barbeau, K., Rue, E. L., Bruland, K. W., and Butler, A. (2001) Photochemical cycling of iron in the surface ocean mediated by microbial iron(III)-binding ligands, *Nature 413*, 409-413.

21. Barbeau, K. (2006) Photochemistry of Organic Iron(III) Complexing Ligands in Oceanic Systems, *Photochem. Photobiol. 82*, 1505-1516.

22. Anderson, M. A., and Morel, F. M. M. (1982) The influence of aqueous iron chemistry on the uptake of iron by the coastal diatom *Thalassiosira weissflogii*, *Limnol. Oceanogr. 27*, 789-813.

23. Shaked, Y., Kustka, A. B., and Morel, F. M. M. (2005) A general kinetic model for iron acquisition by eukaryotic phytoplankton, *Limnol. Oceanogr. 50*, 872-882.

24. Küpper, F. C., Carrano, C. J., Kuhn, J.-U., and Butler, A. (2006) Photoreactivity of iron(III)-aerobactin: photoproduct structure and iron(III) coordination, *Inorg. Chem. 45*, 6028-6033.

25. Abergel, R. J., Zawadzka, A. M., and Raymond, K. N. (2008) Petrobactin-Mediated

Iron Transport in Pathogenic Bacteria: Coordination Chemistry of an Unusual 3,4-Catecholate/Citrate Siderophore, *J. Am. Chem. Soc. 130*, 2124-2125.

26. Shouldice, S. R., Skene, R. J., Dougan, D. R., Snell, G., McRee, D. E., Schryvers, A. B., and Tari, L. W. (2004) Structural basis for iron binding and release by a novel class of periplasmic iron-binding proteins found in Gram-negative pathogens, *J. Bacteriol. 186*, 3903-3910.

27. Alexeev, D., Zhu, H., Guo, M., Zhong, W., Hunter, D. J. B., Yang, W., Campopiano, D. J., and Sadler, P. J. (2003) A novel protein-mineral interface, *Nat. Struct. Mol. Biol. 10*, 297-302.

28. Shaked, Y., Kustka, A. B., and Morel, F. M. M. (2005) A general kinetic model for iron acquisition by eukaryotic phytoplankton, *Limnol. Oceanogr. 50*, 872-882.

29. Myklestad, S. M. (1995) Release of extracellular products by phytoplankton with special emphasis on polysaccharides, *Sci. Tot. Environ. 165*, 155-164.

30. Worden, A. Z., Cuvelier, M. L., and Bartlett, D. H. (2006) In-depth analyses of marine microbial community genomics, *Trends Microbiol. 14*, 331-336.

31. Kamykowski, D., Milligan, E. J., and Reed, R. E. (1998) Relationships between geotaxis/phototaxis and diel vertical migration in autotrophic dinoflagellates, *J. Plankton Res. 20*, 1781-1796.

32. Durham, W. M., Kessler, J. O., and Stocker, R. (2009) Disruption of vertical motility by shear triggers formation of thin phytoplankton layers, *Science 323*, 1067-1070.

33. Richardson, L. L., and Stolzenbach, K. D. (1995) Phytoplankton cell size and the development of microenvironments, *FEMS Microbiol. Ecol. 16*, 185-191.

34. Lewis, B. L., Holt, P. D., Taylor, S. W., Wilhelm, S. W., Trick, C. G., Butler, A., and Luther, G. W. (1995) Voltammetric estimation of iron(III) thermodynamic stability constants for catecholate siderophores isolated from marine bacteria and cyanobacteria, *Mar. Chem. 50*, 179-188.

35. Boukhalfa, H., and Crumbliss, A. L. (2002) Chemical aspects of siderophore mediated iron transport, *BioMetals 15*, 325-339.

36. Kirchman, D. L., Meon, B., Cottrell, M. T., Hutchins, D. A., Weeks, D., and Bruland, K. W. (2000) Carbon versus iron limitation of bacterial growth in the California upwelling regime, *Limnol. Oceanogr. 45*, 1681-1688.

37. Dyksterhouse, S. E., Gray, J. P., Herwig, R. P., Lara, J. C., and Staley, J. T. (1995) *Cycloclasticus pugetii* gen. nov., sp. nov., an aromatic hydrocarbon-degrading bacterium from marine sediments, *Int. J. Syst. Bacteriol. 45*, 116-123.

38. DeSantis, T. Z., Hugenholtz, P., Larsen, N., Rojas, M., Brodie, E. L., Keller, K., Huber, T., Dalevi, D., Hu, P., and Andersen, G. L. (2006) Greengenes, a Chimera-Checked 16S

rRNA Gene Database and Workbench Compatible with ARB, *Appl. Environ. Microbiol. 72*, 5069-5072.

39. Ludwig, W., Strunk, O., Westram, R., Richter, L., Meier, H., Yadhukumar, Buchner, A., Lai, T., Steppi, S., Jobb, G., Forster, W., Brettske, I., Gerber, S., Ginhart, A. W., Gross, O., Grumann, S., Hermann, S., Jost, R., Konig, A., Liss, T., Lussmann, R., May, M., Nonhoff, B., Reichel, B., Strehlow, R., Stamatakis, A., Stuckmann, N., Vilbig, A., Lenke, M., Ludwig, T., Bode, A., and Schleifer, K.-H. (2004) ARB: a software environment for sequence data, *Nucl. Acids Res. 32*, 1363-1371.

40. Guillard, R. R. L. (1975) Culture of phytoplankton for feeding marine invertebrates, In *Culture of marine animals* (Smith, W. L., and Chanley, M. H., Eds.), pp 26-60, Plenum Press, New York.

41. Weisburg, W. G., Barns, S. M., Pelletier, D. A., and Lane, D. J. (1991) 16S ribosomal DNA amplification for phylogenetic study, *J. Bacteriol. 173*, 697-703.

42. Hudson, R. J. M., and Morel, F. M. M. (1989) Distinguishing between extra- and intracellular iron in marine phytoplankton, *Limnol. Oceanogr. 34*, 1113-1120.

43. Price, N. M., Harrison, G. I., Hering, J. G., Hudson, R. J., Nirel, P. M. V., Palenik, B., and Morel, F. M. M. (1988/1989) Preparation and chemistry of the artificial algal culture medium Aquil, *Biol. Oceanogr. 6*, 443-461.

44. Buck, K. N., Lohan, M. C., Berger, C., and Bruland, K. W. (2007) Dissolved iron speciation in two distinct river plumes and an estuary: Implications for riverine iron supply, *Limnol. Oceanogr. 52*, 843-855.

5. Vibrioferrin, an unusual marine siderophore: iron binding, photochemistry, and biological implications

5.1. Introduction

Iron is an essential element for nearly all living organisms due to its ubiquitous role in redox enzymes, especially in the context of respiration and photosynthesis. However although it is the fourth most abundant element in the Earth's crust, it is present under aerobic conditions at neutral pH only in the form of extremely insoluble minerals like hematite, goethite, and pyrite or as polymeric oxide-hydrates, -carbonates, and -silicates that severely restrict the bioavailability of this metal. The iron level in open ocean waters is even lower than in most terrestrial environments (*1-3*), since a large fraction of the limited iron available is already tightly complexed (although the nature of the complexing ligands remains unknown) (*1, 4, 5*). To deal with this low bioavailability bacteria and fungi have evolved sophisticated systems based on high-affinity iron-specific binding compounds called siderophores to acquire, transport and process this essential metal ion. Their major role is the extracellular solubilization of iron from minerals and/or organic substrates and its specific transport into microbial cells. Several hundred siderophores, whose biosyntheses are repressed by high iron levels, are known and extensive studies of their isolation, structure, transport and molecular genetics have been undertaken in the last three decades (*6*). The structural variety of siderophores has been comprehensively reviewed (*7*). However the study of marine siderophores is less extensive as compared to their terrestrial counterparts and the structures of only a relatively few have been fully elucidated (*8-11*). It is noteworthy that a large percentage of the characterized marine siderophores can be classified as amphiphilic, suggesting a different iron uptake strategy than that typically found in terrestrial microorganisms (*8, 10, 12*). In addition the presence of α- or β-hydroxy carboxylate groups in many marine siderophores renders their iron complexes photoactive (*13, 14*). It has been proposed that sunlight-driven photoreduction of the Fe(III) in such siderophores would transiently produce Fe(II) which might be utilizable by other organisms (*15*). However it was subsequently shown that the photooxidized siderophore is still

capable of rapidly rebinding the iron (*16, 17*) and in the one case studied, transporting it into the cell of the producing bacteria (*17*).

Algal blooms are ubiquitous phenomena that have been increasingly observed in the coastal and upwelling parts of the world's oceans. Even in the absence of toxin production these events often alter the chemical and ecological milieu by changing nutrient distribution and consequently the biodiversity of marine ecosystems. Although many physical and biological factors influence bloom dynamics, emerging evidence suggests that bacterial-algal interactions may be contributing to the development and sustenance of blooms(*18*). Indeed, some bacterial associates of harmful algal species are clearly important to the physiological welfare of algal cells as evidenced by the fact that many such species including the dinoflagellate *Gymnodinium catenatum* cannot be grown axenically indicating an obligatory requirement(s) that is supplied by bacteria (*18*). One attractive hypothesis concerning the nature of this inter-species interaction that we are pursuing is that phytoplankton can 'share' iron, an element often limiting to their growth and previously shown to impact bloom formation (*19, 20*), bound to extracellular siderophores produced by their bacterial associates. Although some diatoms have been shown to assimilate iron bound to bacterial siderophores (*21*), the iron acquisition systems of another important group of phytoplankton, the dinoflagellates, are for the most part unknown (*22, 23*).

Vibrioferrin (VF) is a member of the carboxylate class of siderophores and contains two α-hydroxy acid groups (Fig. 5.1A). It was originally isolated from *Vibrio parahaemolyticus*, an enteropathogenic estuarine bacterium often associated with seafood-borne gastroenteritis and has been extensively studied by Yamamoto *et al* (*24-32*). Our interest in VF stems from the fact that we have also isolated this siderophore from several species of marine bacteria, including *Marinobacter* spp. DG870, 879 and 979 and *M. algicola* DG893, which are closely associated or "symbiotic" with toxic, bloom-forming dinoflagellates such as *Gymnodinium catenatum (33)*.

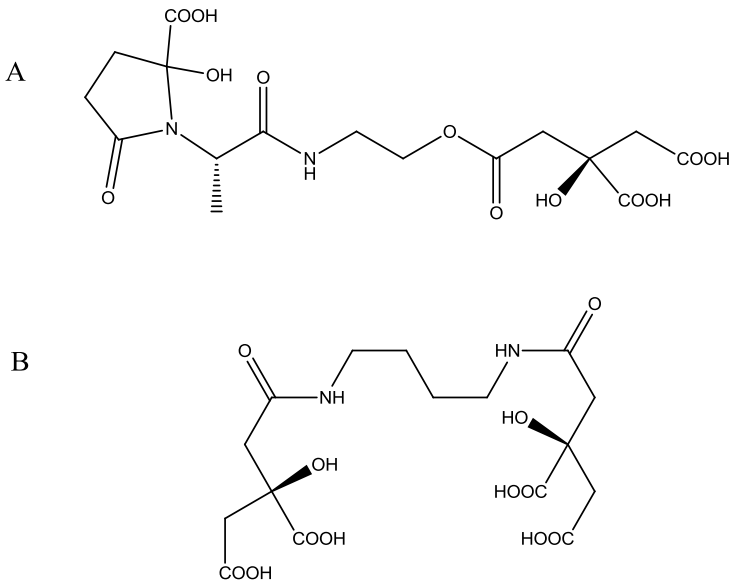

Figure 5.1. Structures of the siderophores (A) vibrioferrin and (B) rhizoferrin.

Despite the fact that VF has been extensively studied from a molecular biology perspective (*24, 27, 28*), its metal binding characteristics remain largely unknown. In this manuscript we describe the iron binding constants for this unusual siderophore and discuss how these, and its unexpected photochemical properties, are related to biological function.

5.2. Results

5.2.1. Ligand Protonation Equilibria. The potentiometric titration curve for apo-vibrioferrin is shown in Figure 5.2. The data below pH 5 and the inflection at three equivalents of base per mole ligand represents the titration of the three free carboxylic acid groups. Ligand protonation constants were determined from the nonlinear refinement of the data to give evaluated constants (log $K_{1\text{-}3}$) of 5.13(3), 3.60(4), and 2.71(1). These compare well with the corresponding values reported for the related siderophore rhizoferrin (5.25, 4.21, 3.05, and 2.86) which has one additional carboxylate group (Fig. 5.1B) (*34*). Therefore we likewise assign the first protonation constant (pK_a = 5.13) to the free carboxylate of the citrate moiety with the

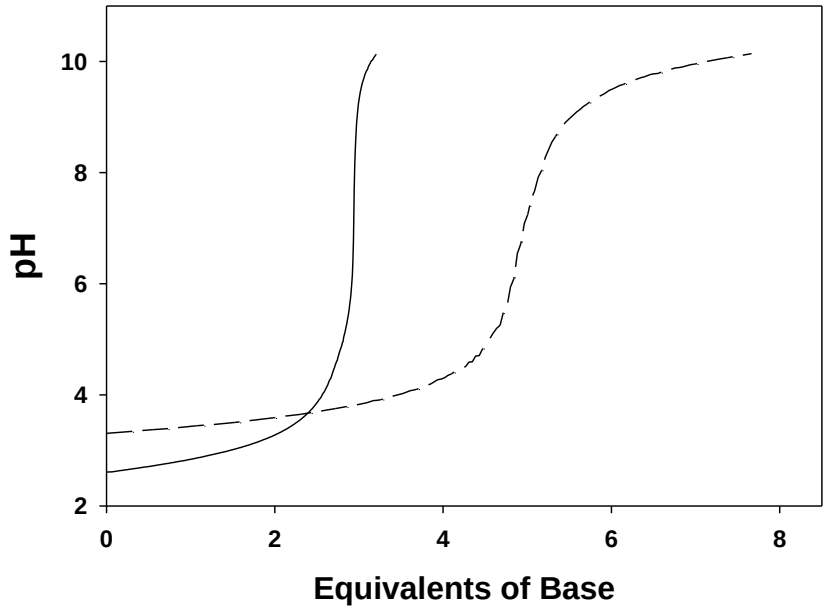

Figure 5.2. Potentiometric titrations of 0.230 mM VF (solid line) and 0.124 mM Fe(III)-VF (dashed line). Titrations were performed at 25°C with I = 0.1 M NaCl. The iron complex titration was performed in the dark to avoid photodegradation.

lower two pK_a's of 3.60 and 2.71 assigned to the carboxylic sites of the two α-hydroxy acid moieties.

5.2.2. Metal-Ligand Equilibria. The potentiometric titration curve of an equimolar mixture of VF and Fe^{3+} below pH 7 shows a breakpoint at 5 equivalents of base (Fig. 5.2) which strongly suggests that, in addition to the three readily titratable carboxylate groups, the two citrate hydroxyl groups are also deprotonated upon iron binding. Between pH 7 and 11 an additional proton is titrated which we assign to the deprotonation of a bound water molecule (*vide infra*). The potentiometic data over the range of pH from 3-11 could be fit using HYPERQUAD (*35*) with a model that assumed just two metal ligand protonation constants. The evaluated constants were log β_{110} = 24.03, log β_{111} = 28.41, and log $\beta_{11\text{-}1}$ = 14.44.

We initially attempted to derive the log β_{110} value used in the initial fit of the potentiometric metal ligand titration curve from an EDTA competition experiment at near neutral pH, as is standard methodology for siderophores (*17*). However this approach failed in

the case of VF as a single equivalent of EDTA effectively removes > 95% of the Fe from FeVF. This set an upper limit of between 10^{24} to 10^{25} as a value for K_{ML} or β_{110}. Therefore we sought a weaker chelator whose optical properties were compatible with its analysis in the presence of Fe-VF. Ultimately we settled on EGTA (Ethylene glycol-bis(2-aminoethylether)-N,N,N',N'-tetraacetic acid). Using a 2-15 fold excess of EGTA over VF at pH 6.0, it is possible to set up a measurable competition of Fe(III) between the two ligands. The measured equilibrium constant, K_m, of 2.21(9) represents the reaction shown in equation 1:

$$\text{Fe(III)-EGTA} + \text{VF} \rightleftharpoons \text{Fe(III)-VF} + \text{EGTA} \qquad (1)$$

where VF and EGTA represent the ligands in all their protonated states. The conditional or pH-dependent formation constant (K*) for the iron(III)-VF is then given by equation 2:

$$K^*_{FeVF} = K_m K^*_{FeEGTA} \qquad (2)$$

which, using the known value of K^*_{FeEGTA} (*36*), yields a value of 14.57(5) for log K^*_{FeVF} at pH 6.0. While this is a valid equilibrium constant under the conditions for which it is measured, it is difficult to compare with the "standard" pH-independent stability constants typically reported which are expressed in terms of the fully deprotonated form of the free ligand. This calculation in turn requires knowledge of the ligand deprotonation constants. Unfortunately only three of the five required deprotonation constants could be determined for VF since the pK_a's of the two citrate hydroxyl groups were not measurable by potentiometric titration at the concentrations of ligand available. If, however, we estimate the values for these two deprotonations as 10.1 and 11.3 (using the dicitrate siderophore rhizoferrin as a model) (*34*), we can estimate the pH-independent stability constant. Given these estimates the overall formation constant, log K_{ML}, for the Fe(III)-VF complex is then determined to be 24.02(5), a value that is unusually small for a confirmed siderophore and somewhat less than that of the related siderophore rhizoferrin (Fig. 5.1B) which has log K_{ML}= 25.3 (*34*). This is presumably the result of VF having one fewer donor group than rhizoferrin. The proposed coordination for Fe(III) to VF involves ligation by

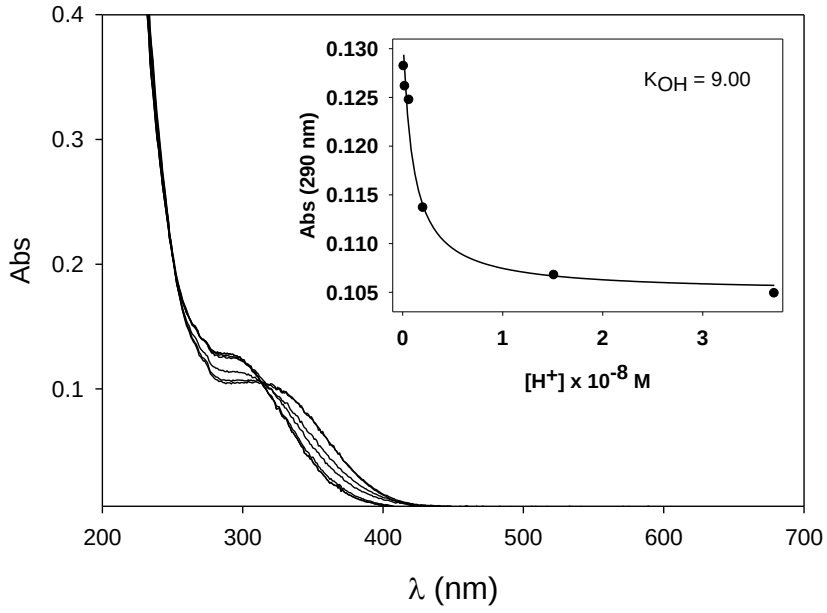

Figure 5.3. Spectrophotometric titration of Fe(III)-VF from pH 7.43-9.96. Experiment was performed in the dark at 25°C with *I* = 0.1 M NaCl. Inset: Schwarzenbach fit of the spectrophotometric titration in the indicated pH range yielding log K_{OH} = 9.0 (R^2 = 0.97).

both hydroxyl groups and the three carboxylates analogous to the proposed coordination of Fe(III) by rhizoferrin with the sixth coordination site presumably occupied by a water molecule. A similar coordination scheme has been proposed by others (*37*).

5.2.3. Spectrophotometric Titrations. At pH values above 7.8 a progressive blue shift and an increase in intensity of the oxygen-to-iron LMCT band of the complex near 330 nm indicates a significant change in the inner coordination sphere. Such changes can be assigned to the deprotonation of the aqua ligand to yield the hydrolyzed species:

$$[FeL(H_2O)]^{2-} \rightleftharpoons [FeL(OH)]^{3-} + H^+ \qquad (3)$$

An alternate structure, which involves deprotonation and coordination of an amide group to the iron as seen in some iron enzymes such as nitrile hydratase, was also considered (*38*). However DFT calculations indicate that the optimized hydroxo form is 27-34 kcal/mol (depending upon basis set used) more stable than the amido plus water formulation indicating that the latter was highly unlikely. Therefore this process was fit to the simple single proton Schwarzenbach equation (*39*),

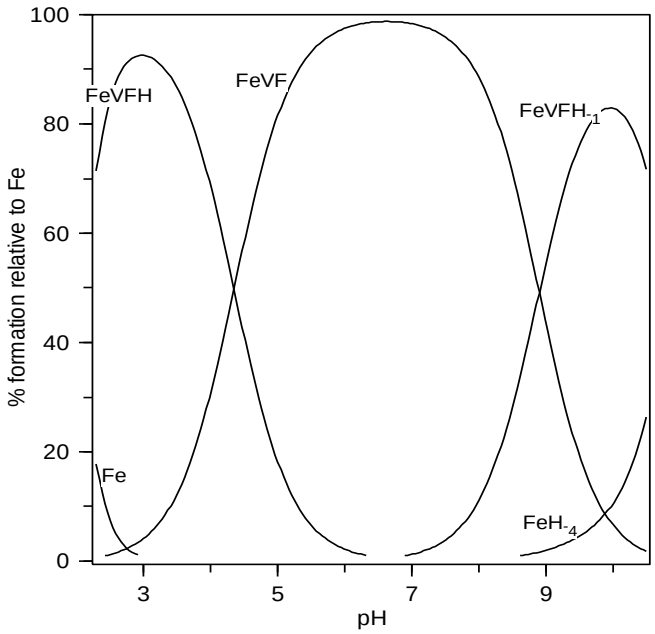

Figure 5.4. Fe-VF species distribution as a function of pH using protonation constants obtained from SpecFit/32. Species distribution was constructed using HySS2006.

$$A_{obs} = (A_{MHL}K[H^+] + A_{ML})/[H^+]K + 1 \qquad (4)$$

where in general A_{obs} is the observed absorbance, A_{MHL} the absorbance due to the protonated species, A_{ML} that of the unprotonated and K the equilibrium constant between them. This analysis yields a hydrolysis constant, log K_{OH} of 9.0 (Fig. 5.3). Such a value is consistent with expectations for a Fe(III)-siderophore with an overall binding constant in the range of $10^{23\text{-}27}$ as there is typically a linear correlation between the overall formation constant of an iron complex and its first hydrolysis constant (*40*). Between pH 7.8 and 3.5 only minor changes in the LMCT band intensity and position were evident indicating no major change in the coordination sphere of the Fe^{3+}. Attempts to fit this region to a single protonation equilibrium via Schwarzenbach analysis gave a log K of 4.40. The minor spectral changes in the LMCT band over this pH range suggest an equilibrium that involves protonation of the terminal carboxylate group rather than the α-hydroxy acid moieties. At pH values lower than 2, a dramatic reduction in the intensity of the LMCT band indicates dissociation of the complex in this pH regime. Using the program

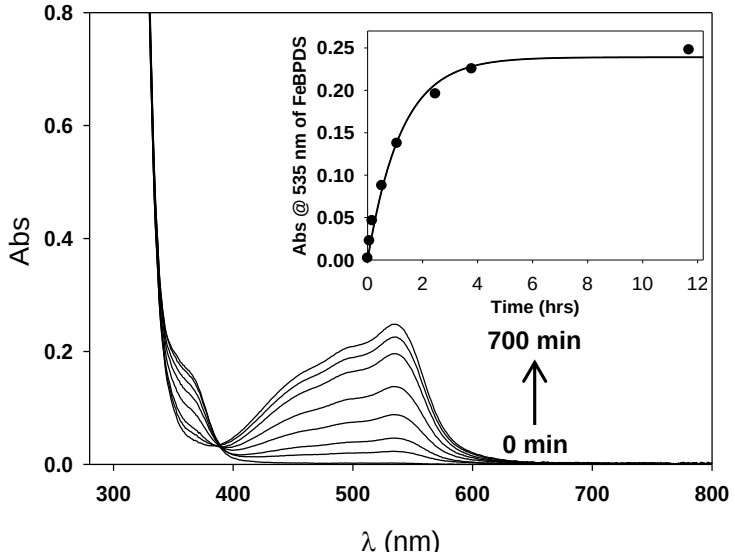

Figure 5.5. Photolysis of Fe-VF over 700 minutes upon exposure to a fluorescent light source in the presence of the Fe(II)-chelating agent, BPDS, at pH 2.9, 20°C and *I* = 0.7 M KNO_3. Inset: Single exponential fit of $Fe(BPDS)_3$ absorbance at 535 nm vs. time ($R^2 = 0.99$).

SPECFIT/32 we were able to construct a global model that satisfactorily accounts for the distribution of various Fe-VF species over the pH regime from 2-10.4 (Fig. 5.4). The constants derived from this global model are given in Table 5.1 and the calculated spectra for individual species are provided in the Appendix (Fig. 5.9). In general there is fair agreement between the values obtained by global refinement of the spectrophotometric titration data, the stepwise Schwarzenbach analysis and the fits to the metal-ligand potentiometric titration (Table 5.1).

5.2.4. Photochemistry. As expected for a siderophore containing two α-hydroxy acid units, Fe-VF was found to be photolabile producing an oxidized ligand photoproduct with concomitant reduction of Fe(III) to Fe(II). Photolysis of Fe(III)-VF by natural sunlight (1500 μEinstein m^{-2} s^{-1}) was monitored by ESI-MS in both positive and negative ion modes which gave qualitatively similar results. In negative ion mode, prior to photolysis only peaks corresponding to free VF (433 amu) and its iron complex (486 amu) are seen. Over the course of an hour the peaks corresponding to VF and Fe-VF are seen to diminish in intensity while new peaks grow in at 389 and 442 amu which correspond to VF* and Fe-VF* (*41*). After two hours

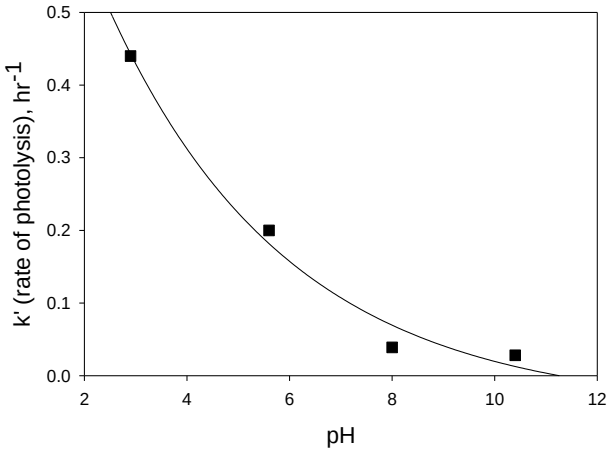

Figure 5.6. Rate constants for photolysis of Fe-VF as a function of pH. Duplicate experiments were performed at 20°C with I = 0.7 M KNO_3 using fluorescent light as the energy source. Error bars were not shown when smaller than the symbol.

only the peak due to free VF* photoproduct remains.

5.2.5. Kinetics of Photolysis. In comparison to other photoactive marine siderophores such as petrobactin, aerobactin, the aquachelins or the marinobactins, Fe-VF proved exceptionally susceptible to photolysis (*13, 14, 17, 42, 43*). For example, when exposed to a mercury-vapor lamp > 95% of a 0.1 mM solution of Fe(III)-VF photolyzes within 6 minutes. Even in the presence of a 1000-fold excess of ligand, 20 minutes of exposure to light resulted in the complete photoxidation of all of the VF, as indicated by the disappearance of the corresponding peak in the HPLC. Thus, to prevent excessive photolysis and to obtain easily measureable reaction rates, we moved from a mercury vapor lamp to standard fluorescent lighting as an energy source. We initially monitored the rate of photolysis by measuring the disappearance of the 330 nm LMCT band of Fe-VF as a function of time. However, this band has a low extinction coefficient that required high concentrations of VF (a product obtained in low yield). Hence we conducted further experiments in the presence of the Fe(II) trapping agent BPDS and used the large extinction coefficient of $Fe(BPDS)_3$ absorbance band at 535 nm to monitor the photolysis (*44*). Under similar conditions the rate constants measured by the two

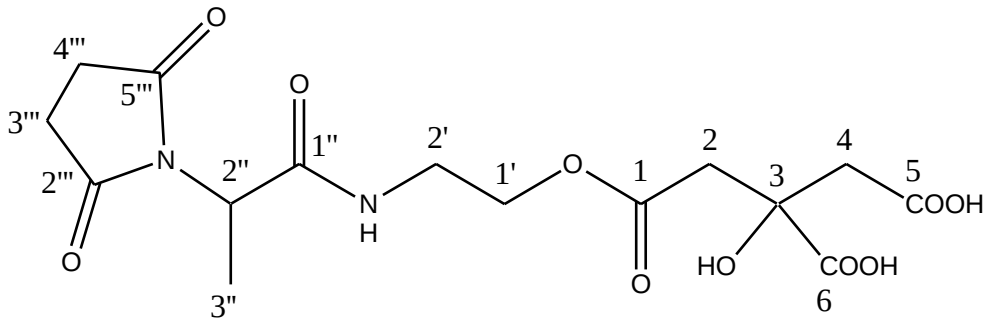

Figure 5.7. Proposed structure of the major photoproduct of vibrioferrin, VF*.

procedures were equivalent within experimental error (Table 5.2), indicating that the presence of the trapping agent did not appreciably affect the rate of photolysis and thus all subsequent experiments were conducted in the presence of BPDS. Clean first order kinetics and tight isosbestic points were observed indicating the presence of only two absorbing species during the photolysis (Fig. 5.5). The reaction rate constant was seen to decrease rapidly as a function of pH (Fig. 5.6) so that near the acidity of seawater (pH 8.0) the photolysis of Fe-VF had a half life of 17.7 hr while petrobactin or the peptidic portion of the marinobactins showed no observable (< 5%) photolysis under the same conditions.

5.2.6. Structure Elucidation. Having observed that Fe-VF was extremely susceptible to photolysis we sought to determine the structure of the photoproduct, VF*. The lack of any apparent appreciable affinity for Fe(II) or Fe(III) by the photoproduct (as indicated by the complete loss of the LMCT band and the negative CAS response of VF*) allowed for its simple isolation by HPLC without the need to extract the iron. Complete structural characterization was obtained by a combination of mass spectral and NMR methods.

The sodium adduct of the photoproduct has an exact mass of 411.1019 (difference between measured and theoretical mass of 411.1010 amu, Δ=2.2 ppm) which gives a molecular formula for the $[M+Na]^+$ ion of $C_{15}H_{20}O_{10}N_2Na$. The most characteristic feature of the ^1H NMR of VF* is its extreme simplification in comparison to VF itself because several protons lose

their diastereotopic nature (*32*). The presence of single sharp methyl doublet from the alanine residue at 1.47 ppm indicates there is only a single form of VF* unlike VF which displays two such doublets in an ca. 2:1 ratio due to the presence of open and closed chain forms (Figs. 5.7, 5.10). Another important feature is the simplification of the citrate region in VF* compared to VF. The latter contains two distinct sets of diastereotopic protons, integrating to four protons each, for the two distinct citrate groups in the molecule while the former contains only a single ABX_2-type system integrating to four protons, centered at 2.89 ppm, assigned to the diastereotopic citrate protons (H-2ab, H-4ab) (Fig. 5.10). The chemical shift values indicate that it is the terminal citrate group that is retained while that associated with the 2-ketoglutarate derived five-membered ring is lost. This is corroborated by the presence of a sharp singlet integrating to four protons corresponding to H-3”’ and H-4”’ centered at 2.79 ppm and further shows that the five-membered ring has two-fold symmetry (Fig. 5.7, Table 5.3). The ^{13}C NMR spectrum shows the presence of only 13 sharp resonances as compared to 16 seen in VF (Fig. 5.11). The most characteristic feature is the disappearance of one of the quaternary carbons of VF (91.9 ppm) due to the loss of CO_2 from the five-membered ring. The carbonyl region shows only five signals, rather than the six seen in VF, with one roughly twice the intensity of the others assignable to the two equivalent succinimidyl carbonyls on the ring (C-2”’ and C-5”’). In addition only six, rather than seven, methylene carbon resonances are seen in VF*, again one of which is twice the intensity of the others, assignable to the two equivalent methylenes of the five-membered succinimidyl ring (C-3”’ and C-4”’). The proposed structure is shown in Figure 5.7 and complete assignments, verified by the appropriate 2-D experiments, are given in tables 5.3 and 5.4.

5.3. Discussion

Vibrioferrin is a member of the carboxylate class of siderophores containing two α-hydroxy acid groups originally isolated from *Vibrio parahaemolyticus*, an enteropathogenic estuarine bacterium often associated with seafood-borne gastroenteritis (*24, 27, 28, 32*). Previously, we isolated VF from two specific clades of *Marinobacter* species (*33*). These clades are a unique subset of bacteria which have been found to be specifically associated with bloom-forming dinoflagellates including toxic species such as *G. catenatum* isolated from places as far apart as the Pacific and Atlantic oceans. This functional conservation is interpreted as indicating that there are specific selective processes operating between the bacterium and dinoflagellate (*45*). Why are dinoflagellates selecting for such a phylogenetically and functionally specific group of marine bacteria? Can we find any clues in the unique features of vibrioferrin as to the nature of this and related algal-bacterial relationships?

The first obvious feature unique to VF is its relatively weak iron binding properties. This is presumably a direct result of the fact that VF lacks the six donor groups required to complete the octahedral coordination geometry preferred by Fe(III) and generally found in other siderophores. While it is difficult to compare the overall formation constants of iron chelators to one another due to differences in ligand pK_a's and/or stoichiometry, the "pM" value has been proposed as a means for more direct comparison (*40*). The pM values express the amount of "free iron" present at equilibrium under particular sets of experimental conditions, typically at a total ligand concentration of 10^{-5} M, a total iron concentration of 10^{-6} M, and a pH of 7.4 (Table 5.5). It is clear that vibrioferrin is not a particularly powerful iron chelator as compared to the more usual tris-(hydroxamate) or tris-(catecholate) or mixed ligand siderophores at this pH (*46*). For example petrobactin and marinobactin E, siderophores known to be produced by closely related, but non-algal associated, *Marinobacter* spp., are 10^4 to 10^7 fold better chelators than VF, a difference that only increases at the higher pH value of seawater.

Beyond its relatively weak Fe(III) binding, the most remarkable feature of VF is the striking sensitivity of its iron complex to photolysis. Similar to citrate, the iron complexes of siderophores that contain a α- or β-hydroxy acid moiety are generally photosensitive and undergo photolysis causing the loss of a carboxylate group from the ligand in the form of CO_2 and the concomitant reduction of the metal and its release as Fe(II). Although the exact mechanism for the photochemical degradation of iron citrate is complex, the reduction of Fe(III) and radical anion generation are generally observed (*47*). It is perhaps significant that most of these hydroxy acid-containing siderophores seem to be associated with the marine environment (*48*). However, the photoproducts formed from the photolysis for all the siderophores studied thus far have been found to retain the ability to coordinate Fe(III) so that the overall photolysis reaction is actually that shown in equations 4 and 5.

$$\text{Fe(III)-Sid} + h\nu \rightarrow \text{Sid*} + \text{Fe(II)} \qquad (4)$$

$$\text{Sid*} + \text{Fe(II)} + O_2 \rightarrow \text{Fe(III)-Sid*} \qquad (5)$$

Indeed in some cases the photoproduct (sid*) is actually a *better* Fe(III) chelator than the parent siderophore (*16, 17*)! It has also been shown in the one case where it was studied that the Fe(III) complex of the photoproduct is recognized by the bacteria that produce the parent siderophore and is taken up via the same transport system with equal affinity (*17*). In light of these observations, we anticipated that Fe-VF would also be photosensitive and undergo photooxidation containing as it does two α-hydroxy acid moieties. Fe-VF did indeed undergo photolysis, and at a faster rate under relatively low illumination conditions, than other photoactive siderophores to produce a monodecarboxylated photoproduct and Fe(II) (*49*). What was unanticipated was the fact that the resulting photoproduct has *no* significant affinity for Fe(III). Thus the photolysis of Fe(III)-VF is an irreversible process that leads to the destruction of the siderophore and the ultimate formation of "free" Fe(III) as in equations 6 and 7

$$\text{Fe(III)-VF} + h\nu \rightarrow \text{VF*} + \text{Fe(II)} \qquad (6)$$

$$Fe(II) + O_2 \rightarrow Fe(III)' \rightarrow Fe(III)\downarrow \qquad (7)$$

where Fe(III)' represents transiently soluble iron hydroxo species and Fe(III)↓ represents the increasingly insoluble mineral phases present at equilibrium.

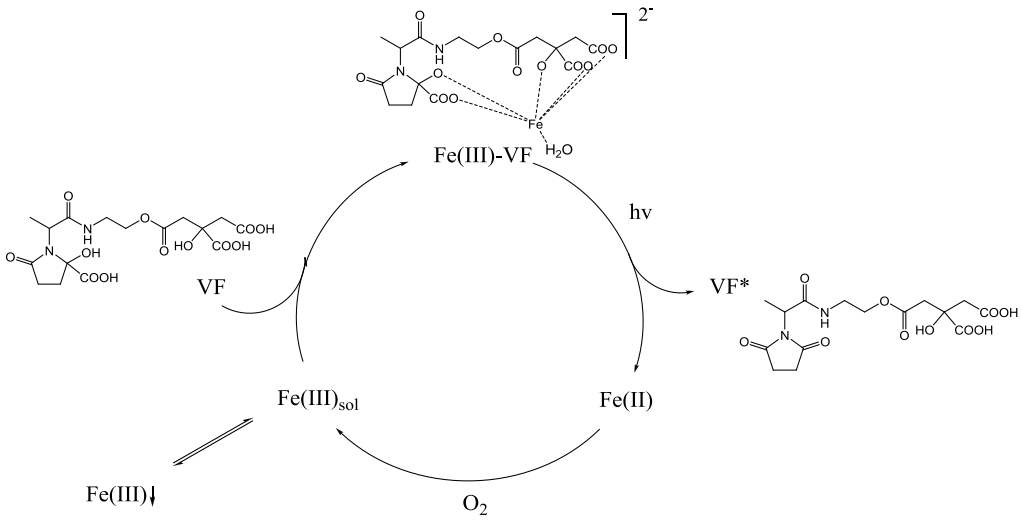

Figure 5.8. Fe catalyzed photochemical oxidation of VF.

Unlike other photosensitive siderophores where the photoproduct retains the ability to coordinate and sequester Fe(III), the lack of affinity for iron of the photoproduct of VF leads to catalytic destruction of the ligand (Fig. 5.8). With such a rapid turnover rate, it appears that even trace amounts of Fe(III) will eventually consume a large excess of VF under high light flux conditions. Such a scenario seems to be metabolically wasteful until one notes that the Fe(II) formed by the photolysis of Fe(III)-VF is expected to be rapidly oxidized to Fe(III) under seawater conditions (*50*). The Fe(III) thus produced is initially in the form of relatively soluble simple hydroxo complexes (Fe(III)') which are only slowly converted into the more refractory oxo-hydroxo polymeric mineral phases. Using ^{55}Fe-labelled VF we have shown that the soluble iron pool i.e. Fe(III)' initially produced after aerobic photolysis is in fact more rapidly and efficiently taken up by the producing bacteria than that of intact Fe(III)-VF itself. Equally significant is the fact that associated phytoplankton are also more capable of assimilating ^{55}Fe

generated from photolyzed Fe(III)-VF than from intact Fe(III)-VF by more than an order of magnitude (*49*). In view of these findings, we propose that VF photodegradation may be an evolutionarily adapted function by which the producing bacteria "share" the soluble, photochemically produced iron with their algal associates possibly in exchange for algal-excreted metabolites. Work designed to further address this hypothesis is underway.

5.4. Methods

5.4.1. Siderophore Isolation. Vibrioferrin was isolated and purified as previously described (*33*).

5.4.2. Potentiometric and Spectrophotometric Titrations. Standard carbonate-free solutions of NaOH were prepared from Baker “Dilut-It” ampoules using boiled, purified water (i.e., 18 MΩ resistance; MilliQ) and were stored under Ascarite™ scrubbed argon. Base solutions were standardized with KHP to the phenolphthalein end point. The absence of carbonate (< 2%) was confirmed by Gran’s plots (*51*). Iron solutions were purchased from Fluka ($FeCl_3 \cdot 6H_2O$ in 4% HCl) and the exact iron concentration determined by EDTA titration with Variamine Blue as an indicator (*17*). Excess acid in the iron solution was determined by passing an aliquot through a well-washed sample of the acid form of AG 50W-X8 cation exchange resin (Bio-Rad) and titrating the liberated acid. The excess acid was the difference between the total acid and three times the known iron concentration. Spectrophotometric and potentiometric titrations were performed in a foil covered, jacketed, three-necked titration vessel and connected to a constant temperature water bath held at 25.0(1)°C. Ionic strength was fixed at 0.1M with NaCl. Hydrogen ion concentration was measured using a Mettler-Toledo DL50 titrator connected to a Mettler-Toledo DG111-5C combination electrode which was standardized with a three buffer sequence and corrected (as needed) to read the negative log of the hydrogen ion concentration directly using dilute HCl solutions. Titrant was added to the cell,

which was kept under a blanket of Ascarite scrubbed argon gas. Ligand protonation constants were determined from the nonlinear refinement of the potentiometric titration data using the program BEST developed by Martell and Motekaitis while metal-ligand constants utilized HYPERQUAD (*35, 52*). Spectrophotometric titration data were analyzed either graphically using the Schwarzenbach equation (*39*) or via nonlinear least squares refinement using the program SPECFIT/32 (*53*). Final species distribution diagram was plotted using the calculated protonation constants using HySS2006 (*35*). UV-Vis spectra were recorded on a Cary 50 spectrophotometer and processed with Varian Win-UV software.

5.4.3. EDTA and EGTA Chelate Competition Experiments. The low pH obtained upon mixing iron (III) with a solution of any of the siderophores indicates that a considerable degree of chelate formation occurs prior to the addition of any base. Since only a small fraction of free metal is present, it is difficult to obtain the overall formation constant from titration data directly. Therefore a chelate competition method was used to obtain the desired formation constant. Solutions for the EDTA or EGTA (Aldrich-Sigma) competition measurements were prepared by adding a known quantity of iron stock to a solution containing 100 mM Bis-Tris (pH 6.0) buffer to avoid Fe-EGTA decomposition at higher pH values (*54*), 0.100 M NaCl to fix the ionic strength, a constant amount of siderophore and varying quantities of EDTA or EGTA in excess and allowing them to come to equilibrium in the dark. The attainment of equilibrium was monitored by optical spectroscopy and appeared to be relatively rapid but samples were left for 1 week as a precaution. The concentration of iron siderophore complex was measured by optical spectroscopy using the known extinction coefficients of the Fe-siderophore and EDTA or EGTA. Data were analyzed using the program SPECFIT/32.

5.4.4. DFT Calculations. Geometry optimizations were carried out on the two possible structures (*vide infra*) for the high pH form of Fe-VF using the B3LYP density functional method and two basis sets: (1) LANL2DZ for all atoms, and a mixed basis of cc-pVDZ for the

main group atoms and (2) the CEP-121G basis and effective core potential for iron. Basis set superposition introduces an error of 3-4 kcal/mol in the hydrido energy using either basis set, and additional thermal and zero-point corrections were not applied.

5.4.5. Photoproduct Isolation and Characterization. Iron(III)-vibrioferrin was prepared by addition of a standard solution of $FeCl_3 \cdot 6H_2O$ to apo-vibrioferrin at pH 2.5 and left to equilibrate overnight then purified by HPLC in the dark. A Phenomenex Luna™ 5 µm C18(2) column was used with the following gradient: (A=H_2O/0.1%TFA, B=CH_3CN/0.1%TFA) 0-10% B in 15 minutes at a flow rate of 5 mL/min and monitoring the eluant at 300 nm. Purified Fe(III)-VF (7.6 mg) was photolyzed under fluorescent light for 4 hours at 20°C. The photolyzed solution was then lyophilized and re-purified by HPLC using the same column with the following gradient: (A = H_2O/0.1%TFA, B = CH_3CN/0.1%TFA) 0-3% B in 5 minutes, 3-12% B in 5 minutes, 12-25% B in 12 minutes, 25-50% B in 13 minutes at a flow rate of 5 mL/min and monitoring the eluant at 210 nm. Purity of the compound was confirmed by analytical reverse phase HPLC. All HPLC fractions were concentrated by lyophilization.

Routine electrospray–ionization mass spectrometry (ESI-MS) was performed on an Agilent LC/MSD Trap XCT Plus mass spectrometer. For high resolution mass measurements a ThermoFinnigan MAT900XL instrument was used (UCSD). NMR experiments (i.e., ^{1}H, ^{13}C, gCOSY, TOCSY, gHMQC, and gHMBC) were run at 30 °C in D_2O with 0.03% DSS (Aldrich-Sigma) on a Varian 400 MHz NMR spectrometer using standard pulse sequences obtained from the VnmrJ™ software (v. 2.2c).

5.4.6. Photolysis Kinetics. All photolysis experiments were conducted at 20 ^{o}C in either a Thermo 818 Illuminated Incubator with temperature controller and fluorescent lighting (80 µE m^{-2} s^{-1}) or using a mercury vapor lamp (350 µE m^{-2} s^{-1}). All samples were photolyzed in borosilicate glass vessels. Samples illuminated with the mercury vapor lamp were placed in a jacketed cuvette connected to a constant temperature water bath at 20^{o}C. Solutions were

prepared by adding a known amount of standardized $FeCl_3 \cdot 6H_2O$ to a known amount of siderophore (1:2) in the presence of 0.7 M KNO_3 and 50 mM of the appropriate buffer (MES for pH 5.60, and HEPES for pH 8.00). Solutions kept at extreme ends of the pH range did not contain buffers but the initial and final pH values did not change appreciably during the photolysis. BPDS (4,7-di(4-phenylsulfonate)-1,10 phenanthroline $Na_2 \cdot 3H_2O$, Fluka) was added as required prior to exposure to light (Fe:BPDS = 1:4). Samples exposed to light were corrected for non-specific reduction by monitoring a control kept in the dark at the same temperature.

Catalytic photooxidation of VF was monitored using a Beckman-Coulter Gold 126 analytical HPLC system equipped with a diode array detector (Gold 168). Fe-VF was prepared as previously described and excess ligand added before the start of the photolysis. After exposure to a mercury-vapor lamp for various times, an aliquot of the reaction mixture was loaded onto a Luna 5 μm C18(2) analytical column and the products separated with the following gradient (A=0.1% TFA in MQ-H_2O, B=0.1% TFA in CH_3CN; flow rate=0.6 mL/min): 3% B in 5 minutes, 12% B in 10 minutes, 12% B in 2 minutes, 0% B in 2 minutes.

5.5. Appendix

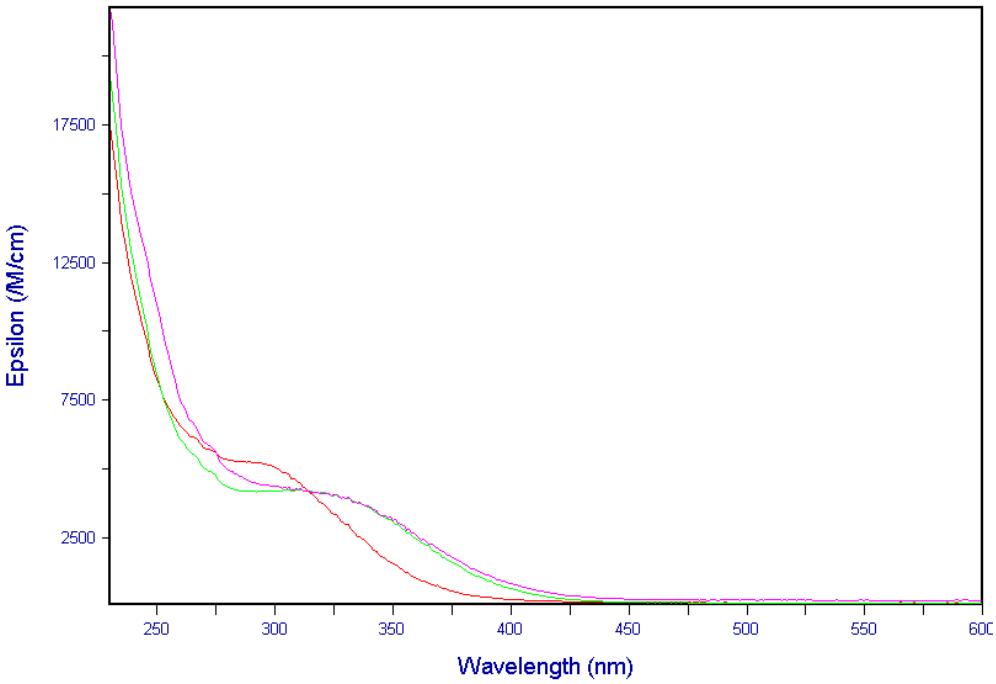

Figure 5.9. Calculated spectra of the various FeVF protonated species using SPECFIT/32. Trace colors represent: $FeH_{-1}VF^{3-}$ (red), $FeVF^{2-}$ (magenta), $FeHVF^{-}$ (green).

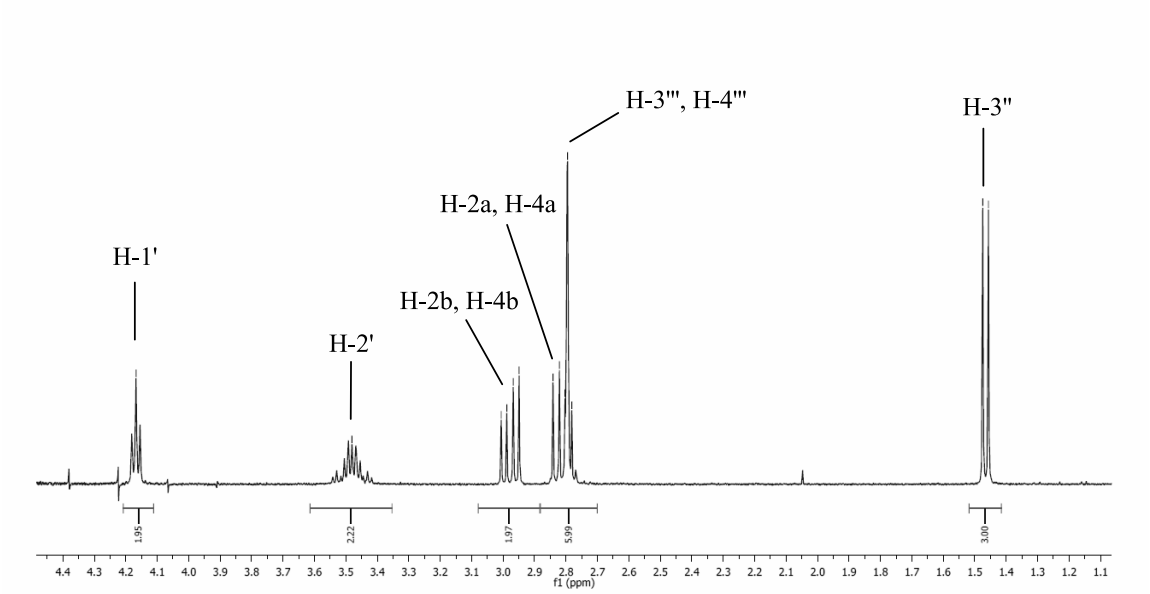

Figure 5.10. ^{1}H NMR of VF* in D_2O (0.03% DSS).

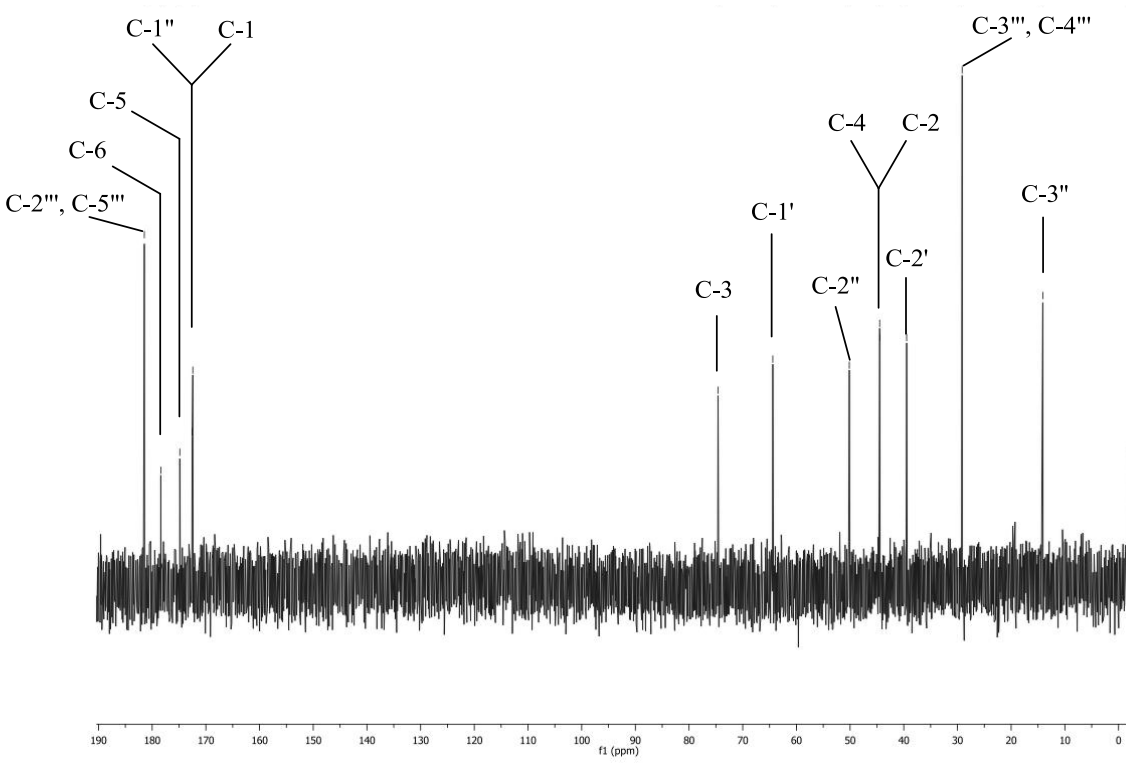

Figure 5.11. ^{13}C NMR of VF* in D_2O (0.03% DSS).

Table 5.1. Deprotonation constants for the Fe-VF complex. Values were extracted via a global fit to the data using SpecFit/32, stepwise fits to the Schwarzenbach equation or fits to the potentiometric titration using Hyperquad.

Species	*Hyperquad*	*Specfit*	*Schwarzenbach*
$\log K_{(MH_{-1}L)}$	9.59	8.90	9.00
$\log K_{(ML)_{fixed}}$	24.03	24.03	-
$\log K_{(MHL)}$	4.38	4.35	4.40

Table 5.2. Rate constants for photolysis of Fe-VF using fluorescent light at 20°C either in the presence of the Fe(II) trapping agent, BPDS (k'_{BPDS}) or without (k'). I = 0.7 M KNO_3.

pH	k'_{BPDS} (h^{-1})	k' (h^{-1})
2.90	0.44	0.46
5.60	0.20	
8.0	0.039	
10.40	0.028	

Table 5.3. ^{1}H chemical shift assignments for VF* in D_2O (0.03% DSS).

^{1}H δ (ppm) in D_2O	Assignment
1.47 (d, 7Hz)	H-3”
2.79 (s)	H-3”’, H-4”’
2.77-2.84 (m)	H-2a, H-4a
2.95-3.02 (m)	H-2b, H-4b
3.48 (m)	H-2’
4.17 (t, 5Hz)	H-1’

Table 5.4. ^{13}C chemical shift assignments for VF* in D_2O (0.03% DSS).

^{13}C δ (ppm) in D_2O	Assignment
14.11	C-3”
29.13	C-3”’, C-4”’
39.47	C-2’
44.44	C-2
44.49	C-4
50.15	C-2”
64.40	C-1’
74.59	C-3
172.43	C-1
172.55	C-1”
174.85	C-5
178.39	C-6
181.46	C-2”’, C-5”’

Table 5.5. pM Values for Various Fe(III)-Siderophore Complexes.

Complex	*pM_1*	*pM_2*
Rhizoferrin[a]	19.7	-
Aerobactin[b]	23.3	-
Petrobactin[c]	23.0	-
Marinobactin E[d]	25.8	27.5
Vibrioferrin[e]	18.4	19.6

pM_1 = -log $[Fe^{3+}]$ where $[L]_0 = 10^{-5}$ M, $[Fe]_0 = 10^{-6}$ M, and pH = 7.4. pM_2 pH 8.0. pM values are based on published stability constants (see references *a*-*e*). *a* (*34*), *b* (*40*), *c* (*16*), *d* (*55*), *e* (*this work*).

5.6. Acknowledgments

This work was supported by NOAA Grants #NA04OAR4170038 and NA08OAR4170669, California Sea Grant College Program Project numbers R/CZ-198 and R/CONT-205, through NOAA's National Sea Grant College Program, U.S. Dept. of Commerce. The authors would like to thank Andrew Cooksy (SDSU) for the DFT calculations. This chapter has been previously published as Amin, S. A., Green, D. H., Küpper, F. C., and Carrano, C. J. (2009) Vibrioferrin, an Unusual Marine Siderophore: Iron Binding, Photochemistry, and Biological Implications, *Inorg. Chem. 48,* 11451-11458.

5.7. References

1. Bruland, K. W., Donat, J. R., and Hutchins, D. A. (1991) Interactive influences of bioactive trace metals on biological production in oceanic waters, *Limnol. Oceanogr. 36*, 1555-1577.

2. Martin, J. H., and Fitzwater, S. E. (1988) Iron deficiency limits phytoplankton growth in the north-east Pacific subarctic, *Nature 331*, 341-343.

3. Wu, J., and Luther III, G. W. (1994) Size-fractionated iron concentrations in the water column of the western North Atlantic ocean, *Limnol. Oceanogr. 39*, 1119-1129.

4. Gledhill, M., and van den Berg, C. M. G. (1994) Determination of complexation of iron(III) with natural organic complexing ligands in seawater using cathodic stripping voltammetry, *Mar. Chem. 47*, 41-54.

5. Vraspir, J. M., and Butler, A. (2009) Chemistry of marine ligands and siderophores, *Annu. Rev. Mar. Sci. 1*, 43-63.

6. Winkelmann, G., and Carrano, C. J. (1997) *Transition metals in microbial metabolism*, Harwood Academic Publishers, Amsterdam.

7. Raymond, K. N. (1994) Recognition and transport of natural and synthetic siderophores by microbes, *Pure Appl. Chem. 66*, 773-781.

8. Martinez, J. S., Carter-Franklin, J. N., Mann, E. L., Martin, J. D., Haygood, M. G., and Butler, A. (2003) Structure and membrane affinity of a suite of amphiphilic siderophores produced by a marine bacterium, *Proc. Natl. Acad. Sci. U. S. A. 100*, 3754-3759.

9. Martinez, J. S., Haygood, M. G., and Butler, A. (2001) Identification of a natural desferrioxamine siderophore produced by a marine bacterium, *Limnol. Oceanogr. 46*, 420-424.

10. Martinez, J. S., Zhang, G. P., Holt, P. D., Jung, H. T., Carrano, C. J., Haygood, M. G., and Butler, A. (2000) Self-assembling amphiphilic siderophores from marine bacteria, *Science 287*, 1245-1247.

11. Reid, R. T., Livet, D. H., Faulkner, D. J., and Butler, A. (1993) A siderophore from a marine bacterium with an exceptional ferric ion affinity constant, *Nature 366*, 455-458.

12. Martin, J., Ito, Y., Homann, V., Haygood, M., and Butler, A. (2006) Structure and membrane affinity of new amphiphilic siderophores produced by *Ochrobactrum* sp. SP18, *J. Biol. Inorg. Chem. 11*, 633-641.

13. Barbeau, K., Rue, E. L., Bruland, K. W., and Butler, A. (2001) Photochemical cycling of iron in the surface ocean mediated by microbial iron(III)-binding ligands, *Nature 413*, 409-413.

14. Barbeau, K., Zhang, G., Live, D. H., and Butler, A. (2002) Petrobactin, a photoreactive siderophore produced by the oil-degrading marine bacterium *Marinobacter hydrocarbonoclasticus*, *J. Am. Chem. Soc. 124*, 378-379.

15. Maldonado, M. T., Strzepek, R. F., Sander, S., and Boyd, P. W. (2005) Acquisition of iron bound to strong organic complexes, with different Fe binding groups and photochemical reactivities, by plankton communities in Fe-limited subantartic waters, *Global Biogeochem. Cycles 19*.

16. Abergel, R. J., Zawadzka, A. M., and Raymond, K. N. (2008) Petrobactin-mediated iron transport in pathogenic bacteria: coordination chemistry of an unusual 3,4-catecholate/citrate siderophore, *J. Am. Chem. Soc. 130*, 2124-2125.

17. Küpper, F. C., Carrano, C. J., Kuhn, J.-U., and Butler, A. (2006) Photoreactivity of iron(III)-aerobactin: photoproduct structure and iron(III) coordination, *Inorg. Chem. 45*, 6028-6033.

18. Kodama, M., Doucette, G., and Green, D. (2006) Relationships Between Bacteria and Harmful Algae, In *Ecology of Harmful Algae* (Granéli, E., and Turner, J. T., Eds.), pp 243-255, Springer-Verlag, Heidelberg.

19. Martin, J. H., Coale, K. H., Johnson, K. S., Fitzwater, S. E., Gordon, R. M., Tanner, S. J., Hunter, C. N., Elrod, V. A., Nowicki, J. L., Coley, T. L., Barber, R. T., Lindley, S., Watson, A. J., Van Scoy, K., Law, C. S., Liddicoat, M. I., Ling, R., Stanton, T., Stockel, J., Collins, C., Anderson, A., Bidigare, R., Ondrusek, M., Latasa, M., Millero, F. J., Lee, K., Yao, W., Zhang, J. Z., Friederich, G., Sakamoto, C., Chavez, F., Buck, K., Kolber, Z., Greene, R., Falkowski, P., Chisholm, S. W., Hoge, F., Swift, R., Yungel, J., Turner, S., Nightingale, P., Hatton, A., Liss, P., and Tindale, N. W. (1994) Testing the iron hypothesis in ecosystems of the equatorial Pacific Ocean, *Nature 371*, 123-129.

20. Boyd, P. W., Watson, A. J., Law, C. S., Abraham, E. R., Trull, T., Murdoch, R., Bakker, D. C. E., Bowie, A. R., Buesseler, K. O., Chang, H., Charette, M., Croot, P., Downing, K., Frew, R., Gall, M., Hadfield, M., Hall, J., Harvey, M., Jameson, G., LaRoche, J., Liddicoat, M., Ling, R., Maldonado, M. T., McKay, R. M., Nodder, S., Pickmere, S., Pridmore, R., Rintoul, S., Safi, K., Sutton, P., Strzepek, R., Tanneberger, K., Turner, S., Waite, A., and Zeldis, J. (2000) A mesoscale phytoplankton bloom in the polar Southern Ocean stimulated by iron fertilization, *Nature 407*, 695-702.

21. Soria-Dengg, S., Reissbrodt, R., and Horstmann, U. (2001) Siderophores in marine coastal waters and their relevance for iron uptake by phytoplankton: experiments with the diatom Phaeodactylum tricornutum, *Mar. Ecol. Prog. Ser. 220*, 73-82.

22. Naito, K., Imai, I., and Nakahara, H. (2008) Complexation of iron by microbial siderophores and effects of iron chelates on the growth of marine microalgae causing red tides, *Phycol. Res. 56*, 58-67.

23. Naito, K., Matsui, M., and Imai, I. (2005) Ability of marine eukaryotic red tide microalgae to utilize insoluble iron, *Harmful Algae 4*, 1021-1032.

24. Funahashi, T., Moriya, K., Uemura, S., Miyoshi, S.-I., Shinoda, S., Narimatsu, S., and Yamamoto, S. (2002) Identification and characterization of *pvuA*, a gene encoding the ferric vibrioferrin receptor protein in *Vibrio parahaemolyticus*, *J. Bacteriol. 184*, 936-946.

25. Takeuchi, Y., Nagao, Y., Toma, K., Yoshikawa, Y., Akiyama, T., Nishioka, H., Abe, H., Harayama, T., and Yamamoto, S. (1999) Synthesis and siderophore activity of vibrioferrin and one of its diastereomeric isomers, *Chem. Pharm. Bull. (Tokyo) 47*, 1284-1287.

26. Takeuchi, Y., Akiyama, T., and Harayama, T. (1999) Total synthesis of the siderophore vibrioferrin, *Chem. Pharm. Bull. (Tokyo) 47*, 459-460.

27. Tanabe, T., Funahashi, T., Nakao, H., Miyoshi, S.-I., Shinoda, S., and Yamamoto, S. (2003) Identification and characterization of genes required for biosynthesis and transport of the siderophore vibrioferrin in *Vibrio parahaemolyticus*, *J. Bacteriol. 185*, 6938-6949.

28. Tanabe, T., Nakao, H., Kuroda, T., Tsuchiya, T., and Yamamoto, S. (2006) Involvement of the *Vibrio parahaemolyticus pvsC* gene in export of the siderophore vibrioferrin, *Microbiol. Immunol. 50*, 871-876.

29. Yamamoto, S., Akiyama, T., Okujo, N., Matsu-ura, S., and Shinoda, S. (1995) Demonstration of a ferric vibrioferrin-binding protein in the outer membrane of *Vibrio parahaemolyticus*, *Microbiol. Immunol. 39*, 759-766.

30. Yamamoto, S., Okujo, N., Matsuura, S., Fujiwara, I., Fujita, Y., and Shinoda, S. (1994) Siderophore-mediated utilization of iron bound to transferrin by *Vibrio parahaemolyticus*, *Microbiol. Immunol. 38*, 687-693.

31. Yamamoto, S., Okujo, N., Miyoshi, S.-I., Shinoda, S., and Narimatsu, S. (1999) Siderophore production of *Vibrio parahaemolyticus* strains from different sources., *Microbiol. Immunol. 43*, 993.

32. Yamamoto, S., Okujo, N., Yoshida, T., Matsuura, S., and Shinoda, S. (1994) Structure and iron transport activity of vibrioferrin, a new siderophore of *Vibrio parahaemolyticus*, *J. Biochem., Tokyo 115*, 868-874.

33. Amin, S. A., Küpper, F. C., Green, D. H., Harris, W. R., and Carrano, C. J. (2007) Boron binding by a siderophore isolated from marine bacteria associated with the toxic dinoflagellate *Gymnodinium catenatum*, *J. Am. Chem. Soc. 129*, 478-479.

34. Carrano, C. J., Drechsel, H., Kaiser, D., Jung, G., Matzanke, B., Winkelmann, G., Rochel, N., and Albrecht-Gary, A. M. (1996) Coordination chemistry of the carboxylate type siderophore rhizoferrin: the iron(III) complex and its metal analogs, *Inorg. Chem. 35*, 6429-6436.

35. Gans, P., Sabatini, A., and Vacca, A. (1996) Investigation of equilibria in solution. Determination of equilibrium constants with the HYPERQUAD suite of programs,

Talanta 43, 1739-1753.

36. Martell, A. E., and Smith, R. M. (1974) *Critical stability constants*, Plenum Press, New York.

37. Budzikiewicz, H. (2005) Bacterial Citrate Siderophores, *Mini-Rev. Org. Chem. 2*, 119-124.

38. Murakami, T., Nojiri, M., Nakayama, H., Odaka, M., Yohda, M., Dohmae, N., Takio, K., Nagamune, T., and Endo, I. (2000) Post-translational modification is essential for catalytic activity of nitrile hydratase, *Protein Sci. 9*, 1024-1030.

39. Schwarzenbach, G., and Schwarzenbach, K. (1963) Hydroxamatkomplexe I. Die stabilität der eisen(III)-komplexe einfacher hydroxamsäuren und des ferrioxamins B, *Helv. Chim. Acta 46*, 1390-1400.

40. Harris, W. R., Carrano, C. J., and Raymond, K. N. (1979) Coordination chemistry of microbial iron transport compounds. 16. Isolation, characterization, and formation constants of ferric aerobactin, *J. Am. Chem. Soc. 101*, 2722-2727.

41. Although an Fe-VF* complex is observed in the ESI-MS, we believe this is a byproduct of the ionization method representing anionic-cationic interactions and not a "real" iron complex.

42. Barbeau, K. (2006) Photochemistry of organic iron(III) complexing ligands in oceanic systems, *Photochem. Photobiol. 82*, 1505-1516.

43. Barbeau, K., Rue, E. L., Trick, C. G., Bruland, K. W., and Butler, A. (2003) Photochemical reactivity of siderophores produced by marine heterotrophic bacteria and cyanobacteria based on characteristic Fe(III) binding groups, *Limnol. Oceanogr. 48*, 1069-1078.

44. Cowart, R. E., Singleton, F. L., and Hind, J. S. (1993) A comparison of bathophenanthrolinedisulfonic acid and ferrozine as chelators of iron(II) in reduction reactions, *Anal. Biochem. 211*, 151-155.

45. Green, D. H., Llewellyn, L. E., Negri, A. P., Blackburn, S. I., and Bolch, C. J. S. (2004) Phylogenetic and functional diversity of the cultivable bacterial community associated with the paralytic shellfish poisoning dinoflagellate *Gymnodinium catenatum*, *FEMS Microbiol. Ecol. 47*, 345-357.

46. Harris, W. R., Raymond, K. N., and Weitl, F. L. (1981) Ferric ion sequestering agents. 6. The spectrophotometric and potentiometric evaluation of sulfonated tricatecholate ligands, *J. Am. Chem. Soc. 103*, 2667-2675.

47. Abrahamson, H. B., Rezvani, A. B., and Brushmiller, J. G. (1994) Photochemical and spectroscopic studies of complexes, of iron(III) with citric acid and other carboxylic acids, *Inorg. Chim. Acta 226*, 117-127.

48. Butler, A. (2005) Marine siderophores and microbial iron mobilization, *BioMetals 18*, 369-374.

49. Amin, S. A., Green, D. H., Hart, M. C., Küpper, F. C., Sunda, W. G., and Carrano, C. J. (2009) Photolysis of iron–siderophore chelates promotes bacterial–algal mutualism, *Proc. Natl. Acad. Sci. U. S. A. 106*, 17071-17076.

50. Morgan, B., and Lahav, O. (2007) The effect of pH on the kinetics of spontaneous Fe(II) oxidation by O_2 in aqueous solution - basic principles and a simple heuristic description, *Chemosphere 68*, 2080-2084.

51. Gran, G. (1952) Determination of the equivalence point in potentiometric titrations. Part II, *Analyst 77*, 661-670.

52. Martell, A. E., and Motekaitis, R. J. (1992) *The determination and use of stability constants*, Wiley-VCH Inc., New York.

53. Gampp, H., Maeder, M., Meyer, C. J., and Zuberbuehler, A. D. (1985) Calculation of equilbrium constants from multiwavelength spectroscopic data- II. SPECFIT: Two user friendly programs in BASIC and standard FORTRAN 77, *Talanta 32*, 257-264.

54. Schröder, K. H. (1963) The stability of the ferric complex with EGTA, *Acts Chem. Scand. 17*, 1509-1514.

55. Zhang, G., Amin, S. A., Küpper, F. C., Holt, P. D., Carrano, C. J., and Butler, A. (2009) Ferric stability constants of representative marine siderophores: Marinobactins, aquachelins, and petrobactin, *Inorg. Chem. 48*, 11466-11473.

6. Diel effects on iron uptake genes in vibrioferrin-producing *Marinobacter* species and their distribution in the North Atlantic

6.1. Introduction

Iron is arguably one of the most important micronutrients in the marine environment due to its poor solubility and tendency to form biologically unavailable colloidal and oxo-polymeric species. The low available concentration of iron in many parts of the open ocean is mostly dominated by organic ligands that tightly complex soluble iron and further complicate its speciation (*1-3*). Multiple iron fertilization experiments in high-nutrient-low-chlorophyll (HNLC) regions corroborated the importance of iron and its limitation to marine microorganisms (*4-6*). To alleviate this limitation, microorganisms have adopted various pathways to acquire this precious metal. For instance, many marine bacteria have been shown to excrete small organic compounds, called siderophores, which bind iron with exceptional affinity in response to iron limitation (*7*). So far, an increasing number of marine siderophore structures have been characterized by various analytical techniques.

An emerging trait that seems to be almost universal among marine siderophores is the presence of α-hydroxy acid moieties, photolabile groups that reduce the bound Fe(III) via a non-reversible electronic transition reaction (*7-9*). The generated Fe(II) rapidly oxidizes under oceanic conditions to yield soluble inorganic iron, Fe(III)' (*10, 11*). Because of the loss of the photolabile functionality from the siderophore in the form of CO_2, it was anticipated that most of the photogenerated, unbound iron would be available to microorganisms (*12*). However, it was shown subsequently that the photooxidized siderophores (photoproducts) had still exceptional affinity to Fe(III), thus, restricting its availability (*12-14*). In two of the three examples examined so far, the photoproducts chelated iron with higher affinity than their parent siderophores (*13, 14*).

Previously, we have shown that algal-associated bacteria belonging to the *Marinobacter* genus release the siderophore vibrioferrin (VF) under iron limitation (*15*). The Fe(III)-VF complex was shown to be more photolabile than all previously examined photoactive

siderophores and generated a photoproduct incapable of chelating iron. The photogenerated iron was shown to be highly available to the producing bacterium as well as to their algal partner. In exchange, algal cells produced dissolved organic matter (DOM) that support bacterial growth and ultimately feeds the biosynthesis of VF (*16*). Here, we examine iron uptake pathways in VF-producers and show that siderophore-related iron uptake genes are co-regulated by iron limitation and light in agreement with the photochemistry of VF. We further examine the abundance of the biosynthesis genes of VF in the North Atlantic during a 2009 research cruise.

6.2. Results and Discussion

6.2.1. Iron uptake. Previously, we have measured VF mediated ^{55}Fe uptake in *Marinobacter sp. DG879* in attenuated sunlight vs. dark incubations. Cells exposed to sunlight (450 µE m^{-2} s^{-1}) assimilated ^{55}Fe more efficiently than controls kept in the dark indicating that Fe' is more bioavailable to the bacteria than iron bound to VF (*16*). Similar results were obtained by photolyzing a concentrated Fe(III)-VF solution prior to addition to cells using a mercury vapor lamp (350 µE m^{-2} s^{-1}). Due to variations in sunlight output depending on daily weather forecast, we resorted to measure uptake rates using the latter method. During two-hour incubations in the dark with either intact ^{55}Fe-VF or ^{55}Fe-VF photolyzed using the mercury vapor lamp, DG879 assimilated photolyzed iron with 30-70% more efficiency than intact ^{55}Fe-VF (Fig. 6.1). The metabolic inhibitor, CCCP, was used as negative control since it was the most effective inhibitor when compared to sodium azide or cell incubation at 4 ^{o}C (Fig. 6.2). In addition, DG879 assimilated iron from intact ^{55}Fe-VF in a concentration-dependent manner with k_m = 17.6 µM, indicating that active transport of iron is utilized when it is bound to VF. However, uptake of photogenerated iron was not concentration-dependent as it did not vary over a wide range of added iron (Fig. 6.3).

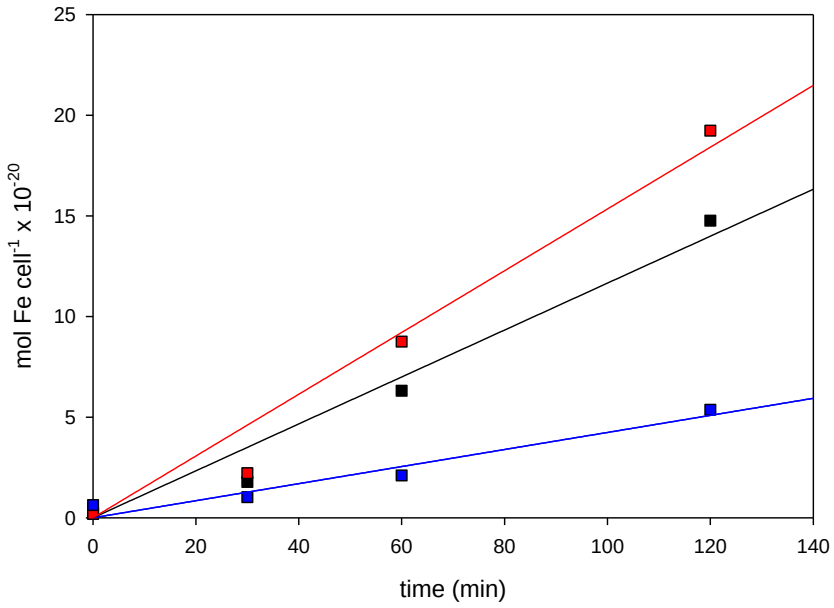

Figure 6.1. VF mediated iron uptake in *Marinobacter* sp. DG879 from photolyzed and intact ^{55}Fe-VF. ^{55}Fe uptake by *Marinobacter* sp. DG879 was performed at 20 ^{o}C using 1 µM Fe(III) and 3 µM total VF either kept in the dark (■) or photolyzed previously (■) using a mercury vapor lamp (350 µE m^{-2} s^{-1}). The uncoupler of oxidative phosphorylation (■), CCCP (carbonyl cyanide 3-chlorophenyhydrazone) was used as a metabolic inhibitor; incubations were carried out in the dark.

These results suggest that iron may be assimilated via two different pathways in VF-producing *Marinobacter* spp. either because Fe' binds to a target other than the Fe(III)-VF siderophore receptor, PvuA, or due to the fact that the bacteria are assimilating Fe(II) before its rapid oxidation to Fe(III), which will presumably require an Fe(II) receptor. Previously we have examined the latter possibility by measuring rates of uptake in the presence of the reductant ascorbate, which reduced the rate of uptake by nearly 4-fold (Fig. 6.2). This rate reduction coupled with the lack of homologs of known Fe(II) transport systems in the genome of *M. algicola* DG893 support the hypothesis that the photogenerated iron is assimilated after its oxidation to the ferric state. It is not clear what the target for Fe(III)' assimilation is; however, the presence of close homologs of a ferric binding protein system (Fbp) in DG893 suggests that this is a likely target.

FbpABC proteins belong to a family of iron binding proteins that include substrates ranging from transferrin (Tbp), lactoferrin (Lbp) to heme and hemoglobin, and are

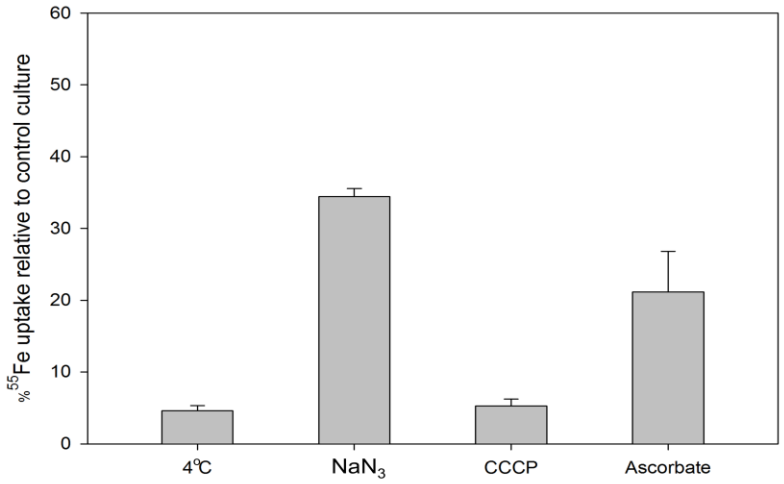

Figure 6.2. Various inhibitors of iron uptake in *Marinobacter* sp. DG879. Cells were either incubated at 4 °C, with 5 mM sodium azide, 30 µM CCCP, or 10 mM ascorbate 60 minutes prior to addition of ^{55}Fe. The former three are known inhibitors of cell growth, while ascorbate slowed the oxidation of photogenerated Fe(II)'. All uptake was measured in the dark at 20 °C except for the 4 °C incubation. Errors bars represent s.d. of triplicate cultures.

overexpressed under iron limitation. FbpA has been shown to be a periplasmic protein that transports inorganic iron species and has been shown to be highly regulated by available iron concentrations (*17*). There has been wide controversy regarding the accessibility of FbpA to the outer cell wall and whether it can bind mineral iron species from the cell surface. X-ray crystallography and site-directed mutagenesis of FbpA from *Haemophilus influenzae* (hFbpA) showed that the active site of the protein is capable of binding multinuclear oxo-iron clusters (*18*). Other results show FbpA from *Neisseria gonorrhoea* (nfbpA) bound to multinuclear oxo-hafnium clusters (*19*). The ability of FbpA to bind these mineral species suggests it may be able to access the outer cell wall where such minerals are accessible. The FbpA homolog in *M. algicola* DG893 belongs to the neisserial FbpA subfamily based on sequence alignment and contains 3 tyrosine residues important for iron coordination. A close homolog of FbpB, the cytoplasmic permease, is contained within the same operon. Some characterized Fbp systems do not contain FbpC, an ATP-binding protein, and this seems to be the case in DG893 since no close homolog of FbpC was found (*20*). In order to test whether the putative FbpA homolog and

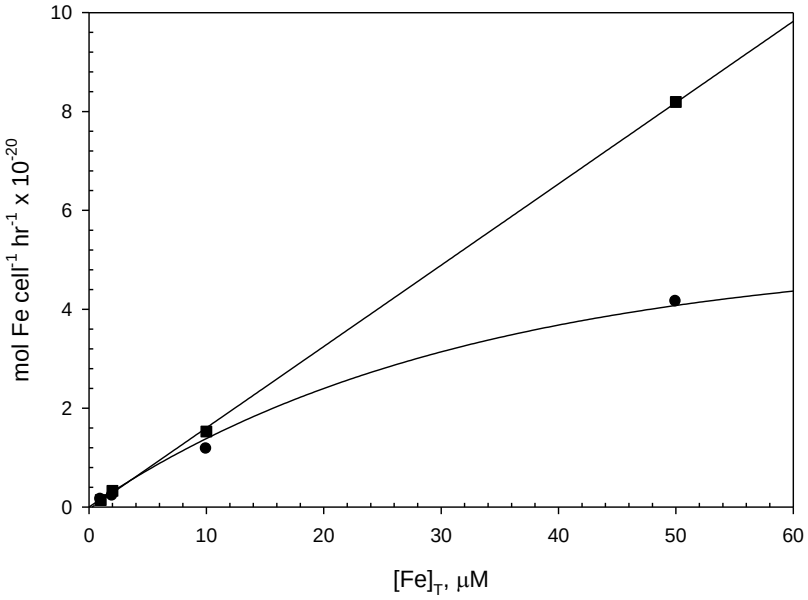

Figure 6.3. Concentration-dependent VF-mediated iron uptake rates by *Marinobacter* sp. DG879. ^{55}Fe uptake was performed at 20^{o}C using varying concentrations of Fe(III)-VF with a 2:1 ratio of VF to iron. Cultures were kept in the dark and either contained intact ^{55}Fe-VF (●) or previously photolyzed ^{55}Fe-VF (■) using a mercury vapor lamp (350 µE m^{-2} s^{-1}).

other putative siderophore biosynthesis and uptake genes are regulated by iron availability, we quantified transcripts of these genes using reverse transcription PCR (RT-PCR) in DG893.

6.2.2. Expression of relevant iron-uptake genes. The biosynthesis operon (*pvs*) of the siderophore vibrioferrin and its receptor (*pvu)* has been previously identified in *Vibrio parahaemolyticus (21-23)*. Homologous genes in *M. algicola* DG893 and other iron uptake relevant genes were identified using bioinformatics analysis. A Fur binding repeat sequence (Fur box) was located near the promoter region of the *pvs/pvu* operon indicating that these genes might be co-regulated by the iron uptake repressor. Besides genes involved in the biosynthesis and uptake of vibrioferrin, we sought to test the influence of iron limitation on putative iron transport genes including *fbpA* and *vciA*, a gene coding for a widely distributed TonB-dependent outer membrane receptor shown to be involved in iron transport in *V. cholera* (*24*). A complete list of primers used in this study is shown in Table 6.1.

Table 6.1. List of primers used in RT-PCR to quantify gene transcripts of important iron uptake genes and in qPCR for the detection of the biosynthesis of VF in the North Atlantic (italics).

Primer Names	Primer Sequences	Target Gene	Putative Function	Accession No.
pvsA532-f pvsA620-r	TGTGATCAGTTCTGGCAAGG CCAATGGTCTCCAGAGTGTG	*pvsA*	vibrioferrin biosynthesis gene	ZP_01892156
fbpA515-f fbpA639-r	TCGCTCACCATGGCGAAGAAGC AATGTCGCACTCGCCGGCAT	*fbpA*	Periplasmic iron binding protein	ZP_01892821
pvuA1107-f pvuA1226-r	GGTTCTGGCCGAAGAAGAAGG ACGAAGCGGACATGAGTCG	*pvuA*	VF outer membrane receptor	ZP_01892151
gyrA130-f gyrA366-r	GTGCATCGCCGCGTACTGTT ATAACGCATGGCAGCCGCGT	*gyrA*	DNA gyrase subunit A	ZP_01895129
vci1196-f vci1343-r	CTGAACCTACCGCCCTGTATCC CGATTGGTGTTCTCGATCTCC	*vciA*	TonB-dependent outer membrane receptor	ZP_01893439
pvsBm1486-f *pvsBm1741-r*	*ARATGTTYACCACCATYACCYTGCA* *CMMKYTTGCCRTAGAAYTTRTTRATRTC*	*pvsB*	Vibrioferrin biosynthesis gene	ZP_01892155

Under iron limitation (50 nM $FeCl_3$) and dark conditions, the biosynthesis and receptor genes of VF, *pvsA* and *pvuA*, were upregulated by 48- and 66-fold respectively compared to iron sufficient cells (10 μM $FeCl_3$). In addition, *fbpA* and *vciA* were upregulated by 22- and 40-fold respectively (Fig. 6.4, black bars). These results are consistent with known behavior of iron regulation of siderophore biosynthesis and iron uptake genes. Cells exposed to a fluorescent lamp (30 μE m^{-2} s^{-1}) under iron-limited conditions showed that gene transcripts of *pvsA*, *pvuA* and *vciA* were upregulated by 36-, 25- and 41-fold respectively, while *fbpA* was upregulated by 4-fold relative to iron sufficient cells (Fig. 6.4, grey bars). Surprisingly, gene transcripts of *pvsA*, *pvuA*, and *fbpA* varied when cultures were exposed to light or grown in the dark under iron limitation. This effect is especially pronounced in *pvuA* and *fbpA* where dark cells upregulated both genes by roughly 3- and 5-fold relative to light-exposed cells (Fig. 6.4).

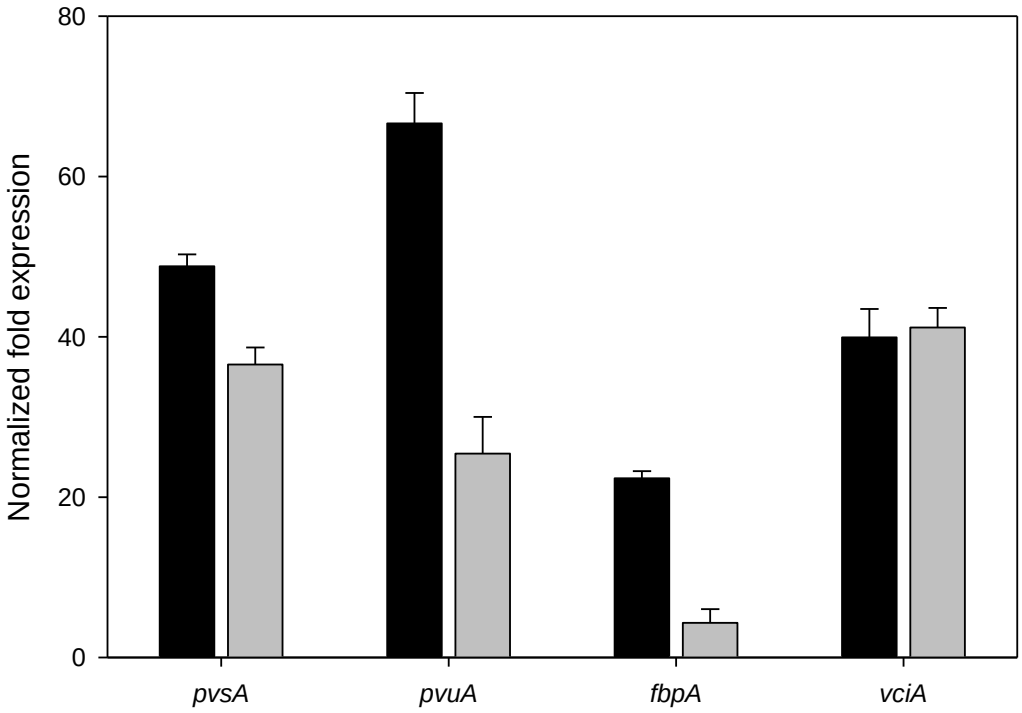

Figure 6.4. Light effects on expression of siderophore biosynthesis and iron uptake genes in iron limited *M. algicola* DG893. Black bars represent iron deficient (50 nM $FeCl_3$**)** cells grown in the dark, while grey bars represent iron deficient cells exposed to a constant fluorescent lamp (30 μE m^{-2} s^{-1}). *pvsA* (VF biosynthesis), *pvuA* (VF outer membrane receptor), *fbpA* (putative iron binding protein), *vciA* (putative TonB-dependent outer membrane receptor). Gene transcripts were normalized relative to transcripts in iron sufficient cultures (10 μM $FeCl_3$). The housekeeping gene, *gyrA*, was used as a control since its expression was constant over all growth conditions. Error bars represent triplicate RT-PCR experiments.

Although this overexpression is modest when compared to iron-induced regulation, there is no *a priori* reason why a non-photosynthetic heterotrophic marine bacterium should exhibit light-induced regulation of its iron uptake genes. This "light regulation" is expected to be more pronounced in attenuated sunlight as judged by measured rates of Fe-VF photolysis and further experiments to elucidate this are underway (*25*). In retrospect, this light effect might be a response to the photochemistry of Fe-VF since previous kinetic studies showed that Fe(III)-VF is expected to photolyze with a half-life of less than 7 minutes at seawater conditions and that the photogenerated Fe(III) is internalized more efficiently than VF-bound iron. By down-regulating the biosynthesis and uptake of VF in the light, bacteria can invest their metabolic

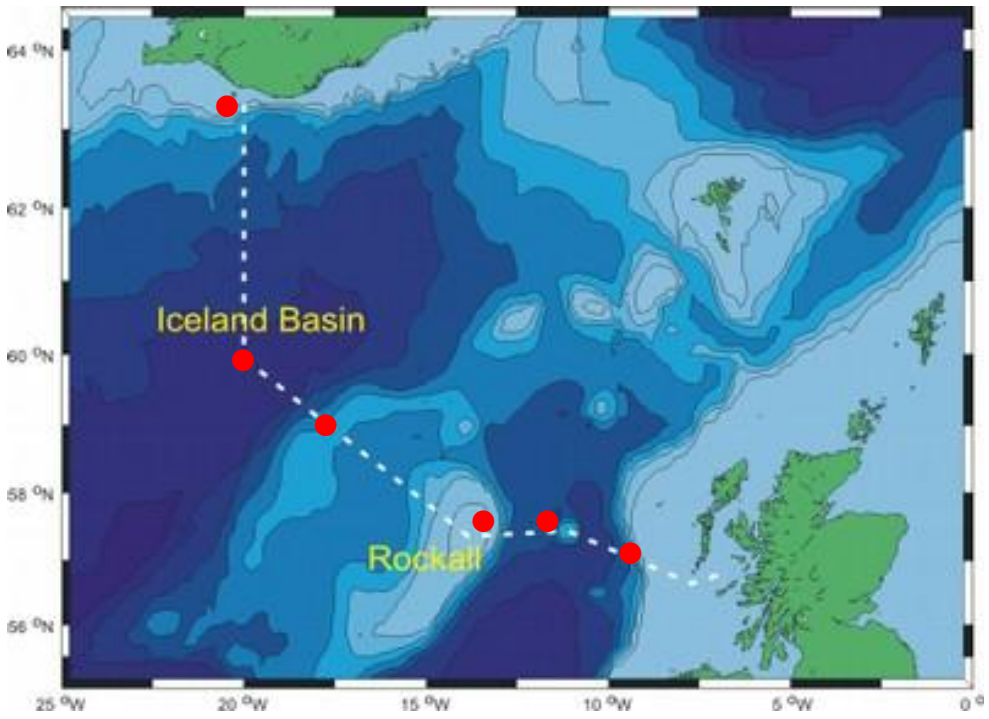

Figure 6.5. The Extended Ellet Line cruise route, June 2009. Stations where samples were collected are highlighted in red.

energy on other physiological functions while still satisfying their iron requirement by activating proteins that can internalize Fe(III)' rather than Fe(III)-VF. Although we have not identified such proteins yet, previous studies indicate that a wide range of heterotrophic bacteria are capable of internalizing Fe(III)'.

An alternative interpretation is that the photochemistry of VF and its consequences on iron speciation and gene transcription is an indirect way of sensing light. Since the physiology of VF-producing *Marinobacter* spp. seems to dictate intimate associations with photosynthetic dinoflagellates, this method of indirect light-sensing might offer an efficient mechanism of nutrient exchange between both organisms. Since dinoflagellates release DOM that will be utilized by the bacteria to support growth and ultimately to continue the synthesis of VF, the ability of the bacteria to indirectly sense light might serve as a regulator of this carbon-iron exchange mechanism. Further work is needed to better understand the role of light in mediating

these interactions and what if any are the effects of iron speciation on gene expression in marine bacteria.

6.2.3. Distribution of the biosynthesis genes of VF in the North Atlantic. In order to assess the ecological importance of the algal-bacterial mutualism mediated by the photochemistry of VF and to examine the importance of VF as an iron binding ligand in seawater, we collected environmental seawater samples during an annual North Atlantic cruise from 10-25 June 2009 along the Ellet Line (Fig. 6.5). The Ellet Line is a time-series established in 1976 to monitor physical changes in the North Atlantic and their impact on Northern Europe and starts traditionally from the Icelandic Shores to the Scottish continental shelf. Sampling occurred during the daytime at six different stations (Table 6.2) from various depths along the line with two bottle replicates for most samples. We sought to distinguish between particle-associated and free-living bacteria by filtering seawater through 1.2 μm GF/C filters followed by a second filtration through 0.2 μm Sterivex filter units. Subsequently, filters were treated as described in the methods section. We utilized real-time quantitative PCR (qPCR) to measure the abundance of the biosynthesis of VF in these samples.

Table 6.2. List of stations where samples were collected and dates of collection.

Station Name	Latitude	Longitude	Sampling Date
IB20S	63.000	-20.000	11 June
IB11S	59.667	-19.117	14 June
IB5	58.883	-17.000	15 June
C	57.550	-13.000	16 June
F	57.508	-12.250	17 June
O	57.150	-9.700	20 June

Using a degenerate primer set (pvsBm1486-f/pvsBm1741-r; Table 6.1), we targeted the second gene in the biosynthetic pathway of VF, *pvsB*, since *pvsA* appears to be involved in the biosynthesis of the siderophore pyoverdine based on previous work by others (*26*). Sequence

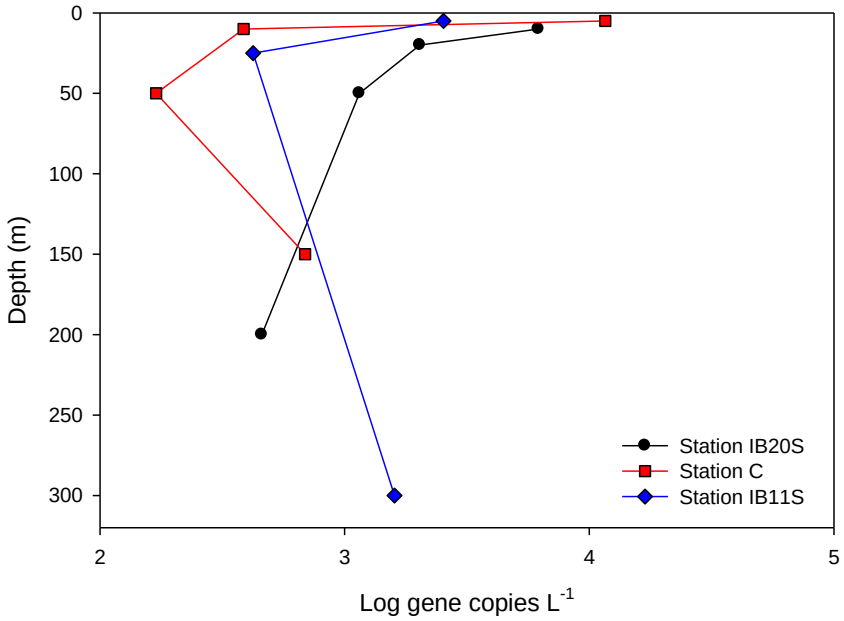

Figure 6.6. Depth distribution of *pvsB* concentration in 3 stations along the Extended Ellet Line. Concentrations represent total *pvsB* detected in the particulate and free-living fractions. Concentrations were determined based on qPCR amplifications relative to *M. algicola* DG893 standards using the $\Delta\Delta C_t$ method.

dissimilarities between *pvsB* in VF-producing *Vibrio* spp. and in *Marinobacter* spp. allowed for the amplification of only the latter as evidenced by PCR and qPCR using *V. splendidus* and a variety of VF-producing and non-producing *Marinobacter* species. The exclusive detection of *pvsB* from *Marinobacter* spp. was deemed important since *Vibrio* spp. are considered more ubiquitous in coastal regions and may bias the results toward non-algal associated VF-producers.

Figure 6.6 shows the depth distribution of total [*pvsB*] in stations IB20S, IB11S and C. All three stations exhibit a consistent localization of *pvsB* genes near the surface than at any other depth. The absence of any DNA amplification from the other three stations, presumably because of inhibitors especially below the chlorophyll a maxima, hampered the inclusion of this data so far. However, a comparison between [*pvsB*] near the surface vs near the chlorophyll a maxima reveal an analogous pattern across all six stations with the exception of Station IB5

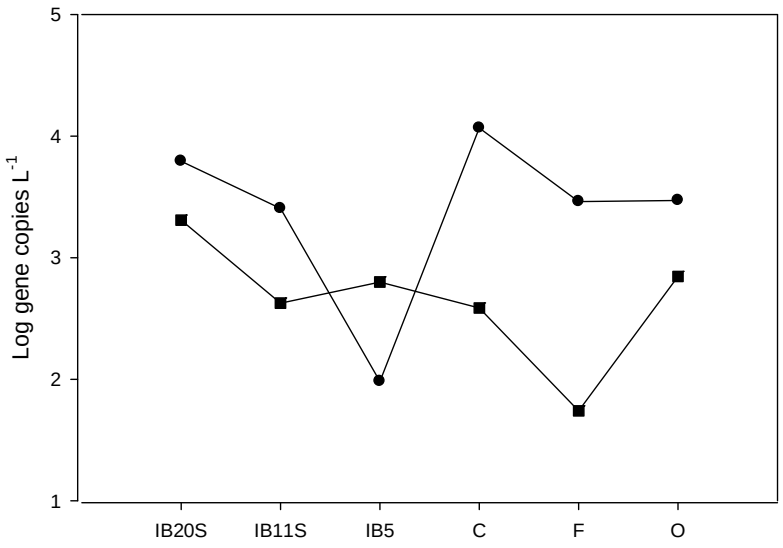

Figure 6.7. Comparison between total *pvsB* concentrations near the surface and near chlorophyll maxima across all six North Atlantic stations. Total surface concentrations (●), total concentration near the chlorophyll a maxima (■).

(Fig. 6.7). These results suggest that *pvsB*, a proxy for VF-producing *Marinobacter* spp., is concentrating near the surface where sunlight will enhance the rate of the photochemical reaction of Fe(III)-VF. Such behavior reinforces the gene expression and iron uptake experiments, that VF-producers might be benefitting from this distribution metabolically and perhaps are using the photochemistry to indirectly sense light. Unfortunately, corrleations between [*pvsB*] in free-living and particulate fractions were ignored at this point because of inconsistencies in bottle replicates and the lack of enough positive data points particularly in the particulate samples. This is presumably due to the lack of physical attachment between the bacteria and particles or algal cells, which would naturally lead to their detection in the free-living fraction.

The detected concentrations of *pvsB* further indicate that though these genes are not dominant, they are relevant to iron biogeochemistry and further work is needed to elucidate the extent of the contribution of these genes to iron speciation and to algal iron uptake. This will include correlations with chlorophyll concentrations, nutrients, DOC, dissolved oxygen and iron

once the CTD data from the Ellet Line becomes available. In addition, calculations of total bacterial DNA and the ratio of VF-producers to total bacteria are underway. Future sampling should include more detailed surface profiles and sampling in areas with high chlorophyll concentrations such as during algal blooms. Since all sampling occurred during the daytime, we can only infer *Marinobacter* spp. distribution when light is available. Additional future sampling should include day and night sampling to examine whether these heterotrophic, motile bacteria can display vertical migration patterns similar to photosynthetic organisms to acquire more nutrients at deeper depths.

6.3. Methods

6.3.1. Bacterial growth and VF Isolation. *Marinobacter* sp. DG879 and *M. algicola* DG893 were grown and harvested and VF was purified as previously described (*15*).

6.3.2. ^{55}Fe Uptake by Marinobacter sp. DG879. ^{55}Fe(III)-VF complex was prepared by adding a standard solution of $FeCl_3 \cdot 6H_2O$ (Aldrich; 1 mg/mL) and $^{55}FeCl_3$ (1522 MBq/mL; Perkin-Elmer) to VF (final Fe_T:ligand = 1:3; final $FeCl_3$:^{55}Fe = 1:0.1) in the dark. The complex was allowed to equilibrate for at least 24 hrs in the dark prior to use.

Cells were grown in ASW (*15*) with the final pH adjusted to 8.0. The ASW was passed through Chelex-100 resin (BioRad) to remove trace metals and supplemented with 100 nM $FeCl_3$. Cultures were harvested at mid-exponential growth phase by centrifuging at 6000 rpm for 20 minutes using Sorvall RC5C+ centrifuge followed by washing 3 times with iron-free ASW. The harvested cells were then diluted with fresh media to an optical density at 600 nm of 0.3 and incubated at 4^{o} C if not used immediately (*14*). Prior to the start of the uptake, cells were shaken at 130 rpm and 20^{o}C for 30 minutes (except for the 4 ^{o}C uptake experiment) after which the experiment was started by adding a 1 µM final concentration of ^{55}FeVF solution. Ascorbate (10 mM), sodium azide (5 mM) and CCCP (30 µM) were added 1 hour prior to adding ^{55}FeVF.

Uptake experiments in the presence of CCCP, sodium azide and 4 ^{o}C were performed in dark with occasional shaking and maintained at 20 ^{o}C (except for the 4 ^{o}C uptake experiment which was kept on ice). Uptake in the presence of the reductant ascorbate was performed by photolyzing the required amount of ^{55}FeVF using a mercury vapor lamp (175W) for 30 minutes at acidic pH and in the presence of 10 mM ascorbate prior to addition to the culture. Photolysis for the uptake of photolyzed ^{55}FeVF was performed *in situ* by exposing the cells directly to the mercury vapor lamp and in a separate experiment by photolyzing the required amount of ^{55}FeVF prior to addition to cells. Results from both experiments were nearly identical.

Concentration dependent ^{55}FeVF uptake rates were measured by growing the cells as described and adding 1, 2, 10 and 50 μM ^{55}FeVF, either kept in the dark or photolyzed briefly before the experiment for 30 minutes using the mercury vapor lamp, to 4 different cultures suspended to a final optical density of 0.4 at 600 nm. All cultures were kept in the dark after adding ^{55}FeVF.

Aliquots were withdrawn at each time point or after 1 hour (for the inhibition and concentration dependence experiments) and filtered using a Millipore 1225 sampling vacuum manifold onto 0.6 μm-pore size polycarbonate filters (Millipore). Filtered cells were washed with 5 mL ASW followed by 5 mL Ti(III)-citrate-EDTA reagent (*27*) and a final 5 mL rinse with ASW to reductively remove iron oxides and iron bound to cell surfaces. ^{55}Fe cellular uptake was measured using a Beckman-Coulter LS6500 liquid scintillation counter.

6.3.3. Two-step RT-PCR amplification of iron uptake genes in M. algicola DG893. Cells were grown using ASW with omission of succinic acid as a carbon source and substitution with casamino acids (Fisher) as succinic acid promotes the formation of biofilms in DG893. ASW salts as well as casamino acids were separately passed through chelex-100 resin column to remove trace metal contaminations and then autoclaved. Cultures were grown in the dark or exposed to a fluorescent lamp (30 μE m^{-2} s^{-1} measured output) with supplemented 50 nM (Fe-

limited) or 10 μM (Fe-sufficient) $FeCl_3$ with constant shaking at 150 rpm and 30 ^oC and harvested at mid-exponential growth phase (ca. 2-3 days) at an optical density of 0.3 at 600 nm. Cells were lysed enzymatically using lysozyme (Fisher) according to RNAprotect® Bacteria Reagent kit (Qiagen). RNA was isolated using RNeasy® Mini kit according to manufacturer's instructions (Qiagen). Genomic DNA digestion was carried out using RNase-free DNase Set (Qiagen), which utilizes DNase I to digest genomic DNA co-purified with RNA. RNA concentrations in post-digestion samples were about ½ to ¼ the original RNA concentrations. Subsequently, cDNA synthesis was performed on 2 μg RNA using iScript cDNA synthesis kit (Bio-Rad), which utilizes oligo(dT) and random hexamer primers. Ten-fold dilutions of the cDNA stocks were prepared to afford a working stock for real-time quantitative PCR. All nucleic acids were quantified spectrophotometrically using a Cary 50 instrument.

Primers were designed using either VectorNTI software package (Invitrogen) or Primer-BLAST searching on NCBI (http://www.ncbi.nlm.nih.gov/tools/primer-blast/). Primer sets were BLAST searched against the *M. algicola* DG893 genome to check for possible non-specific targets and were subsequently used to amplify targets from genomic DNA using standard PCR to ascertain the presence of only one target using 0.2 μM primers, 2 mM $MgCl_2$, and Taq polymerase (PCR profile: Initial 2 min at 95 ^oC, followed by 30 cycles of 95 ^oC for 10 s, 60 ^oC for 30 s, and 72 ^oC for 1 min and a final extension of 72 ^oC for 5 min). The complete list of primers used in this study is provided in table 1. Primers specific for *gyrA* were used as a housekeeping gene, which was confirmed to not vary across all growth conditions using RT-PCR.

Real-time Quantitative PCR (RT-qPCR) was performed on four cDNA conditions (Fe-limited and Fe-sufficient in the dark and in the light) to quantify relative abundance of iron uptake genes using the iQ SyberGreen Supermix kit (Bio-Rad) and relevant primers (0.2 μM)

specific to *M. algicola* DG893. Temperature profiles for RT-PCR consisted of an initial incubation at 50 ^{o}C for 10 min, 95 ^{o}C for 5 min, followed by 45 cycles of 95 ^{o}C for 10 s and 60 ^{o}C for 1 min. Six dilutions of DG893 genomic DNA were used to construct a standard curve for sample quantification. Experiments were carried out using iQ cycler (Bio-Rad) with efficiencies of the PCR reaction ranging from 92-104% in any given experiments.

6.3.4. Environmental Sampling and Nucleic acid extraction from the North Atlantic. Samples along the Extended Ellet Line were collected using 20 L Niskin bottles fixed onto a stainless steel or a Titanium frame from 4 different depths ranging from 5 m to 300 m during 10-25 June, 2009. All sampling occurred during the daytime ranging from 10:00 am to 2:00 pm local time. Samples were collected in Polypropylene plastic bottles and immediately filtered onto 1.2 μm GFC filters (typically 1.3 L filtered) followed by filtration onto 0.22 μm sterivex filter unit (typically 0.75 L). Filters were frozen in sterile small polypropylene tubes at -80 ^{o}C aboard the ship.

Nucleic acid extractions from Sterivex filter units were performed using the XS method based on nucleic acid isolation from cyanobacteria using potassium ethyl xanthogenate buffer (*28*). Nucleic acid extractions from GFC filters required more processing as the amount of extracted DNA was miniscule. Thus, we used a modified XS method based on Yilmaz et al, which uses a DNA precipitation step with 7% PEG 8000 (*29*). Extracted nucleic acids were quantified using a Nano-drop spectrophotometer (Implen) and were frozen at -80 ^{o}C until further use.

6.3.5. Quantification of pvsB from environmental samples. Degenerate primers targeting *pvsB* were designed based on sequence alignments of known *pvsB* genes. The primers were then tested on various VF-producing and non-producing *Marinobacter* spp. and on *V. splendidus* (a VF-producer) to confirm the amplification of correct products from *Marinobacter*

VF-producers only using real-time Quantitative PCR (RT-qPCR). RT-qPCR was performed on all samples in triplicates to quantify relative abundance of *pvsB* using the iQ SyberGreen Supermix kit (Bio-Rad) and the *pvsB* primers (1 μM). Temperature profiles for RT-qPCR consisted of an initial incubation at 95 ^{o}C for 5 min, followed by 45 cycles of 95 ^{o}C for 10 s and 60 ^{o}C for 1 min. Five dilutions of DG893 genomic DNA were used to construct a standard curve for sample quantification. Experiments were carried out using iQ cycler (Bio-Rad) with efficiencies of the PCR reaction averaging to 94%. Samples that did not exhibit any background fluorescence including primer dimmers were assumed inhibited and DNA was repurified using QIAamp DNA Stool Mini Kit (Qiagen). Calculated concentrations in nanograms were converted to genomes assuming 1 copy of *pvsB* per genome and using an average size of 4.41 Mb for *M. algicola* DG893.

6.4. Acknowledgements

This work was supported by California SeaGrant. We would like to thank Frithjof Küpper for providing space on the ship, Toby Sherwin for leading the scientific team and coordinating CTD sampling, Estelle Dumont for calibrating the CTD data, Andrew Mogg for assistance on the ship, David H. Green for designing the degenerate *pvsB* primers, DHG, Mark C. Hart and Debra Brennan for assisting with nucleic acid isolations, Lyndsay Trimble for assisting with the qPCR experiments and Ariel Romano for assisting with gene expression.

6.5. References

1. Rue, E. L., and Bruland, K. W. (1995) Complexation of iron(III) by natural organic ligands in the Central North Pacific as determined by a new competitive ligand equilibration/adsorptive cathodic stripping voltammetric method, *Mar. Chem. 50*, 117-138.

2. Wu, J., and Luther, G. W. (1995) Complexation of Fe(III) by natural organic ligands in the Northwest Atlantic Ocean by a competitive ligand equilibration method and a kinetic approach, *Mar. Chem. 50*, 159-177.

3. Gledhill, M., and van den Berg, C. M. G. (1994) Determination of complexation of iron(III) with natural organic complexing ligands in seawater using cathodic stripping voltammetry, *Mar. Chem. 47*, 41-54.

4. Boyd, P. W., Watson, A. J., Law, C. S., Abraham, E. R., Trull, T., Murdoch, R., Bakker, D. C. E., Bowie, A. R., Buesseler, K. O., Chang, H., Charette, M., Croot, P., Downing, K., Frew, R., Gall, M., Hadfield, M., Hall, J., Harvey, M., Jameson, G., LaRoche, J., Liddicoat, M., Ling, R., Maldonado, M. T., McKay, R. M., Nodder, S., Pickmere, S., Pridmore, R., Rintoul, S., Safi, K., Sutton, P., Strzepek, R., Tanneberger, K., Turner, S., Waite, A., and Zeldis, J. (2000) A mesoscale phytoplankton bloom in the polar Southern Ocean stimulated by iron fertilization, *Nature 407*, 695-702.

5. Coale, K. H., Johnson, K. S., Fitzwater, S. E., Gordon, R. M., Tanner, S., Chavez, F. P., Ferioli, L., Sakamoto, C., Rogers, P., Millero, F., Steinberg, P., Nightingale, P., Cooper, D., Cochlan, W. P., Landry, M. R., Constantinou, J., Rollwagen, G., Trasvina, A., and Kudela, R. (1996) A massive phytoplankton bloom induced by an ecosystem-scale iron fertilization experiment in the equatorial Pacific Ocean, *Nature 383*, 495-501.

6. de Baar, H. J. W., Boyd, P. W., Coale, K. H., Landry, M. R., Tsuda, A., Assmy, P., Bakker, D. C. E., Bozec, Y., Barber, R. T., Brzezinski, M. A., Buesseler, K. O., Boye, M., Croot, P. L., Gervais, F., Gorbunov, M. Y., Harrison, P. J., Hiscock, W. T., Laan, P., Lancelot, C., Law, C. S., Levasseur, M., Marchetti, A., Millero, F. J., Nishioka, J., Nojiri, Y., van Oijen, T., Riebesell, U., Rijkenberg, M. J. A., Saito, H., Takeda, S., Timmermans, K. R., Veldhuis, M. J. W., Waite, A. M., and Wong, C.-S. (2005) Synthesis of iron fertilization experiments: From the iron age in the age of enlightenment, *J. Geophys. Res., [Oceans] 110*, C09S16/01-C09S16/24.

7. Sandy, M., and Butler, A. (2009) Microbial iron acquisition: marine and terrestrial siderophores, *Chem. Rev. 109*, 4580-4595.

8. Barbeau, K. (2006) Photochemistry of organic iron(III) complexing ligands in oceanic systems, *Photochem. Photobiol. 82*, 1505-1516.

9. Barbeau, K., Zhang, G., Live, D. H., and Butler, A. (2002) Petrobactin, a photoreactive siderophore produced by the oil-degrading marine bacterium *Marinobacter hydrocarbonoclasticus*, *J. Am. Chem. Soc. 124*, 378-379.

10. Sunda, W., and Huntsman, S. (2003) Effect of pH, light, and temperature on Fe-EDTA chelation and Fe hydrolysis in seawater, *Mar. Chem. 84*, 35-47.

11. Morgan, B., and Lahav, O. (2007) The effect of pH on the kinetics of spontaneous Fe(II) oxidation by O_2 in aqueous solution - basic principles and a simple heuristic description, *Chemosphere 68*, 2080-2084.

12. Barbeau, K., Rue, E. L., Bruland, K. W., and Butler, A. (2001) Photochemical cycling of iron in the surface ocean mediated by microbial iron(III)-binding ligands, *Nature 413*, 409-413.

13. Abergel, R. J., Zawadzka, A. M., and Raymond, K. N. (2008) Petrobactin-mediated iron transport in pathogenic bacteria: coordination chemistry of an unusual 3,4-catecholate/citrate siderophore, *J. Am. Chem. Soc. 130*, 2124-2125.

14. Küpper, F. C., Carrano, C. J., Kuhn, J.-U., and Butler, A. (2006) Photoreactivity of iron(III)-aerobactin: photoproduct structure and iron(III) coordination, *Inorg. Chem. 45*, 6028-6033.

15. Amin, S. A., Küpper, F. C., Green, D. H., Harris, W. R., and Carrano, C. J. (2007) Boron binding by a siderophore isolated from marine bacteria associated with the toxic dinoflagellate *Gymnodinium catenatum*, *J. Am. Chem. Soc. 129*, 478-479.

16. Amin, S. A., Green, D. H., Hart, M. C., Küpper, F. C., Sunda, W. G., and Carrano, C. J. (2009) Photolysis of iron–siderophore chelates promotes bacterial–algal mutualism, *Proc. Natl. Acad. Sci. U. S. A. 106*, 17071-17076.

17. Tam, R., and Saier, M. H., Jr. (1993) Structural, functional, and evolutionary relationships among extracellular solute-binding receptors of bacteria, *Microbiol. Mol. Biol. Rev. 57*, 320-346.

18. Shouldice, S. R., Skene, R. J., Dougan, D. R., McRee, D. E., Tari, L. W., and Schryvers, A. B. (2003) Presence of ferric hydroxide clusters in mutants of *Haemophilus influenzae* ferric ion-binding protein A, *Biochemistry 42*, 11908-11914.

19. Alexeev, D., Zhu, H., Guo, M., Zhong, W., Hunter, D. J. B., Yang, W., Campopiano, D. J., and Sadler, P. J. (2003) A novel protein-mineral interface, *Nat. Struct. Mol. Biol. 10*, 297-302.

20. Ferreiros, C., Criado, M. T., and Gomez, J. A. (1999) The neisserial 37 kDa ferric binding protein (FbpA), *Comp. Biochem. Physiol. B: Biochem. Mol. Biol. 123*, 1-7.

21. Funahashi, T., Moriya, K., Uemura, S., Miyoshi, S.-I., Shinoda, S., Narimatsu, S., and Yamamoto, S. (2002) Identification and characterization of *pvuA*, a gene encoding the ferric vibrioferrin receptor protein in *Vibrio parahaemolyticus*, *J. Bacteriol. 184*, 936-946.

22. Tanabe, T., Funahashi, T., Nakao, H., Miyoshi, S.-I., Shinoda, S., and Yamamoto, S. (2003) Identification and characterization of genes required for biosynthesis and transport of the siderophore vibrioferrin in *Vibrio parahaemolyticus*, *J. Bacteriol. 185*, 6938-6949.

23. Tanabe, T., Nakao, H., Kuroda, T., Tsuchiya, T., and Yamamoto, S. (2006) Involvement of the *Vibrio parahaemolyticus pvsC* gene in export of the siderophore vibrioferrin, *Microbiol. Immunol. 50*, 871-876.

24. Mey, A. R., Wyckoff, E. E., Hoover, L. A., Fisher, C. R., and Payne, S. M. (2008) *Vibrio cholerae* VciB Promotes Iron Uptake via Ferrous Iron Transporters, *J. Bacteriol. 190*, 5953-5962.

25. Amin, S. A., Green, D. H., Küpper, F. C., and Carrano, C. J. (2009) Vibrioferrin, an unusual marine siderophore: iron binding, photochemistry, and biological implications, *Inorg. Chem. 48*, 11451-11458.

26. Mossialos, D., Ochsner, U., Baysse, C., Chablain, P., Pirnay, J.-P., Koedam, N., Budzikiewicz, H., Fernández, D. U., Schäfer, M., Ravel, J., and Cornelis, P. (2002) Identification of new, conserved, non-ribosomal peptide synthetases from fluorescent pseudomonads involved in the biosynthesis of the siderophore pyoverdine, *Mol. Microbiol. 45*, 1673-1685.

27. Hudson, R. J. M., and Morel, F. M. M. (1989) Distinguishing between extra- and intracellular iron in marine phytoplankton, *Limnol. Oceanogr. 34*, 1113-1120.

28. Tillett, D., and Neilan, B. A. (2000) Xanthogenate nucleic acid isolation from cultured and environmental cyanobacteria, *J. Phycol. 36*, 251-258.

29. Yilmaz, M., Phlips, E. J., and Tillett, D. (2009) Improved methods for the isolation of cyanobacterial DNA from environmental samples, *J. Phycol. 45*, 517-521.